DESIGN OF FRAMEWORK FOR ENHANCEMENT OF UNDERWATER IMAGES

A Thesis Submitted
In Partial Fulfillment of the Requirement
for the Degree of

DOCTOR OF PHILOSOPHY

by

Nishant Singh
(2K20/PHDCO/02)

Under the supervision of
Prof. Aruna Bhat
Delhi Technological University

Department of Computer Science and Engineering

DELHI TECHNOLOGICAL UNIVERSITY
(Formerly Delhi College of Engineering)
Shahbad Daulatpur, Bawana Road, Delhi-110042. India

July, 2024

CERTIFICATE

This is to certify that **Nishant Singh** (2K20/PHDCO/02) has carried out their research work presented in this thesis entitled **"Design of framework for enhancement of underwater images"** for the award of **Doctor of Philosophy** from Delhi Technological University, New Delhi, under my supervision. The thesis embodies results of original work, and studies are carried out by the student himself and the contents of the thesis do not form the basis for the award of any other degree to the candidate or to anybody else from this or any other University/Institution.

Prof. Aruna Bhat
Associate Professor
Department of Computer Science and Engineering
Delhi Technological University, Delhi 110042

Date:

CANDIDATE'S DECLARATION

I, **Nishant Singh**, a full-time scholar (Roll No: 2K20/PHDCO/02), hereby declare that the thesis entitled "**Design of Framework for Enhancement of Underwater Images**" which is submitted by me to the Department of Computer Science and Engineering, Delhi Technological University, Delhi in partial fulfilment of the requirement for the award of the degree of Doctor of Philosophy, is original and not copied from any source without proper citation. This work has not previously formed the basis for the award of any Degree, Diploma Associateship, Fellowship or other similar title or recognition.

Mr. Nishant Singh
Roll No: 2K20/PHDCO/02
Department of Computer Science and Engineering
Delhi Technological University, Delhi

Place: Delhi
Date:

ABSTRACT

Underwater image processing has received tremendous attention in few past years. In the last few years underwater image processing has attracted much attention because of its importance in marine engineering and aquatic robotics. The reason for increased research in this area is due to the process of image taken in under water. When we capture the image in under water then the quality of image is degraded. To address this problem, we need some other methods to increase the quality of image while capturing it under water. But capturing the image in normal circumstances as well as in under water are same, thus once we get an image, some mechanism to increase the quality of captured image will be required. Though some methods are already present in image enhancement and restoration, still some comparative and deep survey is required to improve the image quality. Various algorithms have been proposed for underwater image enhancement, but for their assessment either synthetic datasets or few selected real-world images are used. There are few latest underwater image enhancement methods based on deep learning and machine learning. These methods not only enhance the images but also provide better results as compared to enhancement and restoration method. These deep learning-based methods increasing the variety in underwater imaging, enhancing underwater image quality and providing wider scope in terms of improvisation. This research work presented the four significant contributions in the underwater image enhancement system.

First, we have conducted a literature review of underwater image enhancement systems to highlight the challenges of the existing work and identify some good quality works in the domain of underwater image enhancement. A complete and in-depth study of relevant accomplishments and developments, particularly the survey of underwater image methods and datasets, which are a critical issue in underwater image processing and intelligent application, has been done. In this, we first provide a review of more than 100 articles on the recent advancements in underwater image restoration methods, underwater image enhancement methods, and underwater image enhancement using deep learning algorithms, along with the techniques, data sets, and evaluation criteria. To provide a thorough grasp of underwater image restoration, enhancement, and enhancement using deep learning, we explore the strengths and limits of existing techniques.

Second, we developed a robust model for improving the quality of underwater images using enhancement techniques. This technique is split into two sections. The first section focuses on boosting contrast, while the second section focuses on improving color. Our enhanced results stand out for their brilliant color, greater contrast, and enhanced features. When compared to other approaches this technique improves image quality by increasing entropy, peak signal to noise ratio (PSNR), and underwater color image quality evaluation (UCIQE) values while lowering mean square error (MSE). It is an entirely algorithm-based technique that is independent by image datasets. The images used to evaluate the results come from a variety of datasets, and their enhanced performance confirms their robustness. Because of its single image-based approach, our method is very

compelling in terms of processing speed. Comprehensive findings on a variety of underwater image datasets demonstrate that our approach outperforms the vast majority of them.

Third, we designed an underwater image enhancement framework to recover deep sea images. In deep sea underwater images, the uneven attenuation of sunlight, when it spreads underwater, they have high color distortion and very low intensity. Furthermore, the amount of attenuation changes with wavelength, yielding in asymmetric color traversing. As the research, this framework demonstrates that assigning the appropriate context based on the color channel traversal range may result in a significant performance speedup for the objective of underwater image enhancement. Furthermore, it is critical to reduce irrelevant multi-contextual characteristics and improve the model's representational strength. Therefore, we included an important reduce method to dynamically modify the learnt multi-contextual characteristics. DeepSeaNet, the suggested framework, is enhanced via conventional pixel-wise and feature-based estimation methods. Comprehensive tests were conducted to demonstrate the efficiency of the proposed technique with the best published paper on standard datasets.

Fourth, we do a comparative result analysis of the developed models with the other existing techniques. The comparative analysis shows that the proposed system is better than the existing techniques. The experimental results, analysis, and performance evaluation demonstrate that the proposed work provides feasible and efficient techniques. Thus, this research work successfully provides an effective and optimal underwater image enhancement system.

ACKNOWLEDGEMENT

I owe a debt of my gratitude to my supervisor, Prof. Aruna Bhat, Associate Professor, Department of Computer Science and Engineering, Delhi Technological University, for their valuable guidance, motivation, constant support, and encouragement, which has helped me in formulating an urge for this research work.

I would like to take this opportunity to thank all the faculty members of the Computer Science & Engineering Department, Delhi Technological University, for their encouragement and support. I am also thankful to all the staff members and research fellows for their untiring support.

I would like to extend deep gratitude to my lovely daughter Chhavishka Singh and my wife, Dr. Keerti Singh who always wanted me to be a doctor, and for always being a pillar of strength and support to manage my personal and professional life.

Finally, without whom I could not imagine being enrolled in a Ph.D., my father, Dr. Vijay pal Singh, and my mother, Gayatri Devi, for their unwavering encouragement, undeterred faith in me, and being the biggest pillar of strength, which supported me till the end.

Mr. Nishant Singh
Roll No: 2K20/PHDCO/02
Department of Computer Science and Engineering
Delhi Technological University
Delhi-110042

CONTENTS

LIST OF TABLES

LIST OF FIGURES

LIST OF ABBREVIATIONS

Abbreviation	Meaning
ACE	Automatic color equalization
AP	Attenuation prior
BM	Blurring map
BP	Bianco prior
C	Color correction
CBAM	Convolutional block attention module
CDCP	color corrected images of dark channel prior
CLAHE	Contrast limited adaptive histogram equalization CLAHE
CNN	Convolutional neural network
CNR	Contrast to noise ratio
CUS	Comparative universal stretching
DBGR	difference between blue green and red channels
DCP	Dark channel prior
DECM	Discrete entropy and contrast measure
DL	Deep Learning
DUO	Dataset for underwater object detection
EUVP	Enhancing underwater visual perception
FDC	From the dark channel
GAN	Generative adversarial networks
GAVE	Gradient ration in visible edge
GB	Global background

GC	Gamma-correction
GCF	Global contrast factor
GDCP	Generalized dark primary color prior
GWAT	Gray world assumption theory
HDR-VDP2	High-dynamic range visual difference predictor2 HDR-VDP2
HE	Histogram Equalization
HSV	Hue-Saturation-value
ICM	Integrated color model
IDBM	Image dehazing based model
IQE	Image quality evaluation
J-MGM	Jaffe-McGlamery model
KD	K-Dimension
LB	Local background
LSUI	Large-scale underwater image dataset
MAI	Maximum attenuation identification
MIL	Minimum information loss
ML	Machine learning
MRF	Markov random field
MSE	Mean square error
NIQE	Natural image quality evaluator
NOM	New optical model
NSCT	Non-sub sampled contourlet transform
PCQI	patch based contrast quality index
PDE	Partial differential equation

PSFM	Point spread function model
PSNR	Peak signal to noise ratio
QMOS	Objective score (Q) to predict mean opinion score
R	Restoration
RCP	Red channel prior
RDCP	Red dark channel prior
ReLU	Rectified linear unit
RET	Retinex
RGB	Red-Green-blue
RMSE	Root mean square error
RQ	Research questions
RUIE	Real-world underwater image enhancement dataset
SRCNN	Super resolution convolutional neural network
SRGAN	Generative adversarial network for single image super-resolution
SSIM	Structural similarity index measure
TDM	Turbulence degradation model
TM	Transmission map
U45	Underwater test dataset
UCIQE	Underwater color image quality evaluation
UCM	Unsupervised color correction model
UDCP	Underwater dark channel prior
UGAN	Unsupervised GAN
UICM	Underwater image colorfulness measure
UIConM	Underwater image contrast measure

UIEB	Underwater image enhanced benchmark dataset
UIQM	Underwater image quality measure
UISM	Underwater image sharpness measure
VGG	Visual geometry group
VIF	Visual information fidelity
VM-CNR	Visibility metrics based on CNR
WB	White-balanced
WCAG	Weighted contrast average grads
WGSA	Weighted gray scale angle

LIST OF SYMBOLS

Symbol	Description
(u, v)	Frequency domain
k	Magnitude of turbulence
E_T	Light coming from the camera
E_d	Reflected light from an object
E_f	Forward scattered light
E_b	Back scattered light
λ	Light wavelength that belongs to red, green, and blue
$I_\lambda(x)$	Underwater image
x	Underwater image pixel point
$J_\lambda(x)$	Light at sight location x
$t_\lambda(x)$	Residual energy ratio
B_λ	Uniform background light
$d(x)$	Path between the camera and the site
p_i	Intensity value of the input pixel
p_o	Intensity value of the output pixel
a, b	Min & max intensity values of the actual image
c, d	Min & max intensity values of the desired output image
R_{avg}	Normalized mean values of the recovered R channel
G_{avg}	Normalized mean values of the recovered G channel
B_{avg}	Normalized mean values of the recovered B channel
M * N	Underwater image size
θ_g	G channel color equalization coefficient
θ_b	B channel color equalization coefficient
p_{in}	Input pixel
p_{out}	Output pixel

I_{min} and I_{max}	Adaptive parameters before the stretching images.
O_{min} and O_{max}	Adaptive parameters after the stretching images.
a	Mode
G	Group of image pixel values for each R, G & B channel
$G.sort$	Increasing sorted data set
$G.sort.index(a)$	Index number of the mode in the histogram distribution
$G.sort[x]$	Value at index x of the positive sorted data set
σ_λ	Rayleigh distribution's standard deviation value
$O_{\lambda\ min}$	Required range's minimum value
L*	Signifies brightness within a range of 0 to 100
a* & b*	Signify chromaticity without numerical boundaries
(–ve) a*	Represents green
(+ve) a*	Represents red
(-ve) b*	Represents blue
(+ve) b*	Represents yellow
Δ	Delta
I_γ	Input pixels
P_γ	Output pixel.
γ	Represents the ‘a’, ‘b’ parameters
φ	Stretching coefficient
$M_s(J)$	Spatial attention mappings
$M_c(J)$	Channel attention mappings
J	Intermediate feature map
p^{7*7}	Convolution operation with a $7 * 7$ kernel
σ	Sigmoid function
F^c	A multilayer perceptron with a hidden layer
M	Represents the maximum pooling
A	Represents the average pooling
J^r	Improved feature

$W(\theta)$	Model for the underwater image enhancement
D	Degraded image
E	Enhanced image
D_R	Red color channels of D
D_G	Green color channels of D
D_B	Blue color channels of D
c	Contextual characteristics channel
i	Stage
s	Receptive field size
$f_{c,s}^{i}$	Contextual characteristics channel c at stage i with receptive field size s
$\odot$	Channel-wise concatenation
$\oplus$	Adding the characteristics pixel-by-pixel
bn	Batch normalization
g	Parametric rectified linear unit layers
$M_{<3,5,7>}^{1}$	Wavelength-driven contextual sizes with channel-specific properties
$M_{<3,5,7>}^{2}$	Color-dependent distortion residuals
$M_{<3,5,7>}^{3}$	Global color-correction residual map
w^{3*3}	2D transpose convolution operation
ℓ_2	Conventional mean squared error
O	Original cleaner underwater image
b	Channels
$V(\Theta)$	Visual geometry group (16)
$\mathcal{L}_P$	Perceptual Loss
x and y	Patches from the E and O
z_1 and z_2	Predefined parameters
μ	Mean
σ	Standard deviation

σ_{xy}	Covariance
r	Center pixels of the patches x, y
$\mathcal{L}_{\text{SSIM}}$	SSIM loss
λ_{P}	0.02 value, empirically determined
λ_{S}	0.5 value, empirically determined

CHAPTER 1

INTRODUCTION

This chapter begins with a general overview of the field of underwater image processing, laying the foundation for a thorough examination of the challenges. After presenting an overview, the chapter explores the issues of underwater imaging in depth and then presents several techniques designed to improve underwater images. This comprehensive discussion covers a range of methods intended to improve the detail and quality of underwater images.

The chapter examines image enhancing techniques and then clarifies the requirements and conceptual structure of an underwater image improvement system. It outlines the main issues that the system aims to solve, explains the reasons behind its investigation, and emphasizes the unique contributions it makes in underwater image processing.

Outlining the thesis's arrangement and structure is a crucial component of this chapter. Through the outline of the topics covered in the next several chapters and how they relate to each other, the chapter provides readers with a road map for understanding what's to come. It functions essentially as a thorough guide, getting the reader ready for a detailed examination of the subtle aspects of underwater image enhancement and processing, as well as the novel approach this thesis proposes.

1.1 Introduction

This section covers the details of underwater image processing, explains the underwater image enhancement techniques, their background details, and identifies the associated challenges.

1.1.1 Introduction to underwater image processing

In recent years, there has been a lot of interest in underwater image processing. Because of its usefulness in marine engineering and aquatic robotics, underwater image processing has received a lot of attention in recent years. The reason for increased research in this area is due to the process of taking images under water. When we take images underwater, the image quality suffers. To overcome this issue, we need to find different ways to improve image quality while capturing it underwater. But capturing the image in normal circumstances as well as under water is the same; thus, once we get an image, some mechanism to increase the quality of the captured image will be required. Though some methods are already present in image enhancement and restoration, some comparative and deep survey is still required to improve the image quality. Various algorithms have been designed for underwater image enhancement, but for their assessment, we used either synthesized datasets or real-world image datasets. There are a few of the latest underwater image enhancement methods based on deep learning. These algorithms not only enhance the images but also provide better results as compared to enhancement and restoration methods. These deep learning-based algorithms are increasing the variety in underwater imaging, enhancing underwater image quality, and providing a wider scope in terms of improvisation.

1.1.2 Background

These entire underwater image enhancement algorithms are differentiated as model-free and model-based image enhancement.

1.1.2.1 Model Free Methods

The model-free algorithms alter the values of pixels in an input image without intervening in the image generation process. The values of the pixels are adjusted either in the spatial domain or in the transformation domain. The methods based on spatial domains are the Gray World (GW) algorithm [1], histogram equalization (HE) [2], automatic white balance [3], contrast-limited adaptive histogram equalization (CLAHE) [4], color constancy [5], bilateral filtering, image fusion [6], and multi-scale retinex with color restoration [7]. The author, Iqbal et al., uses unsupervised color balance and histogram stretching enhancement techniques [8]. The author Hitman et al. defined mixture Red-Green-Blue (RGB) and Hue-Saturation-Value (HSV) CLAHE techniques based on model-free methods [9]. The author, Ghani et al., uses minimize under-enhanced and over-enhanced area enhancement techniques based on real-world images [10]. The methods based on transformation domain map the image pixel values in a predefined, specific domain where we develop the physical properties to carry out modification. The most frequently used transformations are the wavelet transformation and the Fourier transformation.

1.1.2.2 Model Based Methods

The The algorithms based on model-based approaches openly distinguish the physical imaging development and assess the parameters of the

imaging model from the inspection and a variety of past experiences. The pure underwater view has been brought back by reversing the degradation procedure. Jaffe McGlamery defined one basic underwater imaging model [11].

Various underwater image enhancement algorithms try to expand the preceding model-based dehazing methods for underwater scenes by notifying that the underwater imaging model shares basic features with one for hazy images. Several model-based underwater image enhancement algorithms use Dark Channel Prior (DCP) [12]. It is one of the best methods for measuring the transmission map in hazy images. The author, Chiang et al., changed the DCP method by compensating for the reduction to bring back the color balance [13]. The author, Drews Jr. et al., used the changed DCP in the green channel and the blue channel [14]. The author Galdran et al. defined Red Channel Prior (RCP) in DCP by differentiating the reduction in red channel [15].

Some researchers have defined other physical-prior underwater image enhancement approaches rather than DCP. The author, Nicholas et al., determines the underwater transmission by using features of channel discrepancies [16]. The author Wang et al. suggested a maximum attenuation identification model (MAI), which determines the atmospheric light and depth map by using red channel information [17]. The author, Peng et al., describe the depth estimation model with the help of light absorption and image blurriness [18]. The author Wang et al. also designed an adaptive attenuation curve, which is useful in underwater image enhancement and image dehazing [19]. One major problem with these prior-based approaches is that these prior algorithms are unacceptable for a specific environment or specific color cast. This is the reason that DCP is not applicable to white regions and objects. Due to this, we required some other mechanisms, like deep learning algorithms, for underwater image enhancement. As very little work has been done on underwater image enhancement algorithms using deep learning,

many researchers are now using these approaches and methods to achieve greater efficiency and accuracy.

1.2 Motivation

There is a different world under the ocean, and now there are many ways to explore it. In today's world, there is very high-vision technology that has attracted attention for carrying high-quality and useful information [20]. Researchers are capturing very high-quality underwater images for enormous purposes and applications like robotics, ecological monitoring, tracking of sea organisms, artifact inspections that are present under water, rescue missions, and various real-time navigation [21].

The underwater images are difficult to capture; the main constraints are light issues, capturing phenomena, dust particles, etc. An artificial mechanism that consists of an optical camera or some methods like spectral imaging, panoramic imaging, and polarization [22] is required, as under the sea, light is not as visible as it is in a normal environment. Other than optical cameras, each of these techniques has its own specific drawbacks, such as complex as well as professional operation, narrow field of view, limited depth, etc.

Underwater images get affected by poor visibility of light, which significantly fades while traveling in the water, thus impacting the result in terms of haziness and poor contrast. The visibility of light gets affected under water by the distance travelled, i.e., around twenty meters in the case of normal clean water or approximately less than or equal to five meters in the case of cloudy water. Scattering and absorption affect the travel of light in water. In scattering, the direction of the light path is changed, while in absorption, light energy is reduced.

Hence, scattering and absorption influence the overall performance of underwater imaging systems.

Scattering is basically of two types: forward scattering and backward scattering. A light deviating randomly while traveling from an object to the camera creates blurriness in the image, which is featured in forward scattering, while in the case of backward scattering, the contrast of the image is impacted. The scattering and absorption effects increase with water itself but are also affected by some other components, like small dust particles, organic particles, tiny observable floating particles, etc. The presence of all these particles will increase the effects of scattering and absorption.

As light propagates in the sea, its amount is reduced, and the color present in the light gets decreased sequentially, depending on the color wavelength. Shorter is the wavelength, higher is the range or distance it covers in sea; similarly, higher is the wavelength, shorter is the range or distance it covers in sea. We all know that, in comparison to other colors, the wavelength of blue is the shortest, so it travels longest in the sea. Hence, the impact of the blue color on objects in the sea is higher than any other color. Therefore, the images on which we are interested in working can be affected by any one of the following reasons: dull contrast, constant range visibility, blurring, haziness, non-uniform light, color diminished, bluish appearance, and various types of noise. To work on these captured images, we require some mechanism so that we can increase the quality of these images.

1.3 Problem Statements

A lot of efforts are being made to improve underwater images. The concrete objective of our thesis is to design an underwater image enhancement

model for improved underwater images with their features. Following are the problem statements and research objectives addressed in this thesis:

Problem Statement 1: To perform the systematic literature review of the models used for underwater image improvement. To achieve this, we required to explore most effective techniques used to enhance the underwater image quality.

Research Objective 1: To perform the systematic literature review of the models used in underwater image enhancement.

Problem Statement 2: For underwater image enhancement system, it does not provide robustness which not only enhances the images captures at different water level but also focuses on the different types of datasets. So, for this we require to develop a robust model for improving the quality of underwater image quality using enhancement algorithms.

Research Objective 2: To develop a robust model for improving the quality of underwater images using enhancement techniques.

Problem Statement 3: Enhancement on Deep Sea underwater images is very difficult because of the unavailability of light as well as uneven presence of artificial light. The use of deep learning-based methodology in this area is less explored. So here we are going to propose an underwater image enhancement framework to recover deep sea underwater images using deep learning approach.

Research Objective 3: To design an underwater image enhancement framework to recover deep sea images.

Problem Statement 4: Need to identify some common parameters to compare the result obtained from different algorithms. So, we do a comparative result analysis of developed models by comparing it with the other existing techniques.

Research Objective 4: To do a comparative result analysis of the developed model with the other existing techniques.

1.4 Contribution of the thesis

The primary goal of this thesis is to provide underwater image enhancement systems that will help improve the quality of underwater images while dealing with the challenges and constraints stated above. The suggested systems provide multiple strategies for color enhancement, contrast improvement, and feature value enrichment.

1. The The literature survey on underwater image enhancement systems is conducted to represent the issues and challenges of the pre-existing work as well as to determine some good-quality works in the underwater image enhancement domain. A complete, in-depth study of relevant accomplishments and developments, particularly the literature review of underwater image methods and datasets, which is a critical challenge in underwater image enhancement, has been done.

2. A robust model for increasing the quality of underwater images using enhancement techniques is developed. This technique is divided into two parts. The first part focuses on boosting contrast, while the second section focuses on improving color. Our enhanced results stand out for their brilliant color, greater contrast, and enhanced features. When compared to other approaches, this technique improves image quality by increasing peak signal-to-noise ratio (PSNR), entropy, and underwater color image quality evaluation (UCIQE) values while lowering mean square error (MSE). It is an entirely algorithm-based technique that is independent of image datasets. The images used to evaluate the results come

from a variety of datasets, and their enhanced performance confirms their robustness.

3. An underwater image enhancement framework to recover deep sea images is designed. In deep-sea underwater images, the uneven attenuation of sunlight, when it spreads underwater, has high color distortion and very low intensity. Furthermore, the amount of attenuation changes with wavelength, resulting in asymmetric color movement. As research demonstrates, this framework demonstrates that assigning the appropriate context based on the color channel traversal range may result in a significant performance speedup for the objective of underwater image enhancement.

4. A comparative result analysis of our developed models with other pre-existing techniques has been performed. The comparative result analysis illustrates how the suggested system outperforms the existing approaches. The results of the analysis, experiments, and performance assessment show that the suggested approach provides good, efficient, and improved models. As a result, this research effort delivers effective and ideal underwater image-enhancement models.

1.5 Thesis Organization

This section explains the overall structure of the thesis, which consists of six chapters, which are given below:

Chapter 1: Introduction

This chapter provides the work done by the researchers in the form of an introduction, background, motivation, problem statements (PS), and research objectives (RO). This chapter also provides a brief structure for the thesis.

Chapter 2: Literature Review

This chapter summarizes prior research work by emphasizing and discussing the research problem thoroughly using formulated research questions. Furthermore, we provided a brief overview of popular underwater image enhancement approaches. This chapter concludes by highlighting research gaps based on previous research. The following research papers have been published based on this work:

N. Singh and A. Bhat, "A systematic review of the methodologies for the processing and enhancement of the underwater images", *Multimedia Tools and Applications*, vol. 82, pp. 38371-38396, 2023. DOI: 10.1007/s11042-023-15156-9. (SCIE, IF: 3.6)

N. Singh and A. Bhat, "A Detailed Understanding of Underwater Image Enhancement using Deep Learning." *International Conference on Information Systems and Computer Networks (ISCON)*, pp. 1-6, 2021. DOI: 10.1109/ISCON52037.2021.9702312.

Chapter 3: Comparative Universal Stretching Model

This chapter includes a detailed explanation of the proposed robust model. It includes a detailed discussion of the model, techniques, datasets, and results achieved by the proposed method. The following research papers have been published based on this work:

N. Singh and A. Bhat, "A Robust Model for Improving the Quality of Underwater Images using Enhancement Techniques", *Multimedia Tools and Applications*, vol. 83, pp. 2267-2288, 2023. DOI: 10.1007/s11042-023-15617-1. (SCIE, IF: 3.6)

N. Singh and A. Bhat, “Deep Sea Underwater Image Enhancement using Convolutional Module”, *Expert System* (2023). (Accepted for Publication) (SCIE, IF: 3.3)

Chapter 4: DeepSeaNet Framework

This chapter includes a detailed explanation of the proposed deep-sea image enhancement model. It includes a detailed discussion of the model, techniques, datasets, and results achieved by the proposed method. The following research papers have been published based on this work:

N. Singh and A. Bhat, “Underwater Image Enhancement using Convolutional Block Attention Module”, *International Conference on Information Systems and Computer Networks (ISCON)*, pp. 1-5, 2023. DOI: 0.1109/ISCON57294.2023.10111974.

Chapter 5: Comparative Result Analysis

In this chapter, we do a comparative result analysis of our developed models by evaluating the performance of our suggested models by comparing them with other pre-existing techniques.

N. Singh and A. Bhat, “Comparative Result Analysis of Underwater Image Enhancement methods”, *International Conference on Computing, Communication and Networking Technologies (ICCCNT)*, pp. 1-5, 2023. DOI: 10.1109/ICCCNT56998.2023.10307108.

Chapter 6: Conclusion

The last chapter discusses the proposed research work's conclusion and future scope. It also considers the significance and importance of the stated underwater image enhancement models.

List of Publications: This section contains the publications list related to our research work that has been published/accepted/communicated in reputed journals/conferences.

References: This section contains the references used in our research.

CHAPTER 2

LITERATURE REVIEW

This chapter presents a broad overview of the terrain of traditional underwater image enhancing methods. These methods, which have been shown to greatly improve the quality of underwater images, are carefully examined, and assessed considering the findings of the research. The chapter identifies research issues that have surfaced during the process in addition to explaining the advantages made possible by these approaches. The chapter highlights areas in which further research and creativity are required to push the limits of underwater image enhancement by highlighting these barriers.

In addition, the chapter adopts a critical perspective by focusing attention to the research gaps that remain in the field of underwater image enhancement. These gaps indicate potential areas for development or places where present approaches may fall short, giving researchers a path forward to investigate and contribute to the continuous advancement of underwater imaging techniques.

This chapter lays the foundation for a deeper knowledge of the difficulties, and possible directions for future study and innovation in the field by providing an extensive summary of the status of the latest underwater image enhancement research.

2.1 Introduction

In this literature survey, it plans to thoroughly review pre-existing research work, identify research gaps, and offer a solution to them. The four phases of the literature review are shown in Figure 2.1. It begins with planning the review process and identifying the review categories. Following that, research questions are developed to examine existing underwater image enhancement methods. The category-wise literature review report is then provided, and research gaps based on the study are demonstrated. At last, the literature survey concludes with recommendations for the future scope.

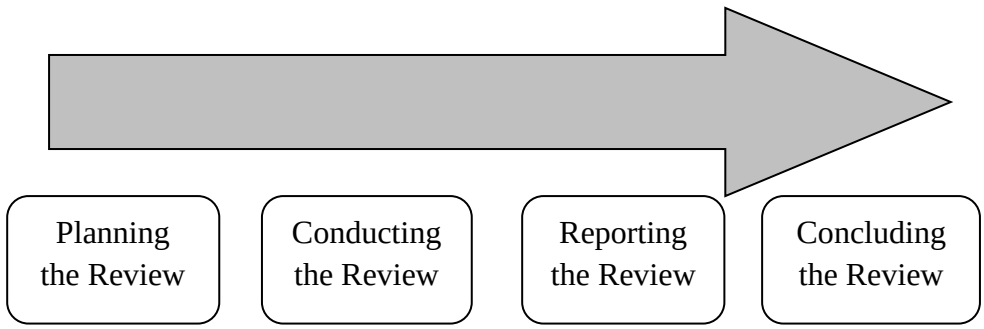

Figure 2.1 Literature Review Steps

2.2 Planning the review

This phase describes the techniques that will be used throughout the literature review process. The current study uses the fundamental literature review technique to identify published articles on the development of underwater images. As a result, we divided the method of assessment into four categories:

- The first category includes work using underwater image restoration methods.

- The second category examines the different techniques for enhancement of underwater images.
- The third category summarizes the underwater image enhancement algorithms using deep learning approaches.
- The fourth category contains the overall information of various types of datasets which have been used in underwater images improvement and the evaluation metrics which have been used to measure the underwater image quality.

2.3 Conducting the Review

In this phase, the research questions must be defined as part of the survey process. The primary goal in the research is to provide an overview of the latest studies in the underwater image enhancement techniques. As a result, we discussed here some research questions.

- **Research Question 1:** What are the most efficient models which have been used to improve the underwater images quality?

To identify the present improvement methods used in the underwater image. This benefits the researchers to explore topics based on the underwater image enhancement algorithms.

- **Research Question 2:** On what parameters we can achieve an efficient model in the underwater image enhancement?

To identify various feature and parameter on which improvement can be done.

- **Research Question 3:** Can we use the same enhancement algorithm for different applications?

To study and understand the robustness of the various pre-existing models. This benefits the researchers to differentiate the algorithms and models based on their real time applications.

- **Research Question 4:** Is there any difference in the algorithms if we enhance the images at different sea level?

To study and understand the robustness of the various pre-existing models. This benefits the researchers to differentiate the algorithms and models based on the standard datasets. As most of the models are very specific to same kind of datasets and few models are datasets independent.

- **Research Question 5:** What enhancements are required in pre-existing models?

To identify the different unique models which have been used in restoration and enhancement of underwater images.

- **Research Question 6:** Is there any change in results if we apply the same model on different datasets?

To identify and understand the behaviour of the enhancement model on different datasets. This helps the researcher understand that the underwater image improvement models will behave in a haphazard manner on different datasets.

- **Research Question 7:** Which common methods are there to compare their results analysis obtained from various approaches?

To explore and understand the methods of comparison utilized to carry out the result analysis on underwater image enhancement techniques. This helps academicians to identify the various result evaluations criteria.

2.4 Reporting the Review

In this phase, we reviewed the three vast approaches and various underwater image datasets and their evaluation criteria, as mentioned in Section 2.2. We subsequently identified the research gaps based on this literature review.

2.4.1 Underwater Image Restoration Techniques

This section contains research on underwater image restoration techniques. In detail, underwater image restoration method is classified in four main groups:

- Turbulence degradation model (TDM)
- Jaffe-McGlamery model (J-MGM)
- Point spread function model (PSFM)
- Image dehazing based model (IDBM)

2.4.1.1 Turbulence Degradation Model

Turbulence generates a non-uniform switch in the refractive index of the atmosphere; it resembles light propagation in water. Degradation model A, designed by Hufnagel and Stanley [23], is totally based on the atmospheric turbulence properties. Based on the frequency domain (u, v), it is defined by Eq. (2.1):

$$A(u, v) = \exp[- k (u^2+v^2)5/6] \quad (2.1)$$

Here, k represents the magnitude of turbulence. The underwater image restoration is realized by merging the degradation model with the evaluation function. Yang and Gong [24] also designed an underwater image restoration technique based on turbulence, where the weighted contrast average grads (WCAG) are applied in determining the standard of underwater images.

2.4.1.2 Jaffe-McGlamery Model

This method of underwater image restoration [25–26] is one of the most widely used models, in which the light (ET) coming from the camera is divided into the following divisions: (i) reflected light from an object (Ed), (ii) light that is emulated from a target known as forward scattered light (Ef), and (iii) non-target reflected light known as back scattered light (Eb), given in Eq. (2.2).

$$E_T = E_d + E_f + E_b \tag{2.2}$$

Based on the simplified model by Jaffe McGlamery, Trucco and Olmos [27] designed a self-calibrated filter. This filter is based on two presumptions: (i) lighting (direct sunlight) underwater is consistent, and (ii) forward scattering is an important component, whereas other components like direct components and backscattering were neglected.

Few researchers not only paid attention to backscattering in the Jaffe McGlamery model but also used the Dark Channel Prior (DCP). In this method, it was presumed that backscattering did not affect a high-contrast region in an image. The parameters of this model were evaluated based on this presumption.

2.4.1.3 Point Spread Function Model

The imaging process in seawater with the help of a linear system was introduced by Hou et al. [28–30]. They also introduced the optical properties of water under the standard underwater image restoration system. Various parameters like attenuation, volume scattering function, absorption, and particle distribution were measured with some specific instruments. Grosso [31], Voss [32], and Chapin [33] also used some specific instruments to measure the PSFM. However, the instruments were too complicated and expensive.

2.4.1.4 Image Dehazing Based Model

This model is divided into two parts: (i) a classical DCP-based underwater image restoration model and (ii) a learning DCP-based underwater image restoration model. Table 2.1 represents these methods, where in model column R, R is restoration, C is color correction, ML is machine learning, and DL is deep learning. In the Hypothesis priori column, DCP is dark channel prior, DBGR is the difference between blue green and red channels, UDCP is underwater dark channel prior, RDCP is red dark channel prior, and CDCP is color-corrected images in dark channel prior. In the background light column, GB is the global background light estimation and LB is the local background light estimation. In the transmission map (TM) estimation column, DEP is depth, AP is attenuation prior, FDC is from the dark channel, RET is Retinex, BM is blurring map, and MIL is minimum information loss.

Table 2.1. DCP based underwater image restoration models.

S.No.	Model	Hypothesis Prior	Color Correction	TM Estimation
1	R	DBGR	N	FDC
2	R	DCP	N	FDC
3	R	DCP	N	DEP+AP
4	R	UDCP	N	FDC
5	R	RDCP	N	FDC
6	R+C	DCP	Y	BM
7	R	UDCP	N	FDC
8	R+C	DCP	Y	DEP
9	R+C+ML	DCP	Y	DEP
10	R+C	DCP	Y	MIL+FDC
11	R	DCP	Y	FDC
12	R+C	DCP	Y	DEP+AP
13	R+C+ML	CDCP	Y	ML+AP
14	R+C+DL	DCP	Y	DL+DEP
15	R+C	CDCP	Y	FDC
16	R+C	CDCP	Y	FDC
17	R+ML	DCP	N	DEP+AP
18	R+ML	DCP	N	DEP+AP
19	R+C	UDCP	Y	FDC
20	R+C+DL	DCP	Y	DL+DEP
21	R+C	DCP	Y	RET+AP

In previous years, the DCP-based underwater image restoration model has gained attention. In it, there is a presumption that red debilitation is agile as compared to other attenuation colors, which is true in the case of open water and is used for calculating dark channel images in both DCP-based restoration models.

Carlevaris et al. [16] initially computed the highest variation in red and blue-green channels. Thereafter, the transmission map is evaluated by setting the maximum variation until it becomes one. Whatever the least value of the transmission map, it is considered background light. Now, the posterior probability is maximized, and the final image is evaluated. The transmission map is further studied by Chiang and Chen [34] in terms of the ratio of residual energy of the input image to the camera after reflection. The average brightness difference between foreground and background is compared to estimate an artificial light source. The red channel was taken underwater prior to Galdran et al. [35]. Here, using the highest value of the red channel, the background light was computed. The red channel was considered the fast-attenuated channel by P. Drews, Jr., et al. [14], because of which no information related to field depth was provided. As a result, a novel approach with an underwater dark channel (UDCP) was presented. This dark channel image was created by calculating the lowest difference between the green and blue channels, and the background light was calculated using the highest value obtained from the dark channel image.

When light is absorbed through water, it causes scattered color projection, which generally causes dark channels prior to failing to identify the transmission map more precisely. Furthermore, an underwater scenario is generally defined by limited or inappropriate light. There will be no change in the dark scene area even after imaging. In some previous work, fuzzy image and field depth were used to enhance the transmission map estimation [36–38], and color correction was

added to adjust the uneven projection caused by absorption [39–42]. Ancuti et al. [43] used the local highest value of dark channels for evaluating background light.

Background's light, whether global or local, is also defined as a flat area [44–45], also known as a blurry region [42]. To compute the blurry area in an underwater image or to identify the background light, Emberton et al. [46] designed a hierarchical model. While the color of the underwater target was near-blurred, this model became unreliable. Emberton et al. [42] again dissolved the underwater image into (i) greenish, (ii) bluish, and (iii) blue greenish, based on the hierarchy technique. Before the DCP-based restoration, different white balance procedures were used for each part. Whereas, if the theoretical highest merit of background light was applied as a denominator for evaluating the transmission map, then this resulted in an oversaturation phenomenon leading to the appearance of artifacts in the background area [47].

In existing approaches, the maximum amount of learning used in DCP-based restoration models is based on supervised scenarios [45]. In some of the approaches, unsupervised methods were used. With respect to the statistical distribution of color images, authors [19, 41] combined the colors present in original images into 500 types. Every pixel present in the color image was presented with a cluster center. In clustering space, a color pixel shows a line segment based on distance with respect to the camera. Using the k-dimensional (KD) tree, an attenuation curve is created by clustering with the logarithmic of the RGB value. The background light was examined after determining the pixel value with the most significant change across RGB channels in the underwater image. To correct the transmission map simultaneously, the saturation constraint is applied; still, the restored image remains oversaturated and dark.

2.4.2 Underwater Image Enhancement Techniques

This section contains research on underwater image enhancement techniques. In this method, information related to the image is extracted even in the absence of prior knowledge of the surroundings. For this reason, these techniques are more generalized in comparison to restoration techniques.

In underwater image processing and analysis, many underwater enhancements are combined, which are taken from methods directly applied to natural images [48–50]. Here we are discussing the most important aspects of underwater image enhancement techniques, in which they focus on contrast stretching, merged improvement, multi-information, and noise removal.

All these methods have been listed in Table 2.2. In detail, underwater image enhancement method is classified in three main groups:

- Filter Based Technique
- Color Correction Based Technique
- Image Fusion Based Technique

Table 2.2. Underwater image enhancement techniques

S. No.	Technique	Quality	Fusion
1	ACE	None	N
2	Gaussian filter, Contrast Stretch	None	N
3	MRF	None	N
4	Homomorphic filtering, Wavelet Transform, Anisotropic filtering, Contrast Stretch	Distribution of gradient histogram	N
5	Integrated color model	None	N
6	Quaternion's rotation	None	N
7	Morphological filter	None	N
8	White Balance, Bilateral Filter, Histogram equalization	None	Y
9	NSCT, ATV	PSNR and Sharpness	N
10	Rayleigh stretching	None	N
11	Rayleigh stretching	None	N
12	Retinex, color correct	None	N
13	Gray World, Gamma Correction, High Pass Filter	PCQI	Y
14	Wavelet	SSIM, PSNR, Entropy	N
15	Retinex	MSE, UIQM, UCIQE	Y

2.4.2.1 Filter Based Technique

Arnold-Bos et al. [51] designed a pre-processing model for luminance components in the underwater image. This model identified a specific noise range in the underwater image by combining enhancement and deconvolution methods. The Log Gabor wavelet is used for denoising, decreasing various quantization errors, and suspending particle noise. This system increases the effect of edge detection.

A model designed by Bazeille [52] contains various filtering steps that enhance the quality of non-uniform illumination, increase contrast, decrease noise, and update the color of an underwater image. To minimize the noise in the underwater image, a non-subsampled contourlet transform (NSCT) that depends on adaptive total variation was designed by Jia and Ge [53].

A partial differential equation (PDE) was also used by the authors to reduce noise in an image and construct frequency components. The amount of improvement in underwater images was examined through the sharpness and peak signal-to-noise ratio (PSNR).

2.4.2.2 Color Correction Based Technique

A model was proposed by Chambah et al. [54] in which automatic color equalization (ACE) was applied on each channel of RGB individually and adjusted the outputs of all three channels to increase the efficiency of identifying the object from the image. The ACE algorithm's various parameters were adjusted internally. A model based on the Rayleigh distribution that contains a sequence of color correction schemes was designed by Ghani and Isa [55–56]. An underwater image was taken by Torres-Méndez and Dudek [57], which was treated like a Markov random field (MRF), and in it, nodes evident in random fields indicated

the poor quality of color values, while those that were not visible indicated the true color values in the underwater image. It explained the relationship between the pixels and their neighbourhood by training the true color of the sample pixels. Iqbal et al. [58] suggested an underwater image enhancement algorithm for the marine environment using the integrated color model. In this model, an RGB color space is used, and it depends on the sequence of sliding stretching, like contrast stretching, whereas in an HSI color space, it depends on brightness and saturation stretching. An underwater image color enhancement algorithm, designed by Petit et al. [59], was based on optical attenuation inversion.

The variational Retinex model was designed by Fu et al. [60] and was based on Retinex theory. Herein, using the linear domain variational Retinex, the spatial luminance parameter of a color-corrected underwater image was disintegrated through 4-6 iterations. In this, triangular and bilateral filters were used on a, b, and L components in place of the Gaussian filter, and then they were combined based on the ratio of values present in the RGB space.

2.4.2.3 Image Fusion Based Technique

There are many methods and models based on observation, which plays a significant part in improvement. Gradually, the fusion procedure was also considered under image enhancement. A fusion-based underwater image enhancement model was designed by Ancuti et al. [6]. Here, white balance color improvement and the output of bilateral filtering were weighted using the outcome of histogram equalization. To get a pixel-level fusion output, four types of fusion weights—Gaussian, local, sensitometry, and saliency contrast—were calculated. However, under the consideration that fast attenuation was of the red channel, they increased the white balance processing in [61].

2.4.3 Underwater Image Enhancement using Deep Learning Techniques

Based on deep learning, underwater image enhancement has challenges like labelling images, difficulty collecting them practically, etc. Some of the approaches are discussed in Table 2.3, wherein training image column N stands for normal images and U stands for underwater images.

A collection of color-corrected underwater images [62] has been used as a training data set in [63], in which, based on a convolutional neural network (CNN), an underwater image enhancement technique is constructed. In this model, 55 elements are used, following which a three-D enhanced underwater image is achieved. In [64], the Water GAN network was designed for underwater image color alteration enhancement, which is used to simulate the attenuation caused by the water body. This is like the Generative Adversarial Networks (GAN) [65], where two training sets were taken into consideration, one containing normal images and their relative depth maps in air and another one containing underwater images that are taken from simulated underwater and laboratory images referred to by the Jaffe-McGlamery model.

Motivated by the cycle-consistent adversarial network (Cycle GAN) [66], a weakly supervised color migration model was suggested by Lie et al. [67] to provide accuracy in color deformation in deep-sea underwater images. Herein, between the underwater and normal images, forward and backward mapping and adversarial discriminators were incorporated. Several distortion functions, like adversarial losses (Loss GAN), structural similarity (Loss SSIM), and periodic continuity (Loss Cyc), were used in the forward mapping and backward mapping generators. All the useful information in the underwater images was the same, while the color was improved. There are some other types of GAN that have been used by various authors [68–69]. These types of GAN enhance the contrast, color,

and de-haziness of real-world underwater images. Details of these types of GAN are given in Table 2.3.

2.4.4 Underwater Image Dataset and Evaluation

This section presents research work related to the various datasets and evaluation of the underwater image quality. This section is classified in two groups:

- Underwater Image Dataset
- Evaluation of underwater image quality

2.4.4.1 Underwater Image Dataset

The underwater image dataset is very useful in the evolution of underwater image processing techniques. Here, various underwater image datasets that have been used by several authors for restoration and enhancement purposes have been summarized in Table 2.4.

2.4.4.2 Evaluation of Underwater Image Quality

There are some parameters, such as image restoration, image enhancement, image classification, image retrieval, image transmission, and optimization, in optical image systems where the measurement of image quality plays an important part. Two main methods, i.e., subjective image quality evaluation and objective image quality evaluation, are used for evaluating the quality of images. The classification of objective image quality evaluation is independent of the reference image. If a reference image for any underwater image is not found, then to obtain the image quality, we need a no-reference image metric.

Table 2.3. Deep learning-based models

S. No.	Model	Source of training sets	Training Images	Effects
1	CNN	Corrected Underwater Images	Not mentioned	Color Correction
2	GAN	Tank and simulated underwater images	5348N+7000U	Color Correction
3	Cycle GAN	Online underwater images	3800N+3800U	Color Correction
4	Fusion-GAN	Real Underwater Images	6128U	Color Correction
5	Unsupervised-GAN	Synthetic Underwater Images	3733U	Color Correction
6	FUnIE-GAN	Paired and Unpaired Underwater Images	20000U	Color & Contrast Correction
7	Spiral GAN	Real World Underwater Images	4757U + 4129U + 726U	Color & Contrast Correction

Table 2.4: Underwater Image datasets

S.No.	Dataset	No. of Images		Total Images	Resolution
		Paired	**Unpaired**		
1	Underwater 45 **(U-45)**	-	45	**45**	256*256
2	Enhancing Underwater Visual Perception Dataset **(EUVP)**	11950	6665	**18615**	320*240
3	Underwater Image Enhancement Benchmark Dataset **(UIEB)**	890	60	**950**	Varied
4	Large Scale Underwater Image Dataset **(LSUI)**	4279	-	**4279**	Varied
5	**UFO-120**	1620	-	**1620**	640*480
6	Real-world Underwater Image Enhancement Dataset **(RUIE)**	300	3630	**3930**	320*240
7	Detecting Underwater Object Dataset **(DUO)**	-	7782	**7782**	Varied
8	Underwater Multiple Object Tracking Dataset **(U-MOT)**	-	514	**514**	1920*1020

We can use several quantitative metrics to assess the restoration and enhancement performance of different types of underwater images. These are (i) global contrast dealing with grayscale underwater image quality; (ii) weighted grayscale angle (WGSA) metrics to evaluate the improvement of the restored image; and (iii) robustness index to identify the proximity of grayscale histograms to their exponential distribution. Some papers define a method to measure the robustness of underwater image noise removal.

In color-based underwater images, two important no-reference evaluation metrics were used. One is the underwater image quality measure (UIQM), in which the following three methods were combined to measure the quality of underwater images: (i) underwater image sharpness measure UISM; (ii) underwater image contrast measure UIConM; and (iii) underwater image colorfulness measure UICM.

The other reference metric is the underwater color image quality evaluation (UCIQE) metric, which is broadly used to estimate the quantity of non-uniform color cast, enhance the quality of the image, and quantify the blur and noise in the underwater image.

In subjective evaluation, some techniques are defined to evaluate the quality of natural images, similar to patch-based contrast quality index (PCQI), mean square error (MSE), global contrast factor (GCF), structural similarity index measure (SSIM), average execution, peak signal to noise ratio (PSNR), entropy, a contrast to noise ratio (CNR), visibility metrics based on CNR (VM-CNNR), discrete entropy and contrast measure (DECM), and gradient ration in visible edge (GAVE).

The overall deterioration dominates all underwater images, including non-uniform light, non-uniform color casts, chroma reduction, poor contrast, blurring, and noise from numerous parameters. Because of the various distortions

present in underwater images, it is difficult to develop a standard image quality metric that can be applied to all kinds of underwater conditions. Using the existing underwater image quality criteria, an incorrect value was given for an underwater image containing dark areas, oversaturation, and non-uniform brightness.

2.4.5 Research Gaps Identification

From the literature survey, few research gaps which have been identified are as follows:

1. Required to explore the most effective techniques used to enhance the quality of underwater images.

2. It has been observed that, most of the previous research is focused only on restoration rather than enhancement methods.

3. Robust image enhancement system is not available which enhances the images captures at different water level.

4. Previous models works on only specific objectives which are mainly focused on the specific datasets.

5. The use of Deep learning-based methodology in this area is less explored.

6. Enhancement on Deep Sea underwater images is very difficult because of the unavailability of light as well as uneven presence of artificial light.

7. Need to identify some common parameters to compare the result obtained from different algorithms.

2.5 Concluding the Review

The literature review has uncovered several challenges in the field of underwater image enhancement, mainly related to the use of deep learning techniques, the resilience of current systems, and traditional enhancement methods. Seeing these challenges, a distinct gap of opportunity comes up for a development of a powerful underwater image enhancement model that solves the problems and improves image quality more effectively and robustly.

Conventional enhancement techniques, although somewhat successful, might not be able to handle the complexities of underwater images. Despite their potential, deep learning techniques may encounter difficulties in reaching peak performance because of the difficulties presented by underwater environments. Moreover, the current technologies may not be as strong as needed to manage changing underwater circumstances, which would reduce their overall efficacy.

Underwater image enhancement is an area that might experience significant changes, and this research opportunity provides a cutting-edge opportunity to contribute to the development of technology and approaches in this field.

CHAPTER 3

COMPARATIVE UNIVERSAL STRETCHING MODEL

The suggested robust model for enhancing underwater images is thoroughly explored in this chapter. It starts with an introduction that places the model's importance and usefulness in the larger context of underwater imaging. After that, the chapter reviews relevant literature, providing insights into current frameworks and approaches that contributed to the development of the proposed model.

A significant section of the chapter is providing the detailed explanation of the robustness of the model. It includes the fundamental and the structural part of the model. This method is analysed and validated on the eight different datasets for their efficiency. This validation shows that we can rely on the improved underwater images.

This chapter shows that the CUS model is a single image based, datasets independent model. It shows that the model is more flexible and adaptable, enable the model to work well on various datasets.

3.1 Introduction

Underwater image enhancement is a main research area that is now being addressed across the world. The primary reason for this is that water scatters and absorbs light, providing images with extremely low contrast and color cast. Hence, to conquer this problem with underwater images, we designed a simple and effective Comparative Universal Stretching (CUS) method. This method is split into two parts.

The first section focuses on boosting contrast, while the second focuses on improving color. To begin with, under the RGB color model, contrast enhancement equalizes the G and B channels. Each R, G, and B channel's histogram is then redistributed using effective parameters connected with the intensity distribution in the input image and the wavelength attenuation of various colors underwater. The noise is subsequently reduced using a bilateral filtering technique, which not only keeps important facts in an underwater image but also increases local information. In the second section, the color is enhanced by increasing the L element and adjusting the 'a' and 'b' elements of the CIE lab color space.

The experiment findings show that the suggested techniques outperform alternative strategies. Our enhanced results stand out for their brilliant color, greater contrast, and enhanced features. When compared to other approaches, the values of peak signal-to-noise ratio (PSNR), entropy, mean square error (MSE), underwater color image quality evaluation (UCIQE), and underwater image quality measures are 7.88, 920.20, 18.92, 0.596, and 2.734, respectively. This technique improves image quality by increasing entropy, PSNR, and UCIQE values while lowering MSE.

It is an entirely algorithm-based technique that is independent of image datasets. The images used to evaluate the results come from a variety of datasets, and their enhanced performance confirms their robustness. Because of its single image-based approach, our method is very compelling in terms of processing speed. Comprehensive findings on different underwater image datasets show that our approach performs well on most of them. For these reasons, the comparative universal stretching approach is better than others.

3.2 Related Work

This section mainly consists of the pre-requisites of the proposed comparative universal stretching (CUS) model. In this section, the basic underwater model approach and histogram stretching approach have been discussed, and how we are using their equations in our proposed work has been explained.

3.2.1 Underwater Model

Various well-defined image hazing models [70-71] are generally used to identify the transmission equation of the scattered background light in an underwater scene. The equation is given below:

$$I_\lambda(x) = J_\lambda(x)t_\lambda(x) + (1 - t_\lambda(x))B_\lambda \quad (3.1)$$

Where λ is the light wavelength that belongs to red, green, and blue. x is the underwater image $I_\lambda(x)$ pixel point. $J_\lambda(x)$ denotes the light at sight location x. $t_\lambda(x)$ denotes the residual energy ratio (RER). RER is the ratio of reflection in underwater from location x to back to camera. Uniform background light is

represented by B_λ . $J_\lambda(x)t_\lambda(x)$ represents the straight attenuation of scene radiant $J_\lambda(x)$ in underwater [72]. The RER $t_\lambda(x)$ is depends upon the λ as well as the site camera distance $d(x)$, which shows the complete impact of color change which has been suffered by the wavelength of light in underwater distance $d(x)$, and light scattering. Therefore $t_\lambda(x)$ can be defined as:

$$t_\lambda(x) = \text{NRER } (\lambda)^{d(x)} \tag{3.2}$$

where NRER is normalized RER, which defines the proportion of residual energy ratio to original energy for a minimum single unit of distance transmitted. As we know, the green & blue light have a higher frequency because of their shorter wavelengths, and therefore they attenuate extremely lower as a comparison to the red light. For this reason, as we move deep inside the sea, the images appear as blue toned images. The values of the light wavelength of NRER (λ) are defined as follows:

$$\text{NRER } (\lambda) = \begin{cases} 0.83\sim0.90 & \text{if } \lambda = 590\sim750 \text{ µm (Red)} \\ 0.90\sim0.95 & \text{if } \lambda = 490\sim590 \text{ µm (Green)} \\ 0.95\sim0.99 & \text{if } \lambda = 400\sim490 \text{ µm (Blue)} \end{cases} \tag{3.3}$$

We are using these values to predict the range of RGB channels in the CUS model.

3.2.2 Histogram Stretching

The underwater images have poor visibility as well as contrast because of the very low range of histograms and relatively concentrated distribution. To overcome this problem, we use histogram stretching, which gives us a fair distribution of pixels in the image channels across the dynamic range. This

increases the visibility and contrast in the underwater image. The contrast stretching function is given in equation (3.4) [73–74].

$$p_0 = (p_i - a) + \frac{c-d}{b-a} + d \tag{3.4}$$

where p_i is the intensity value of the input pixel, p_o is the intensity value of the output pixel. The min & max intensity values of the actual image and the desired output image is represented by a, b & c, d, respectively. c & d are constant in a global stretching and are frequently fixed to 255 & 0 respectively; a & b are chosen at 0.2 % & 99.8 % in the original image's entire histogram.

3.3 Proposed Work

Generally, our suggested model is consisting of three basic steps: contrast improvement, color improvement, and quality evaluation as shown in Figure 3.1.

In contrast improvement, first we are doing RGB channel decomposition. After that, we perform color equalization on the green and blue channels. Then we determine the adaptive stretching range. After that, we perform comparative universal stretching on the image. Finally, while keeping the information about the needed colorful underwater image, we use a bilateral filter to eliminate the noise created by the aforesaid transformation [72]. This will not only diminish the color cast result because of the light absorption and scattering, but also reduce the effect of the low contrast. Once we performed all the steps in contrast improvement, we got the resultant image. After that, we performed color improvement on the resultant image [75]. In color improvement, first we change the image into a CIELAB color model. We extend the parameters of the image using basic global histogram stretching and correct the parameters in the CIE Lab

color model. The adaptive stretching improves the image's brightness and saturation, resulting in a more vibrant color. After performing contrast improvement and color improvement, to estimate the quality of our designed model, we use a few quality evaluation parameters. Now we are going to elaborate in detail on contrast improvement and color improvement.

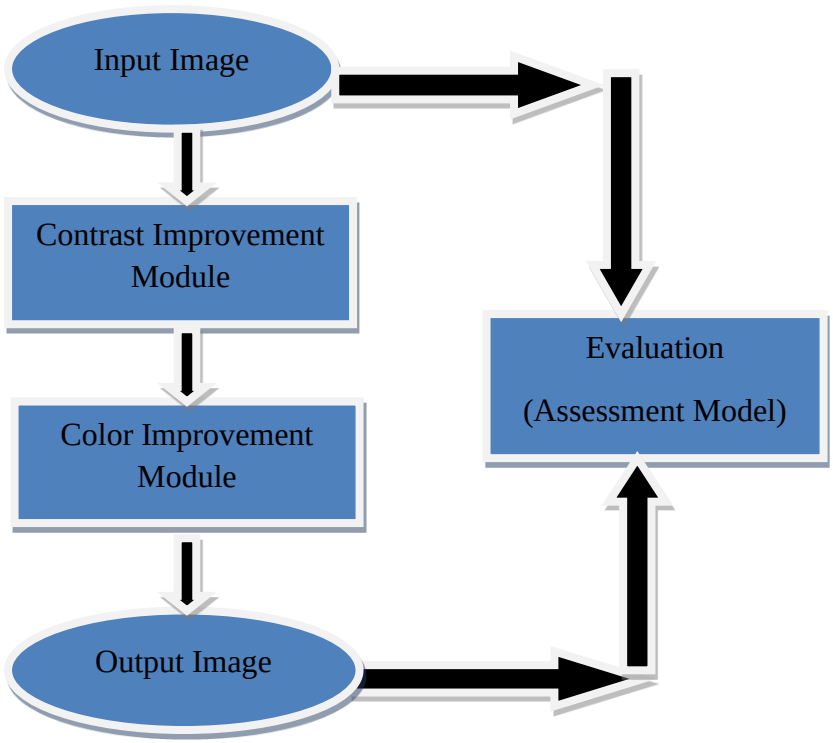

Figure 3.1. Comparative Universal Stretching (CUS) Model

3.3.1 Contrast Improvement

Figure 3.2 presents the sequence used in contrast improvement, which consists of five main phases. These are (i) RGB Channel Decomposition, (ii) Color Equalization on GB Channel, (iii) Determining Adaptive Stretching Range, (iv) Comparative Universal Stretching, (v) Bilateral filter on the RGB Channels.

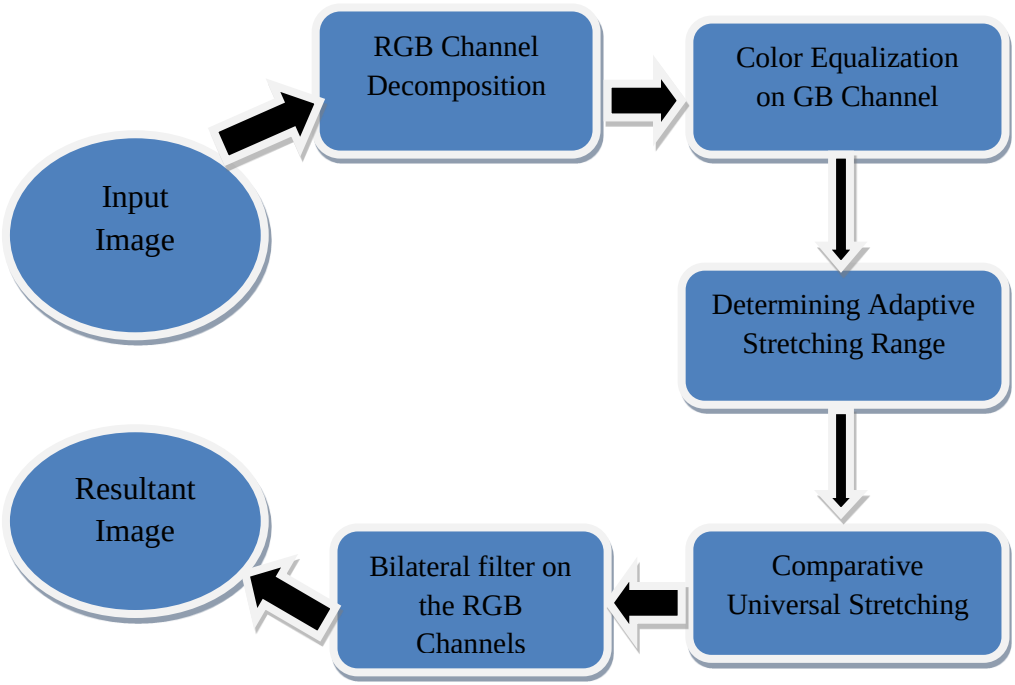

Figure 3.2. Sequence used in contrast improvement.

3.3.1.1 Color Equalization on GB Channel

Images are rarely color-balanced appropriately when taken underwater. We begin color equalization for the underwater image after RGB channel decomposition. According to the Von Kries hypothesis [76], Iqbal et al. (2010) modified color values in RGB elements, keeping the leading color cast channel constant. As per the unsupervised color correction model (UCM), if one channel's average is very low, the channel must increase with a larger multiplier, resulting in incorrect image color processing. As motivated by the Gray World Assumption Theory (GWAT) [16], in a perfect image, the mean value of any color object is always gray. Hence, we improve the green as well as the blue channels with the help of the following assumptions:

$$(R_{avg} + G_{avg} + B_{avg})/3 = 0.5 \quad (3.5)$$

where R_{avg}, G_{avg} and B_{avg} are the normalized mean values of the recovered RGB channels.

$$G_{avg} = \frac{1}{255 * MN}\sum_{i=1}^{M}\sum_{j=1}^{N} I_g(i,j), \theta_g = \frac{0.5}{G_{avg}}$$

$$B_{avg} = \frac{1}{255*MN}\sum_{i=1}^{M}\sum_{j=1}^{N} I_b(i,j), \theta_b = \frac{0.5}{B_{avg}} \quad (3.6)$$

Pixel values can vary between 0 and 256. Every value denotes a color code. The calculation of these large numerical values may get more difficult when processing the image as it is, i.e., by taking the simple mean value. It can be minimized by normalizing the numbers to the range between 0 and 1. As a result, the numbers would be minimal, and the calculation would be easy as well as quicker. Pixel values vary between 0 and 256; apart from 0, the range is 255. Hence, dividing all the numbers by 255 (i.e., the standard deviation) will convert them to a range of 0 to 1. That is the reason for taking the normalized mean value instead of the simple mean value in equation (3.6).

With the help of GWAT, we improve the G & B channel. The R channel is not taken into attention here since the red light in water is difficult to correct with basic color equalization. If we consider the red light, then it brings red over saturation. The above equation is defined for computing G & B channels color equalization coefficient i.e., θ_g & θ_b, respectively. The underwater image size is given by M * N. Depends upon the color equalization coefficients θ_g & θ_b, the intensity of the G channel and B channel is modified by changing θ_g and θ_b respectively. After this, we now must perform comparative universal stretching for image channels.

3.3.1.2 Comparative Universal Stretching (CUS) Model

The overall histogram stretching method typically employs equal values for each channel of an image, neglecting the histogram allocation features of individual channels and images. If predefined values, for example, have been used in (3.4), some color channels are either over or under stretched, causing destruction to the input image's features. Due to the transmission principle of light underwater, to repair the distorted images, we must use the contrast improvement approach. According to the following study of underwater images, the RGB channel's histogram distribution requirements are as follows: The histogram of red light in most underwater images is in the band [50, 150], whereas in the G & B channel, values are in [70, 210]. Due to this, the histogram stretching is sensitive to channels. We rewrite the comparative universal stretching in equation (3.7) to distinguish it from global histogram stretching in equation (3.4).

$$p_{out} = \left(p_{in} - I_{min}\right)\left(\frac{O_{max} - O_{min}}{I_{max} - I_{min}}\right) + O_{min} \tag{3.7}$$

where $p_{in}$is the input pixel, p_{out} is the output pixel. I_{min} and I_{max} are the adaptive parameters before the stretching images. O_{min} and O_{max} are the adaptive parameters after the stretching images. After this, we'll go through how to calculate the stretching range (I_{min}, I_{max}) and the desired range (O_{min}, O_{max}).

3.3.1.3 Determining Adaptive Stretching Range

If we consider the histogram distribution of different underwater images, it is seen that the histogram distribution in the RGB channel is comparable to a variant of the Rayleigh distribution described as (3.8), and that is an ongoing probability proportion for positive-valued random variables.

$$Rayleigh\ Distribution = \frac{x}{a^2} e^{-x^2/2a^2},\ x \geq 0,\ a > 0 \quad (3.8)$$

In equation (3.8), the distribution's scaling parameter a is the mode, which is the highest in the R, G & B channel histogram. It is worth noting that, when a channel's allocation follows a regular pattern, its midpoint and mode are almost identical. In the histogram stretching, we use the mode result as a borderline to determine the minimum intensity level on the left and the maximum intensity level on the right of the original input image.

Because underwater images are impacted by a variety of causes, stretching ranges between 0.1 % and 99.9 % of the histogram are commonly used to decrease the impact of certain high pixels in comparative universal stretching. If the histogram is not regularly distributed, the procedure of removing the same quantity of pixels from both ends of the histogram is not appropriate. To compute the I_{min} and I_{max} for each RGB channel, we partition the top and bottom portions of the intensity values, as shown in equation (3.9).

$$I_{min} = G.sort\ [\ G.sort.index(a) * 0.1\%\ ]$$

$$I_{max} = G.sort[\ -(\ G.length - \ G.sort.index(a)) * 0.1\%\ ] \quad (3.9)$$

where G is the group of image pixel values for each R, G & B channel, $G.sort$ is the increasing sorted data set, $G.sort.index(a)$ is the index number of the mode in the histogram distribution, and $G.sort[x]$ is the value at index x of the positive sorted data set. To implement the unique approach, we extract pixels values in the lowest 0.1 % of the left side and the largest 0.1 % of the right side from histogram distribution using Equation (3.9). The RGB channels and different images of the Rayleigh distribution, the I_{min} and I_{max} are both channel and image sensitive.

Global histogram stretching of [0, 255] range typically produces excessive blue and green light in underwater images. We dynamically decide the highest (O_{max}) and lowest (O_{min}) intensity level values by each RGB channel to obtain a perfect intended band of stretching.

We begin by calculating the Rayleigh distribution's standard deviation values σ_λ, as shown in equation (3.10).

$$\sigma_\lambda = \sqrt{\frac{4-\pi}{2}}\, a_\lambda = 0.655 a_\lambda \ , \ \lambda \in \{ \mathrm{R}, \mathrm{G}, \mathrm{B} \} \tag{3.10}$$

Where a denotes the channel mode, λ belongs to RGB Channels. After that, we establish the required range's minimum value $O_{\lambda\,\min}$, as shown in equation (3.11)

$$O_{\lambda\,\min} = a_\lambda - \beta_\lambda * \sigma_\lambda \ , \ 0 \leq O_{\lambda\,\min} \leq I_{\lambda\,\min} \tag{3.11}$$

Here β_λ is derived from equation (3.11) and substitute σ_λ from equation (3.10)

$$\beta_\lambda = \frac{a_\lambda - O_{\lambda\,\min}}{\sigma_\lambda} \ , \ \frac{a_\lambda - I_{\min}}{\sigma_\lambda} \leq \beta_\lambda \leq \frac{a_\lambda}{\sigma_\lambda} \tag{3.12}$$

In the right side of equation (3.12), we get $\beta_\lambda \geq 0$, as $a \geq I_{min}$.

Now, substitute the value of σ_λ in the right side in equation (3.12), we obtain $\beta_\lambda \leq 1.526$.

Now describe $\beta_\lambda \in Z$, it must have a unique solution that is $\beta_\lambda = 1$. Hence equation (3.11) is rewritten in the form of equation (13) as shown below:

$$O_{\lambda\,\min} = a_\lambda - \sigma_\lambda \tag{3.13}$$

Because of the varying degrees of depletion of the various bands of light in underwater, we should study individual R, G, B channel to compute optimum parameters of the required range. Based on the simple fuzzy image method (3.1), the image dehazing function $J_\lambda(x)$ is improved as given in equation (3.14).

$$J_\lambda(x) = \frac{I_\lambda(x) - (1 - t_\lambda(x))B_\lambda}{k\, t_\lambda(x)} \tag{3.14}$$

Where the red and the green-blue channel have experienced values of 1.1 and 0.9, respectively. When maximizing the recovered image $J_\lambda(x)$, as shown in equation (15), the maximum value of the required range O*max* is obtained.

$$Max\,(J_\lambda(x)) = Max\left(\frac{I_\lambda(x) - (1 - t_\lambda(x))B_\lambda}{k\, t_\lambda(x)}\right) \tag{3.15}$$

B_λ is 0, when $J_\lambda(x)$ reaches its maximum value. Then, for each color channel O*max* is defined as shown in equation (3.16).

$$O_{\lambda\,\max} = \frac{I_\lambda}{k\, t_\lambda} = \frac{a_\lambda + \mu_\lambda * \sigma_\lambda}{k * t_\lambda}\ ,\ I_{\lambda\,\max} \leq O_{\lambda\,\max} \leq 255 \tag{3.16}$$

$t_\lambda(x)$ is calculated with the help of equation (3.2), where $NRER$ (λ) values are 0.83, 0.95 and 0.97 for the RGB channels, respectively (also look at equation (3.3)). Due the estimated path between the camera and the site, $d(x)$ is fixed to 3. I_λ values always lie on the right side of the mode in channels histogram, and therefore it is represented in the form of $a_\lambda + \mu_\lambda * \sigma_\lambda$.

The coefficient μ_λ fulfils the inequality as shown in equation (3.17), depending on the overall range value of $O_{\lambda\,\max}$.

$$\mu_\lambda = \frac{(O_{\lambda\,\max} * k * t_\lambda) - a_\lambda}{\sigma_\lambda}$$

$$\frac{k * t_\lambda * I_\lambda}{\sigma_\lambda} \leq \mu_\lambda + 1.526 \leq \frac{k * t_\lambda * 255}{\sigma_\lambda} \quad (3.17)$$

In equation (3.17), in the integer field μ_λ has either no solution or specific solutions. We take the mean of all solutions when μ_λ are many solutions. When there are no solutions of μ_λ, $O_{\lambda\,\max}$ is set to 255. These adaptive parameters, which are derived from the histogram distributions from several channels, may substantially enhance the contrast of stretched images while also reducing noise and preserving features.

3.3.2 Color Improvement

Figure 3.3 shows the sequence used in color improvement, which consists of three important phases. These are (i) Conversion from RGB to CIE lab, (ii) Adaptive Stretching in CIE lab, (iii) Conversion from CIE lab to RGB.

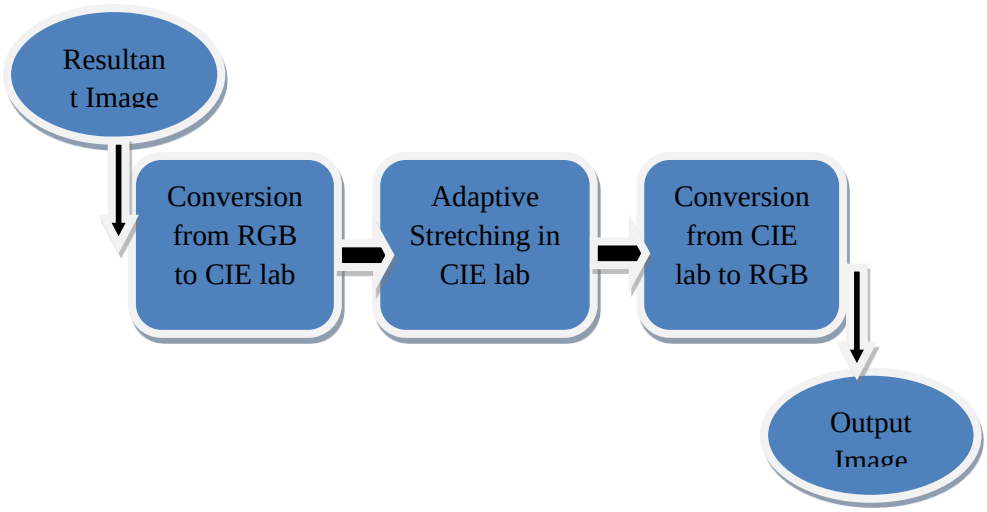

Figure 3.3 Sequence used in color improvement.

3.3.2.1 CIELAB Color Model

The human eye can see large numbers of colors. However, it does not always differentiate between colors properly. Based on our viewing position and illumination, we may see two slightly different colors as the same or detect distinctions in things of equal color. These create challenges when we try to enhance the color component. To enhance the color of underwater images every time, we require strategies to define a color's qualities and identify the quantitative difference between shades. CIELAB, generally CIE L*a*b*, is a three-dimensional color space that is device-independent and enables the exact analysis and measurement of all observable colors via three color variables. In this color space, numerical changes between values generally correlate to the degree of difference in colors that humans perceive.

Each of the three variables used by the CIELAB color space to measure objective color and calculate color differences is given by L*, a*, and b*. L* signifies brightness within a range of 0 to 100. Whereas a* & b* signify chromaticity without numerical boundaries. (–ve) a* represents green, (+ve) a* represents red, (-ve) b* represents blue, and (+ve) b* represents yellow. The CIELAB color space plots a color's location in a chart that comprises an unlimited range of different colors, including colors outside the visible spectrum, by measurements of its L*, a*, and b* values. We may utilize formulas to quantify the difference between distinct colors with the values on the L* a* b* chart, which is referred to as delta (Δ). To compute L*, for example, reduce the L* value of the standard color from the L* value of the sample. L*a*b* values can also be used to transform to a different color scale. Because of these various qualities of the CIE Lab color model, it is chosen over other models.

3.3.2.2 Adaptive Stretching in CIE Lab

The resultant image will be color corrected after the contrast enhancement in the RGB color space. To enhance color quality, the image is altered further in the CIELAB color space in this step. The 'L' parameter, is like image lightness in CIE-Lab color space, provides the darkest assessment at L= 0, whereas the brightest assessment is at L = 100. The color channel will show true neutral gray values when ‘a’ and ‘b’ are both zero. As a result, the output color successions in ‘a’ and ‘b’ parameters are updated to obtain proper color improvement, while the intensity of the full image is tuned using the 'L' component.

The 'L' element is used in conjunction with linear slide stretching, as described in equation (3.8), which lies within 0.1% to 99.9% is stretched to [0 to 100]. The minimum and maximum 0.1 % of the image's value are adjusted to 0 and 100, respectively.

‘a’, ‘b’ has values ranging from [128, 127], where 0 represents the median. An S-model curve is used to define the extending of 'a' and 'b' parameters as shown in equation (3.18).

$$P_\gamma = I_\gamma * \left(\varphi^{1-\left|\frac{I_\gamma}{128}\right|}\right) , \ \gamma \in \{a, b\} \tag{3.18}$$

Where I_γ is the input pixels, P_γ is the output pixels. γ represents the ‘a’, ‘b’ parameters. φ is the ideally suitable value which is 1.3. The stretching coefficient in Equation (3.18) is an exponential function, in which case if the value is close to 0, the more it will be stretched.

The importance of contrast and color in an image's clarity and visibility cannot be overstated. As a result, the background and foreground objects in an image are easily distinguished. The channels are assembled and turned into an

RGB color model once the stretching process for $L, a \,\&\, b$ elements in CIE Lab have been completed. As the observed and viewable final output image, a contrast- and color-improved result can be formed.

3.4 Datasets and Evaluation Parameters

This section describes the datasets, competing methods, and evaluation metrics that have been used to evaluate the designed algorithm.

3.4.1 Datasets

For underwater image improvement, we currently utilize eight different datasets: Underwater Test Dataset (U45) [67], Enhancing Underwater Visual Perception (EUVP) [68], Underwater Image Enhanced Benchmark dataset (UIEB) [77], Large-scale Underwater Image (LSUI) dataset [78], UFO-120 dataset [79], Underwater MOT dataset [69], Real-world Underwater Image Enhancement (RUIE) dataset [80], and dataset for underwater object detection (DUO) [81].

3.4.2 Competing Methods

We are using different competing approaches for underwater image enhancement. These competing approaches are given below. We compared our proposed model with the following methods: We compared our comparative universal stretching model with Bianco Prior [82], Dark Channel Prior [12], New Optical Model [83], Integrated Color Model [76], and Unsupervised Color Correction Method [73]. In the assessments, our method of comparative universal stretching gets the highest outcomes, while unsupervised color correction gets the

second highest outcomes. The Bianco Prior and Dark Channel Prior methods depend on the underwater image restoration method. The new optical and integrated color models depend on underwater image enhancement techniques. The comparative universal stretching method also uses a fusion-based algorithm in the underwater image enhancement method.

3.4.3 Evaluation Parameters

We use objective metrics such as entropy, peak signal-to-noise ratio (PSNR) [84], mean square error (MSE), High-Dynamic Range Visual Difference Predictor 2 (HDR-VDP2) [85], and underwater color image quality evaluation (UCIQE) [86] to perform quantitative analysis. The amount of information is represented by entropy, which is understood as the mean unpredictability of the information source. The more information there is, the greater the entropy value. MSE and PSNR are standard image quality evaluation measures that primarily measure image noise deterioration. The HDR-VDP2 predicts both the presence of artifacts and the overall quality of images using a pretty complex model of human perception. It generates a QMOS value ranging from 0 (best) to 100 (worst) to represent image quality. The UCIQE, which is an appropriate analytical predictor of hue, brightness, and contrast, is a relatively new non-reference metric for the evaluation of color image quality. However, MSE, PSNR, and Q-MOS are full reference metrics that take an actual image as a reference. They can be used to show how the created image compares to the original in terms of the observed loss in quality and increase in noise.

The detailed comparative analysis has been done in Chapter 5. Where we provide a detailed description of datasets, evaluation criteria, and result comparison in terms of qualitative and quantitative analysis.

3.5 Conclusion

This chapter provides a detailed explanation of the difficulty which have been occurred during the enhancement of the underwater images. A novel approach called CUS is designed to address this issue. This model generates the very high quality of the underwater images on various datasets.

In first phase of the CUS model we improve the contrast by using adaptive feature in histogram stretching. These adaptive features have been taken from the RGB color space of the degraded image; it evaluates the light propagation features as well as extract the histogram distribution parameter from the degraded images.

In second phase of the CUS model we perform the color improvement by utilizing the efficiency of the CIELAB color space. This phase is important to improve the color representation in the enhanced underwater images. A more subtle and context-aware color improvement is possible in the CIE Lab color space because of the adaptive stretching technique, which takes into consideration the unique qualities of underwater environments.

The CUS model offers a complete approach for enhancing underwater images by fusing contrast improvement in the RGB color space with adaptive color stretching in the CIE Lab color model. This two-step process results in a strong and efficient enhancement technique that is customized to the unique challenges presented by underwater environments.

A thorough comparative analysis against traditional dehazing models, like DCP, and other enhancement models, such UCM and ICM, is an essential phase in verifying the efficiency of the CUS model. We use both qualitative and quantitative analyses to determine how well the CUS model performs relative to

these well-established methods. Through this rigorous assessment, the CUS model shows its superiority in achieving these goals, exhibiting a significant advantage for enhancement of visibility, fine-tuning of details, and improvement in contrast and color.

In addition, these comparison assessments demonstrate how robust the CUS model is. Its success applies to other underwater image datasets and is not limited to any specific dataset. This universality highlights the CUS model's flexibility and applicability, which makes it a flexible option for improving images in a variety of applications and datasets.

The results of the comparison analysis verify the CUS model's effectiveness and robustness. It is proven to be a useful and adaptable technique for enhancing underwater image quality due to its superior performance over other dehazing and enhancement models on both qualitative and quantitative analysis. This validates the concept that the CUS system is fundamentally reliable, producing positive results on various datasets and establishing its status as a potential development in the field of underwater image enhancement.

CHAPTER 4

DEEPSEANET FRAMEWORK

In this chapter, the suggested DeepSeaNet model is explained in detail, with the architecture divided into two sections: convolutional, which consists of the first three steps, and deconvolutional, which consists of the fourth step. The first step considers the channel-specific features of each image channel to generate wavelength-driven contextual sizes. The second step uses the multi-contextual features that were learnt in the previous stage to construct color-dependent distortion residuals. Then these residuals have been used to generate the global color-correction features, which is the objective of the third step of the DeepSeaNet model. The restoration phase, which consists of a deconvolution layer, residual block, and an additional deconvolution layer, is the last and fourth step.

This chapter is organized as follows, with an introduction placing the scene for the importance of the DeepSeaNet model in the context of deep-sea image improvement. Reviewing related content gives light on present methods and prepares the reader for a thorough analysis of the suggested model.

The chapter describes the datasets utilized for evaluation, assuring a representative and varied range of deep-sea underwater images for verifying the proposed model. The assessment criteria, involving both qualitative and quantitative evaluations to fully evaluate the model performance.

4.1 Introduction

In deep-sea underwater images, the uneven attenuation of sunlight, when it spreads underwater, has high color distortion and very low intensity. Furthermore, the amount of reduction with respect to their wavelength causes asymmetric color movement. Irrespective of several efforts at deep-sea image enhancement via deep learning, this asymmetry has not been addressed earlier. As part of the research, this paper demonstrates that assigning the appropriate context based on the color channel traversal range may result in a significant performance speedup for the objective of underwater image enhancement. Furthermore, it is critical to reduce inappropriate characteristics and improve the model's representational strength. Therefore, we included an important reduction method to dynamically modify the learned characteristics. DeepSeaNet, the suggested framework, is enhanced via conventional pixel-wise and feature-based estimation methods. Comprehensive tests were conducted to demonstrate the efficiency of the proposed technique with the best published paper on standard datasets.

4.2 Related work

Despite the vast literature on previous deep learning and machine learning-based algorithms, the enhanced underwater images still suffer from color distortion. One of the key problems might be the use of deep CNN without appropriately overseeing the spatial formation of receptive fields among all the channels depending upon traversal lengths. Underwater images, unlike outside images, need specific measures due to varying attenuation ranges all over the channels.

As a result, a ready-made outdoor system is not appropriate in an underwater situation. Additionally, it was discovered in a prior study [87] that

specific channels contribute so much to dehazing, whereas the rest contribute to spatial color improvement. Because of these meaningful differences in various subtasks, the channels may need differing receptive field dimensions. Furthermore, the bulk of the approaches [88–90] rely on adversarial training [65], which could result in training instability. Due to adversarial learning, the generator model may soon begin to create images to fool the discriminator rather than generating improved or enhanced underwater images if not carefully designed [91]. Furthermore, unlike [77, 92], the suggested method does not use some priors, such as histogram equalization (HE), gamma correction (GC), or white-balanced (WB), to estimate the improved images. Due to the absence of semantic guidance and a vast dataset, such priors may assist in avoiding constructing a model that may not function well on unknown data. An example is estimating alpha matte out of a single image without using any before, so this is a significant issue [93]. The DeepSeaNet, on the other hand, is reasonably self-sufficient in learning these meaningful characteristics without some previous knowledge while predicting an enhanced version of the noisy deep-sea image at the same time. Furthermore, unlike [79], DeepSeaNet does not include several residual dense blocks [94] or multi-modal loss functions. The proper and accurate design of contextual sizes, together with the optimal usage of convolutional block attention modules, is sufficient to achieve significant improvement increases in enhanced deep sea underwater images.

4.3 Proposed work

In this section, we are going to discuss our approach to the problem statement, followed by one of the pre-requisites of the proposed work, which is the convolutional block attention module, followed by the proposed model. In the end, we also discussed model learning and how we trained our model to reduce the error so that the trained model worked well for the deep-sea underwater images.

4.3.1 Our Approach

Given the disadvantages highlighted above, we present the DeepSeaNet architecture, a four-step process containing convolutional in the first three steps and deconvolutional in the fourth step that enhances the degraded underwater images. We controlled the receptive field size, depending upon color channels of attenuation-guided global as well as local coherence. It is commonly known that a bigger or smaller receptive field understands the global or local characteristics of an image very well. In the deep-sea underwater image, the global coherence is generally aligned with blue. As a result, depending on our previous studies of the wavelength-driven spatial size connection, we decided to give the blue color channel a bigger receptive field, green's smaller, and reds even smaller. Moreover, to dynamically control the channel-specific information flow throughout the designed DeepSeaNet, we used a block attention-based [95] skip refinement technique. Our major contributions are outlined below:

• We introduce a deep convolutional neural network structure with multiple stages for deep-sea underwater image enhancement. The first phase analyzes the color channel of the damaged image, which has varied spatial sizes, while considering its global and local semantics depending on its attenuation length. Using an attention mechanism, the intermediate levels combine the learned multi-contextual characteristics, which also reduces the extraneous color-localized data from the preceding layer. The final phase is concerned with the restoration of the improved image.

• Although the scale of such advances may appear trivial, it is sometimes exactly what is required to produce the highest quality.

• We use the feature reconstruction loss [96] in addition to the standard mean squared error for training.

• We provided a thorough set of trials versus various current best research papers on enhancement of underwater images on the 10 image quality measures to demonstrate efficacy.

4.3.2 Convolution Block Attention Module (CBAM)

The CBAM module developed by Woo et al. [95] has been integrated into the proposed framework to retrieve the channel attention module and spatial attention module characteristics for the provided intermediate feature map as input. As illustrated in Figure 4.1, the resulting attention maps are multiplied by specified input features for adaptive enhancement [97]. In DeepSeaNet, we use the convolutional block attention module advantage after the color-localized skip connections in stages II and IV rather than directly after the convolution layer.

To formalize its operation, consider $M_s(I)$ as the spatial attention mappings and $M_c(I)$ as the channel attention mappings for the intermediate feature map I. They are represented as:

$$\begin{aligned} M_s(I) &= \sigma\left(c^{7*7}\left([\,AP(I); MP(I)\,]\right)\right) \\ &= \sigma\left(c^{7*7}\left(\left[\,I^s_{avg};\, I^s_{max}\,\right]\right)\right) \\ M_c(I) &= \sigma\left(F^c\left(I^c_{avg}\right) + F^c\left(I^c_{max}\right)\right) \end{aligned} \tag{4.1}$$

c^{7*7} is a convolution operation with a $7 * 7$ kernel, σ is a sigmoid function, F^c denote a multilayer perceptron with a hidden layer. While MP represents the maximum pooling and AP represents the average pooling. The improved feature I^r is defined as:

$$H = M_c(I) \otimes I$$
$$I^r = M_s(H) \otimes H \quad (4.2)$$

For further information, we recommend that readers consult [95]. In Section 7.2, we demonstrated how the improved characteristics aided in the creation of visually pleasing, enhanced underwater images.

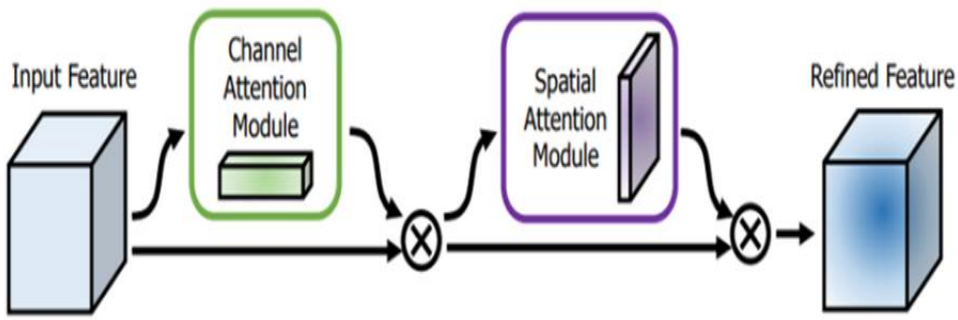

Figure 4.1. Convolutional Block Attention Module Structure

4.3.3 Proposed Model

Goal: As seen in Figures 4.2 – 4.5, we develop a model for the enhancement of underwater images. Figure 4.2 – 4.5, represent the structure of the suggested technique for enhancement of underwater images. The suggested technique receives a degraded underwater image as input and produces an enhanced image in terms of both visual appeal and spatial quality.

Description: The underwater images that are deteriorated and enhanced, respectively, are D and E.

Additionally, we use the abbreviations D_R, D_G and D_B to refer to the red color channel, blue color channel, and green color channel of the deteriorated image. $f_{c,s}^{i}$ referred as i^{th} step, having channel c belongs to red, green, and blue, and field size s. The planned DeepSeaNet operational regimes for each level are described below. While ⊙ means channel-wise concatenation, ⊕ means adding the characteristics pixel-by-pixel.

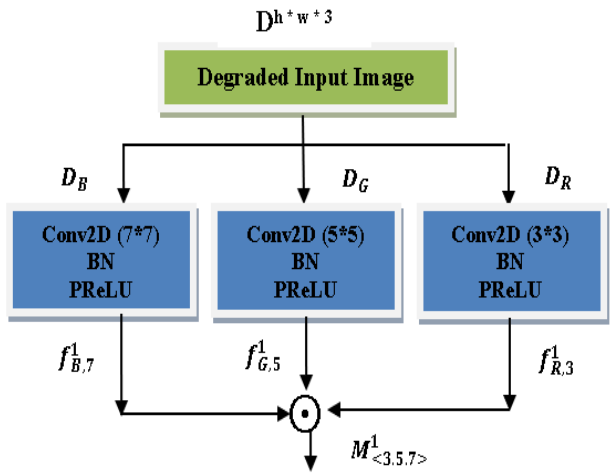

Figure 4.2 Structure of the suggested technique for enhancement of underwater image Step I.

Step I: The first step tries to provide wavelength-driven contextual sizes with channel-specific properties as shown in Figure 4.2. We do this by channel-wise inputting the degraded underwater image D to acquire the multi-contextual characteristics as follows:

$$M_{<3,5,7>}^{1} = f_{R,3}^{1} \odot f_{G,5}^{1} \odot f_{B,7}^{1} \tag{4.3}$$

where these color specific features are calculated as:

$$f_{R,3}^{1} = g(bn(p^{3*3}(D_R)))$$
$$f_{G,5}^{1} = g(bn(p^{5*5}(D_G))) \tag{4.4}$$

$$f^{1}_{B,7} = g(bn(p^{7*7}(D_B)))$$

here bn is the batch normalization and g is the parametric rectified linear unit (ReLU) layers.

Step II: Like step I, the initial layer of stage II is composed of just a pile of convolution layers with varied receptive fields as shown in Figure 4.3. The specific purpose of step II is to generate the color-dependent distortion residuals from multi-contextual features learned in step I as follows:

$$\begin{aligned} f^{2}_{R,3} &= g(bn(p^{3*3}(M^{1}_{<3,5,7>}))) \odot f^{1}_{R,3} \\ f^{2}_{G,5} &= g(bn(p^{5*5}(M^{1}_{<3,5,7>}))) \odot f^{1}_{G,5} \\ f^{2}_{B,7} &= g(bn(p^{7*7}(M^{1}_{<3,5,7>}))) \odot f^{1}_{B,7} \end{aligned} \tag{4.5}$$

The resulting residuals are dynamically improved using CBAM [16] modules.

$$\begin{aligned} f^{2}_{R,3} &= CBAM(f^{2}_{R,3}) \\ f^{2}_{G,5} &= CBAM(f^{2}_{G,5}) \\ f^{2}_{B,7} &= CBAM(f^{2}_{B,7}) \end{aligned} \tag{4.6}$$

The two objectives were achieved by doing this: (i) the color-specific, noisy features will not propagate to the next steps; and (ii) the model preserve the color related features when predicting the "global color correction residual," as it may while handling the complete input image all at once. Step II's output may be described as:

$$M^{2}_{<3,5,7>} = f^{2}_{R,3} \odot f^{2}_{G,5} \odot f^{2}_{B,7} \tag{4.7}$$

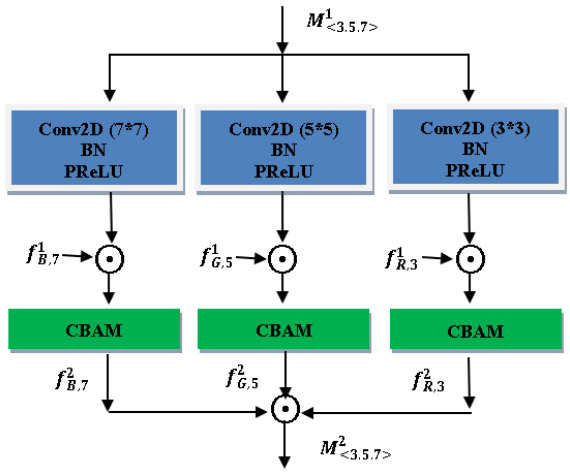

Figure 4.3. Structure of the suggested technique for enhancement of underwater image Step II.

Step III: It generates the global color-correction features from the intermediate features residuals, shown in Figure 4.4. It is given as follows:

$$M^3_{<3,5,7>} = f^3_{R,3} \odot f^3_{G,5} \odot f^3_{B,7} \tag{4.8}$$

where,

$$\begin{aligned} f^3_{R,3} &= g(bn\,(p^{3*3}\,(M^2_{<3,5,7>}))) \oplus D_R \\ f^3_{G,5} &= g(bn\,(p^{5*5}\,(M^2_{<3,5,7>}))) \oplus D_G \\ f^3_{B,7} &= g(bn\,(p^{7*7}\,(M^2_{<3,5,7>}))) \oplus D_B \end{aligned} \tag{4.9}$$

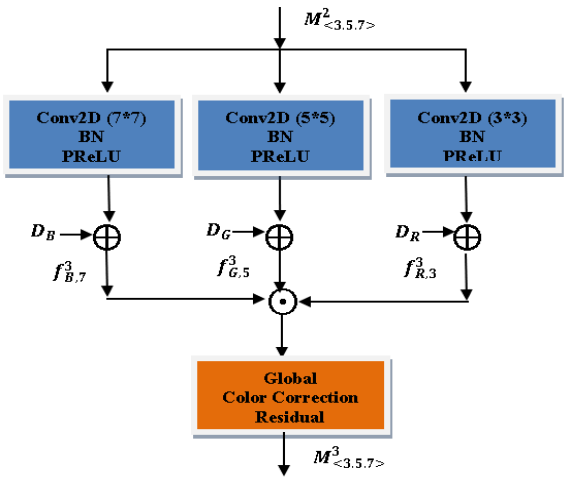

Figure 4.4 Structure of the suggested technique for enhancement of underwater image Step III.

Step IV: The last step serves as the restoration method and consists of a deconvolution layer, a residual block that is attentive, and the final deconvolution layer as shown in Figure 4.5. The improved underwater image is produced in step IV using the overall color correction residual in the form of input. The step IV operational regimes are given below:

$$f^4 = \mathrm{CBAM}(\, g\,(\, bn\,(d^{3*3}\,(M^3_{<3,5,7>}))) \odot M^3_{<3,5,7>})$$
$$E = g\,(\, bn\,(d^{3*3}\,(f^4))) \qquad (4.10)$$

where d^{3*3} is the deconvolution operation and E is the enhanced image.

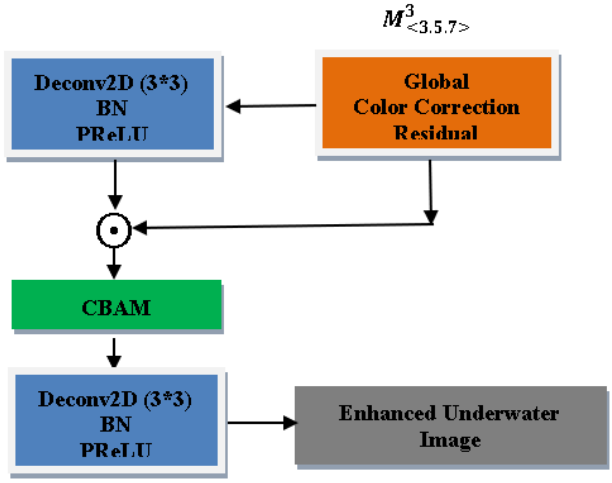

Figure 4.5 Structure of the suggested technique for enhancement of underwater image Step IV.

4.3.4 Model Learning

As per the prior image enhancement efforts [98-99], to train the DeepSeaNet, we initially integrated the conventional Mean Squared Error ℓ_2 as,

$$\mathcal{L}_2(\theta) = \frac{1}{b} \sum_{j=1}^{b} || \ W(\theta;\ D_j) - \ O_j \ ||_2^2 \tag{4.11}$$

here O is the original cleaner underwater image. The ℓ_2-norm based reduction result in fuzzy artefacts in recovered image.

To address this issue, we have included the Perceptual Loss $\mathcal{L}_P$ [96] function, which aids in keeping the image's high-frequency information. We used the visual geometry group (VGG16) ($V(\Theta)$)[100] technique, which was pre-trained on the ImageNet [101] database. We define the ℓ_2 norm as a cost function between the relu2_2 feature [102] derived via employing a speculated enhanced

underwater image and their respected ground truth image, which can be represented as:

$$\mathcal{L}_{\mathrm{P}}(\theta) = \frac{1}{\mathrm{b}} \sum_{\mathrm{j}=1}^{\mathrm{b}} || \mathrm{V}(\mathrm{W}(\theta;\ \mathrm{D}_{\mathrm{j}}); \Theta) - \mathrm{V}(\mathrm{O}_{\mathrm{j}};\ \Theta) ||_2^2 \tag{4.12}$$

The structural difference between the enhanced underwater image generated by DeepSeaNet and the original cleaner underwater images has been reduced with a structural similarity index measure (SSIM) [103] like loss relation in continuation to the $\mathcal{L}_2$ loss and $\mathcal{L}_{\mathrm{P}}$ loss. It calculates the similarities between two images and states them as:

$$SSIM\ (r) = \frac{2.\mu_x.\mu_y + Z_1}{\mu_x^2 + \mu_y^2 + Z_1} . \frac{2.\sigma_{xy} + Z_2}{\sigma_x^2 + \sigma_y^2 + Z_2} \tag{4.13}$$

here x and y are the patches from the E and O. z_1 and z_2 are the predefined parameters. μ is a mean, σ is a standard deviation and σ_{xy} is a covariance, provided r is the center pixels of the patches x, y from the E and O underwater images. The SSIM loss that has been absorbed may then be expressed as:

$$\mathcal{L}_{\mathrm{SSIM}}(\theta) = \frac{1}{2\mathrm{b}} \sum_{\mathrm{j}=1}^{\mathrm{b}} 1 - \mathrm{SSIM}(\mathrm{W}(\theta;\ \mathrm{D}_{\mathrm{j}}); \mathrm{O}_{\mathrm{j}}) \tag{4.14}$$

Here after, the suggested technique is refined with the help of objective function shown below:

$$\arg\min\ \mathcal{L}_2(.) + \lambda_{\mathrm{P}}.\mathcal{L}_{\mathrm{P}}(.) + \lambda_{\mathrm{S}}.\mathcal{L}_{\mathrm{SSIM}}(.) \tag{4.15}$$

here λ_{P} is 0.02 and λ_{S} is 0.5, these both values are empirically determined.

During our experiments, we discovered that $\mathcal{L}_2$ & $\mathcal{L}_{\mathrm{P}}$ losses are enough on their own. However, for more improved performance, $\mathcal{L}_{\mathrm{SSIM}}$ loss has also been integrated for image enhancement. This is mainly concerned with color correction in an underwater environment.

4.4 Datasets and Evaluation Parameters

In this section, the datasets and training setup, competing methods, and evaluation parameters have been described. They are all used to evaluate the DeepSeaNet model.

4.4.1 Datasets and training setup

For underwater image improvement, we utilized currently accessible benchmarks, especially the EUVP [68] dataset, the UIEB [77] dataset, and the UFO-120 [79] dataset. For underwater image enhancement, we use the EUVP dataset, which contains 11435 paired images of dimensions 256 * 256. The EUVP testing dataset contains 515 image pairs that are identical. The model that was trained on the EUVP dataset has been further fine-tuned to share our findings on the UIEB dataset. This dataset consists of 890 pair-wise underwater images. A random set of any 800 images is selected as the training and testing dataset. Given the memory restriction, we downsized the training images to 512 * 512. For a fair comparison, we used 5-fold cross-validation and published the mean findings. We also used the UIEB dataset challenge set for validation, which includes 60 deteriorated underwater images with no ground truth references. Once the model was fully trained, we tested it on the UFO-120 dataset for the enhancement of the underwater images.

The DeepSeaNet model is designed using the Pytorch [104] platform with the Adam [105] optimizer. The training went on for around two thousand three hundred iterations. The DeepSeaNet model requires a memory of 5GB and a batch size of 5. It is light weight, with a file size of 3.23 MB, and can analyze a 640 * 480 pixel image in 0.38 seconds.

4.4.2 Competing Methods

We are using different competing methods for underwater image enhancement. These competing methods are given below. We compared the suggested strategy to the following best-published works for this task: Fusion-based [6], Retinex-based [60], Histogram Prior [106], Blurriness-based [18], generalized dark primary color prior (GDCP) [107], Water Cycle GAN [67], Dense GAN [89], Water-Net [77], Haze Lines [108], unsupervised GAN (UGAN) [88], Funie-GAN [109], Deep SESR [79], Ucolor [92], SRCNN [115], SRResNet [116], SRGAN [116], SRDRM [90], SRDRM GAN [90].

4.4.3 Evaluation Parameters

For a more comprehensive evaluation of the proposed approach, we have included both reference-based and non-reference-based image quality measurements, as shown here: Structural similarity index measure (SSIM), Peak Signal-to-Noise Ratio (PSNR), Mean-Squared Error (MSE), Patch-based Contrast Quality Index (PCQI) [110], Natural Image Quality Evaluator (NIQE) [111], Visual Information Fidelity (VIF), Underwater Image Contrast Measure (UIConM) [112], Underwater Image Quality Measure (UIQM) [112], Underwater Image Sharpness Measure (UISM) [112], Underwater Color Image Quality Evaluation (UCIQE) [86].

The detailed comparative analysis has been done in Chapter 5. Where we provide a detailed description of datasets, evaluation criteria, and result comparison in terms of qualitative and quantitative analysis.

4.5 Conclusion

This chapter presents an innovative deep learning-based method designed to improve deep-sea underwater images. Our method is unique because we carefully consider the receptive field size for every single image channel, which is established by its appropriate wavelength. This novel architecture allows for a multi-contextual formulation, which makes it easier to understand the various global and local features present in every channel of deep-sea images.

The implementation of a multi-contextual formulation is found to be crucial in ensuring that the model can identify both global and local details, as well as the complex features encountered in deep-sea images. We integrate the Convolutional Block Attention Mechanism (CBAM), an adaptive change that considerably increases the performance of our suggested DeepSeaNet model, to further optimize the learnt features.

We perform comprehensive evaluation and comparisons among several standard datasets to validate the effectiveness of our proposed DeepSeaNet model. The outcomes show how well our model performs when compared to current state-of-the-art methods, demonstrating its superiority in deep-sea underwater image improvement.

CHAPTER 5

COMPARATIVE RESULT ANALYSIS

This chapter highlights the minute details of the suggested method through a comprehensive examination of datasets, evaluation criteria, outcome analysis, and method comparisons. The first part of the chapter provides the detailed description of the datasets that have been used and taken for the evaluation. We have taken eight various datasets to prove the robustness of the model whereas we have taken three deep-sea images datasets for a representative analysis and to provide an accuracy.

The evaluation parameters have been taken which include both the quantitative and qualitative analysis to provide the detailed view of the various pre-exists methods.

This chapter is a key component of the detailed assessment of the suggested approach. By thoroughly going over the datasets, evaluation criteria, result analysis, and method comparisons, the chapter provides valuable knowledge about the benefits and effectiveness of the suggested method for underwater images enhancement and deep-sea image enhancement respectively.

5.1 Result analysis of CUS Model

Our designed technique, which includes saturation equalization, sharpness improvement, and contrast improvement, is quantitatively and qualitatively comparable to other standard enhancement techniques. He [12] utilized image haze reduction with DCP and is taken as a comparison with our proposed work since it is a traditional approach for dehazing, and underwater images are frequently termed haze images. Unsupervised color correction models (UCM) and integrated color models (ICM) [73, 76] are the other comparison techniques since they are the most efficient imaging models and have the best similarities to the suggested approach in the context of histogram modification. Because the Rayleigh distribution method failed to run out in [74, 113–114], we only provide the UCM images in the comparative outcomes because the ICM has comparable outcomes to the UCM. Bianoc Prior (BP) [16] and New Optical Model (NOM) [82] are also compared with our approaches, as they are also based on the single image enhancement system.

(a) (b) (c) (d) (e) (f)

Figure 5.1. Represents the (a) Input Image and enhanced images using methods (b) Bianco Prior (c) Dark Channel Prior (d) New Optical Model (e) Unsupervised Color Correction Method (f) Comparative Universal Stretching.

Our designed technique, as shown in Figure 5.1, appears to provide an improved visual image compared to the other way. An UCM and NOM model produces a general sense of fish that has simple changes that do not boost image quality or reduce brightness and visibility. The BP and DCP oversaturate the color

because the image's blue and green colors are dominant in nature, which causes noise and decreases the overall visual effect. As the fisher is more distinguished from the background, the contrast and the color saturation of the image created by our approach improve, and a smaller amount of blue-green lighting is preserved.

The x-axis in the histogram in input as well as output images lies from 0 to 255, as shown in the other part of Figure 5.2. In (a) and (b), the gray-level values of histogram distributions are relatively dense, which helps to explain why two vibrant pictures have poor contrast and visibility. The gray level values in (c) and (d) spread in comparison to (a) and (b), but not as well with respect to (e) and (f). The gray level values of histogram distribution in (e) and (f) are dispersed throughout the x-axis, but according to GWAT [83], because of the accurate histogram stretching, the histogram of the improved image as shown in (f) has a better distribution.

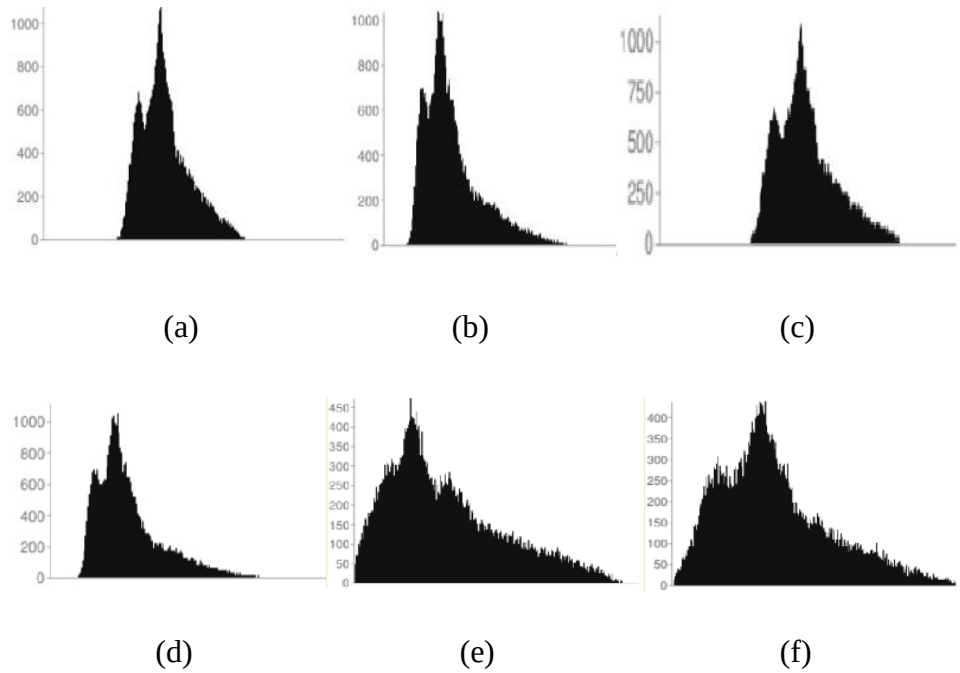

Figure 5.2. Represents the histogram distribution of (a) Input Image (b) Bianco Prior (c) Dark Channel Prior (d) New Optical Model (e) Unsupervised Color Correction Method (f) Comparative Universal Stretching.

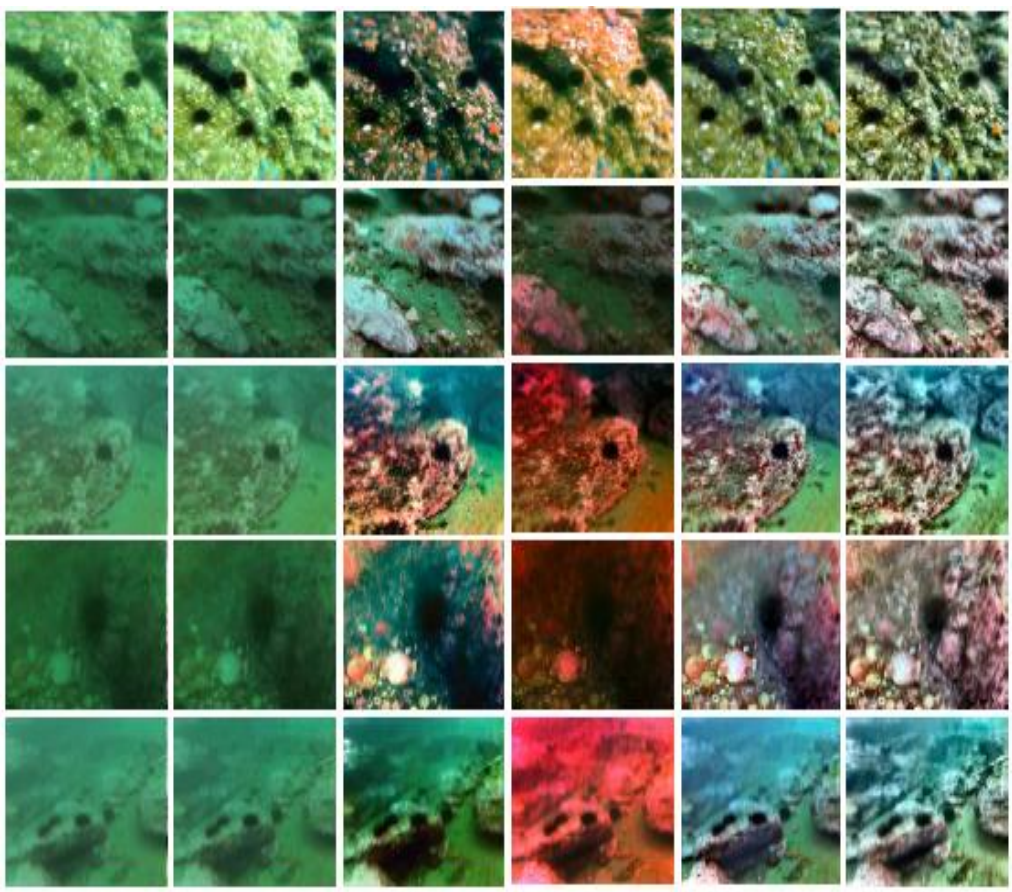

(a) (b) (c) (d) (e) (f)

Figure 5.3. (a) Input Image (b) Bianco Prior (c) Dark Channel Prior (d) New Optical Model (e) Unsupervised Color Correction Method (f) Our proposed method

Various approaches used for image improvement attain the outcome given in Figure 5.3. The input images are from the Real-World Underwater Image Enhancement Dataset (RUIE). Clearly, the images are not enhanced by BP and NOM, as shown in Figures 5.3 (b) and 5.3 (d). In Figures 5.3 (c) and 5.3 (e), the top two images of the DCP and UCM oversaturate the image color when the image's blue as well as green color gets too intense, resulting in enhanced images that are less realistic than those produced by our technique, as shown in Figure 5.3 (d) (top two images). The UCM's output underwater images have considerable noise; however, our technique successfully reduces the noise while preserving image features, as represented in the below three images in Figures 5.3 (e) and 5.3 (f), respectively.

We use objective metrics like entropy, peak signal-to-noise ratio (PSNR) [84], mean square error (MSE), High-Dynamic Range Visual Difference Predictor 2 (HDR-VDP2) [85], and underwater color image quality evaluation (UCIQE) [86] to perform quantitative analysis. The amount of information is represented by entropy, which is understood as the mean unpredictability of the information source. The more information there is, the greater the entropy value. MSE and PSNR are standard image quality evaluation measures that primarily measure image noise deterioration.

The HDR-VDP2 predicts both the presence of artefacts and the overall quality of images using a pretty complex model of human perception. It generates a QMOS value ranging from 0 (best) to 100 (worst) to represent image quality. The UCIQE, which is an appropriate analytical predictor of hue, brightness, and contrast, is a relatively new non-reference metrics for the evaluation of the quality of a color image. However, MSE, PSNR, and Q-MOS are full reference metrics that take an actual image as a reference. They can be used to show how the created image compares to the original in terms of observed loss in quality and increase in noise.

The comparative outcomes with the following evaluation models are given in Table 5.1. We compared our comparative universal stretching model with Dark Channel Prior [12], Unsupervised Color Correction Method (UCM) [73], Integrated Color Model (ICM) [76], Bianco Prior [82], and the New Optical Model. In the assessments, our method of comparative universal stretching gets the highest outcomes, while unsupervised color correction gets the second highest outcomes. The Bianco Prior and Dark Channel Prior methods depend on the underwater image restoration method. The new optical and integrated color models depend on underwater image enhancement techniques. The comparative universal stretching also uses a fusion-based approach in the underwater image enhancement method.

TABLE 5.1. Evaluation of various methods based on entropy, MSE, PSNR, HDR-VDP2, UCIQE and UIQM

Methods	Entropy	MSE	PSNR	HDR-VDP2	UCIQE	UIQM
Bianco Prior	5.43	3201.66	12.64	55.89	0.401	0.114
Dark Channel Prior	6.17	3116.78	13.36	53.68	0.419	1.396
New Optical Model	6.55	2224.36	15.51	48.36	0.453	1.327
Integrated Color Model	7.22	1440.12	16.58	42.65	0.485	2.236
Unsupervised Color Correction Method	7.56	1355.56	16.97	38.66	0.528	2.668
Comparative Universal Stretching	7.88	920.20	18.92	33.69	0.596	2.734

It keeps the most details and information, provides excellent visibility and overall quality, and reduces noise. The greatest UCIQE score indicates that our approach can properly balance the improved underwater images' chroma, saturation, and contrast. In all four approaches, the DCP delivers the lowest results, which is consistent with the viewing experience of low brightness and poor visibility. This implies that basic haze elimination with the DCP for underwater enhancement should not be employed straight away. The UCM and ICM techniques generate images with visible noise, resulting in a high MSE and low PSNR value.

To be more precise, we are using graphs to compare our proposed model with various other pre-existing models to represent the quantitative analysis of each evaluation parameter. It is very difficult to analyze the complete table straight-forward. So here we are going to compare all models with every evaluation parameter and identify the performance of all methods.

In the graphs, the x axis consists of the methods, which are arranged in order of their performance. The methods that are present on the left-most side are the lowest in terms of efficiency, and the methods that are on the right-most side have the highest efficiency. By doing so, we can easily find out the relationship between the various models, like which model is more or less efficient than the others.

Table 5.1 has been further analyzed with the help of graphs for each evaluation parameter, as shown in Figures 5.4.–5.9.

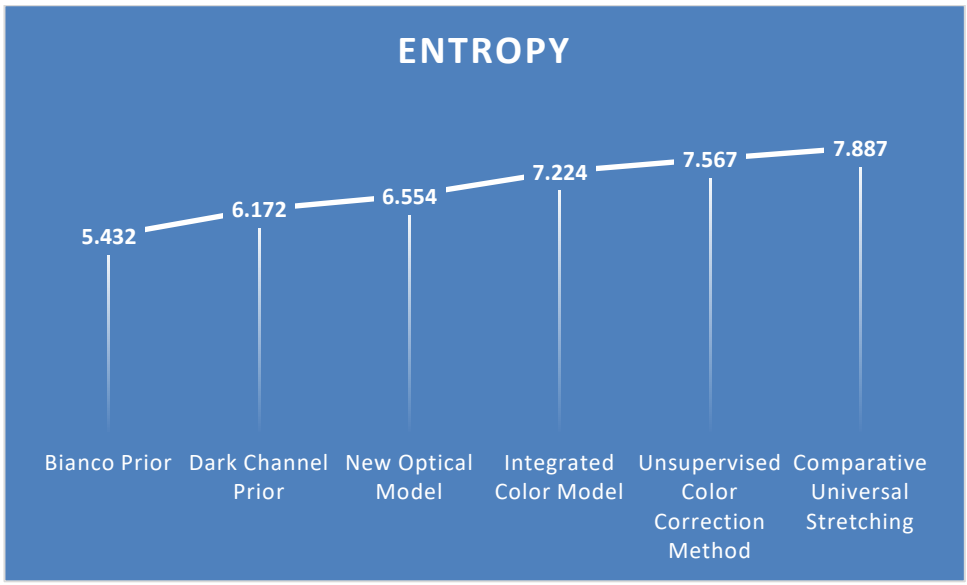

Figure 5.4. Analysis of the Entropy evaluation parameter shown in Table 5.1

By analyzing Figure 5.4, we can easily understand that the Bianco Prior method is performing the lowest with an entropy value of 5.432 and the CUS method is performing the best with an entropy value of 7.887 among all the methods that have been compared in Table 1.1.

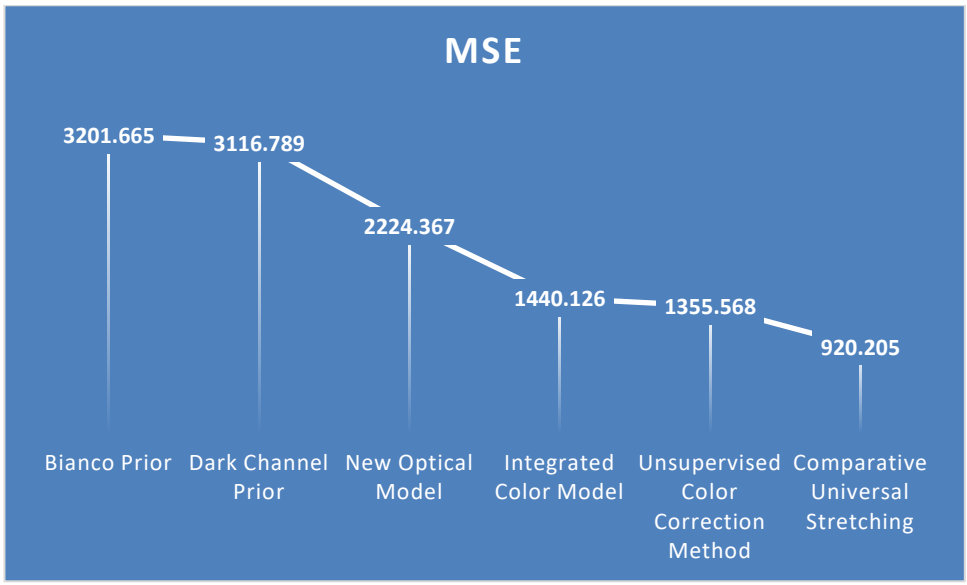

Figure 5.5. Analysis of the MSE evaluation parameter present in Table 5.1

By analyzing Figure 5.5, we can easily understand that the Bianco Prior method is performing the lowest with an MSE value of 3201.663 and the CUS method is performing the best with an MSE value of 920.205 among the methods that have been compared in Table 5.1.

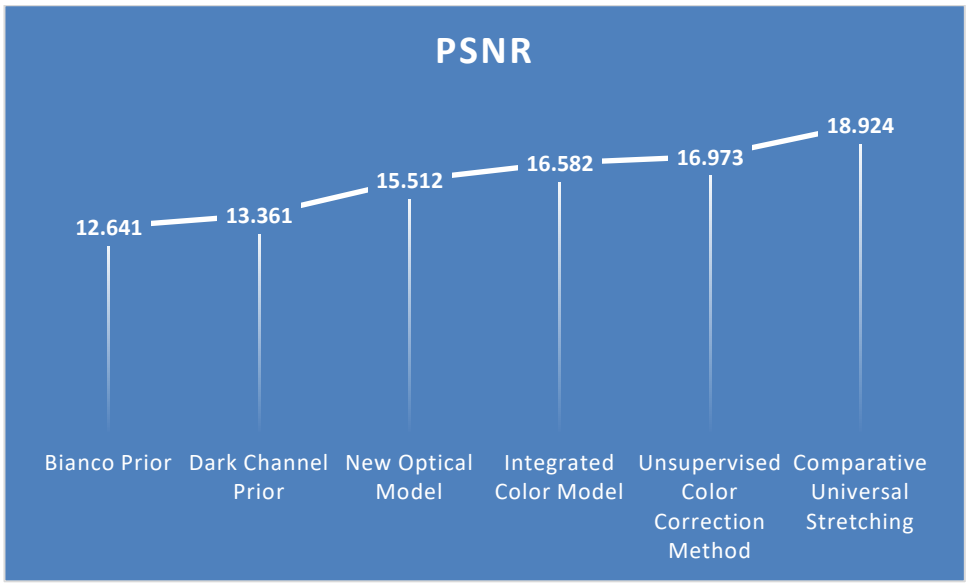

Figure 5.6. Analysis of the PSNR evaluation parameter present in Table 5.1

By analyzing Figure 5.6, we can easily understand that the Bianco Prior method is performing the lowest with a PSNR value of 12.641 and the CUS method is performing the best with a PSNR value of 18.924 among the methods that have been compared in Table 5.1.

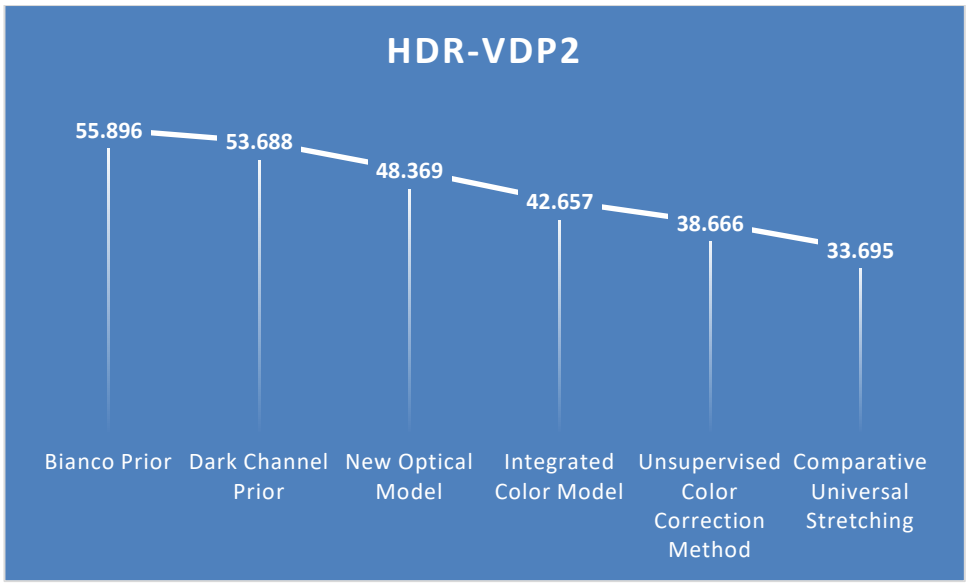

Figure 5.7. Analysis of the HDR-VDP2 evaluation parameter present in Table 5.1

By analyzing Figure 5.7, we can easily understand that the Bianco Prior method is performing the lowest with an HDR-VDP2 value of 55.896 and the CUS method is performing the best with an HDR-VDP2 value of 33.695 among the methods that have been compared in Table 5.1.

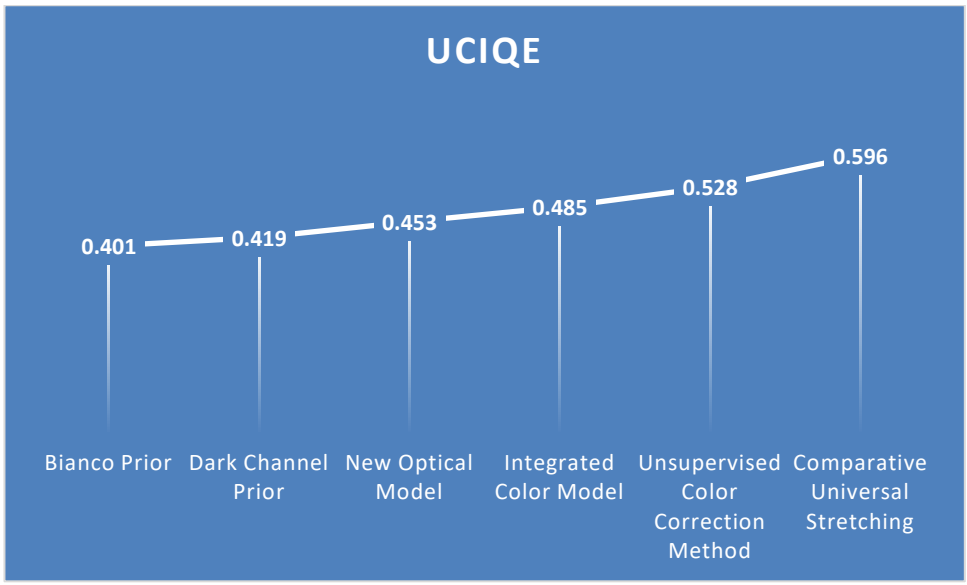

Figure 5.8. Analysis of the UCIQE evaluation parameter present in Table 5.1

By analyzing Figure 5.8, we can easily understand that the Bianco Prior method is performing the lowest with a UCIQE value of 0.401 and the CUS method is performing the best with a UCIQE value of 0.569 among the methods that have been compared in Table 5.1.

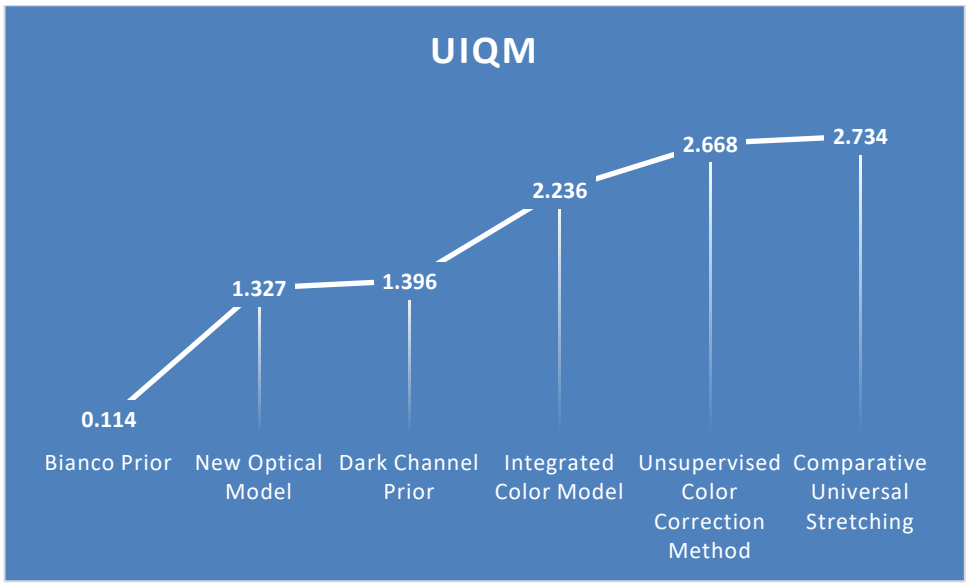

Figure 5.9. Analysis of the UIQM evaluation parameter present in Table 5.1

By analyzing Figure 5.9, we can easily understand that the Bianco Prior method is performing the lowest with a UIQM value of 0.114 and the CUS method is performing the best with a UIQM value of 2.734 among the methods that have been compared in Table 5.1.

Table 5.2. Evaluation Metrics of our proposed method CUS on various datasets using MSE, PSNR, UCIQE and UIQM

Datasets	Images	MSE	PSNR	UCIQE	UIQM
U45	Figure 5.4 (i)	1389.985	17.369	0.489	2.123
	Figure 5.4 (ii)	1458.398	16.254	0.456	1.965
	Figure 5.4 (iii)	1187.325	17.321	0.496	1.587
	Figure 5.4 (iv)	1255.985	15.323	0.532	2.321
EUVP	Figure 5.5 (i)	1026.987	16.548	0.498	2.541
	Figure 5.5 (ii)	826.698	17.896	0.562	2.365
	Figure 5.5 (iii)	855.258	17.549	0.554	2.897
	Figure 5.5 (iv)	812.987	18.369	0.589	3.168
UIEB	Figure 5.6 (i)	750.357	19.398	0.599	3.245
	Figure 5.6 (ii)	712.987	19.687	0.601	3.112
	Figure 5.6 (iii)	650.325	18.368	0.532	2.987
	Figure 5.6 (iv)	623.245	19.967	0.491	2.645
LSUI	Figure 5.7 (i)	1055.325	15.359	0.402	1.987
	Figure 5.7 (ii)	1032.357	16.356	0.425	2.665
	Figure 5.7 (iii)	1652.365	16.245	0.489	1.986
	Figure 5.7 (iv)	984.325	17.554	0.487	1.889

Datasets	Images	MSE	PSNR	UCIQE	UIQM
UFO-120	Figure 5.8 (i)	820.125	15.748	0.523	2.568
	Figure 5.8 (ii)	850.256	15.356	0.432	2.325
	Figure 5.8 (iii)	1052.658	16.958	0.489	2.578
	Figure 5.8 (iv)	981.854	17.698	0.502	2.222
RUIE	Figure 5.9 (i)	752.995	19.689	0.569	3.568
	Figure 5.9 (ii)	715.658	19.584	0.635	3.115
	Figure 5.9 (iii)	655.358	19.284	0.555	2.998
	Figure 5.9 (iv)	620.356	19.657	0.489	2.897
Underwater MOT	Figure 5.10 (i)	1110.879	16.358	0.502	3.589
	Figure 5.10 (ii)	1204.689	16.325	0.565	3.456
	Figure 5.10 (iii)	1002.359	18.658	0.486	2.154
	Figure 5.10 (iv)	995.987	17.658	0.466	2.753
DUO	Figure 5.11 (i)	1056.337	16.526	0.416	3.129
	Figure 5.11 (ii)	985.401	15.469	0.337	2.101
	Figure 5.11 (iii)	1054.159	16.334	0.499	3.825
	Figure 5.11 (iv)	9987.232	17.567	0.562	2.219

Table 5.2 represents the evaluation metrics in the form of MSE, PSNR, UCIQE, and UIQM values of four enhanced images of each of the eight datasets, which have been given in Figures 5.10–5.17.

Figures 5.10–5.17 represent the underwater images and their corresponding enhanced images from eight different datasets: Underwater Test Dataset (U45) [67] in Figure 5.10; Enhancing Underwater Visual Perception (EUVP) [68] in Figure 5.11, Underwater Image Enhanced Benchmark dataset (UIEB) [77] in Figure 5.12, Large-scale Underwater Image (LSUI) dataset [78] in Figure 5.13, UFO-120 dataset [79] in Figure 5.14, Real-world Underwater Image Enhancement dataset (RUIE) [80] in Figure 5.15, Underwater MOT dataset [69] in Figure 5.16, and dataset for underwater object detection (DUO) [81] in Figure 5.17.

(i) (ii) (iii) (iv)

Figure 5.10. U45 datasets input and enhanced images.

(i) (ii) (iii) (iv)

Figure 5.11. EUVP datasets input and enhanced images.

(i) (ii) (iii) (iv)

Figure 5.12. UIEB datasets input and enhanced images.

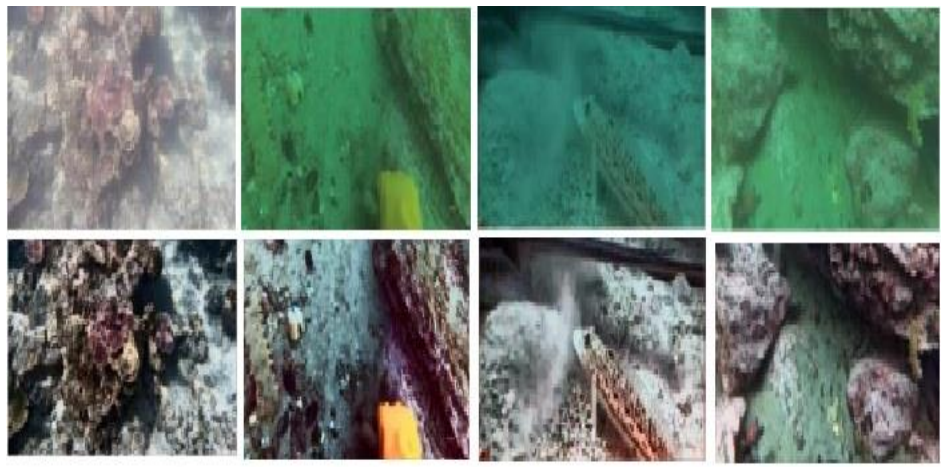

(i) (ii) (iii) (iv)

Figure 5.13 LSUI datasets input and enhanced images.

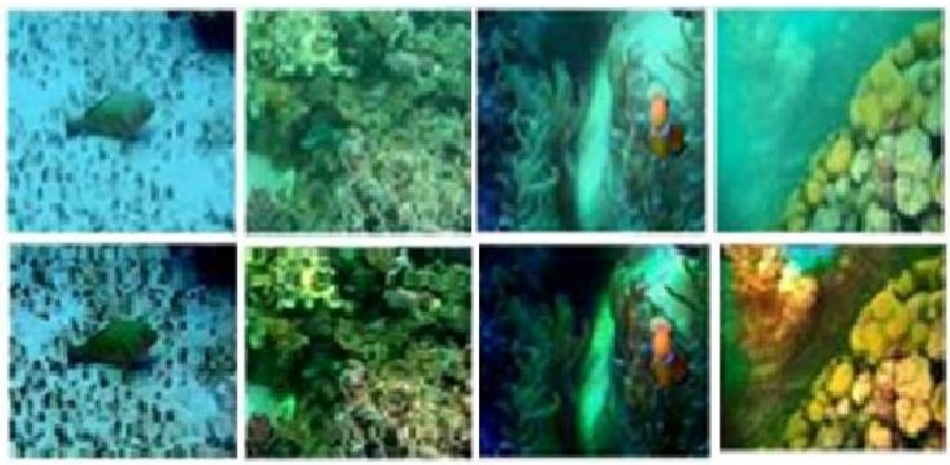

(i) (ii) (iii) (iv)

Figure 5.14 UFO-120 datasets input and enhanced images.

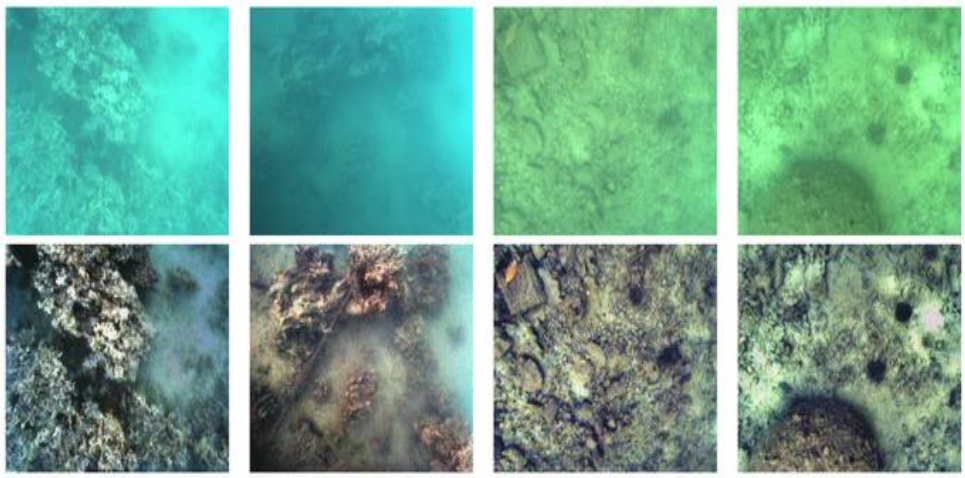

(i) (ii) (iii) (iv)

Figure 5.15 RUIE datasets input and enhanced images.

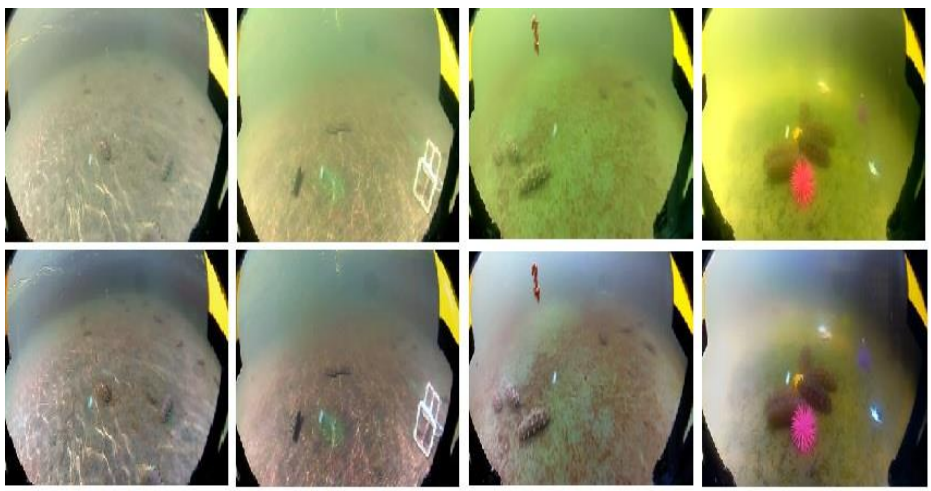

(i) (ii) (iii) (iv)

Figure 5.16 Underwater MOT datasets input and enhanced images.

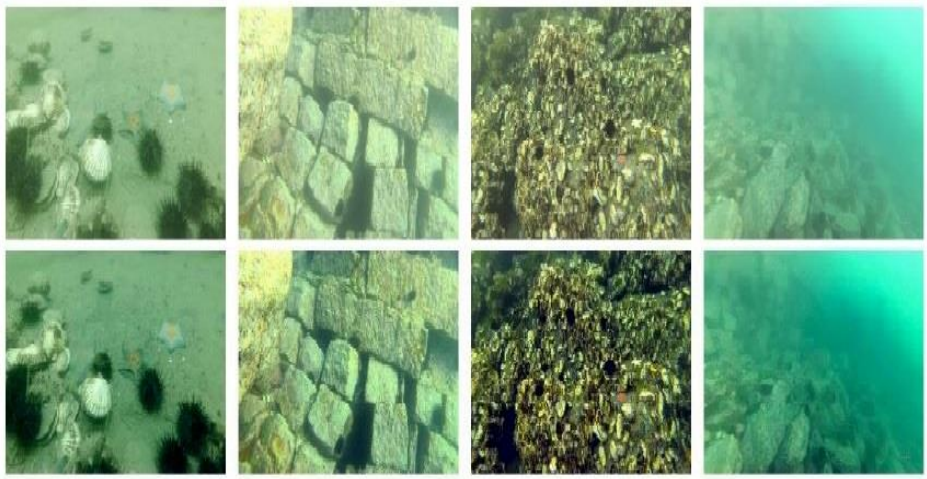

(i) (ii) (iii) (iv)

Figure 5.17. DUO datasets input and enhanced images.

Tables 5.3 to 5.10 represent the quantitative analysis of all eight datasets in detail. In each table, ten random test sample images have been chosen to compute evaluation metrics. The chosen images are totally different from all the above images, which have been used in Figures 5.10 – 5.17.

To prove the robustness of our approach, we took input images from different datasets and then performed our model to enhance the underwater images. If the MSE value is lower, then the image quality is better, whereas if the PSNR, UCIQE, and UIQM values are higher, the image is better. If the average value of any dataset in the test samples is less than 1000 in RMSE and greater than 16.700, 0.450, and 2.500 in PSNR, UCIQE, and UIQM, respectively, we consider our method to be above average for the datasets; otherwise, we consider our method to be below average for the datasets.

Table 5.3. Evaluation Metrics of our proposed model on U45 dataset using MSE, PSNR, UCIQE and UIQM

Datasets	Images	MSE	PSNR	UCIQE	UIQM
U45	Image 1	1040.709	17.441	0.436	2.302
	Image 2	905.390	17.435	0.441	3.589
	Image 3	989.783	17.000	0.478	1.666
	Image 4	822.131	16.255	0.423	1.863
	Image 5	1071.325	16.235	0.456	2.365
	Image 6	1074.658	17.321	0.569	3.265
	Image 7	1018.698	17.256	0.444	1.325
	Image 8	979.258	17.369	0.565	2.325
	Image 9	1085.147	16.357	0.462	2.654
	Image 10	906.963	17.238	0.423	3.698
	Image Average	**989.406**	**16.991**	**0.470**	**2.505**

Table 5.4. Evaluation Metrics of our proposed model on EUVP dataset using MSE, PSNR, UCIQE and UIQM

Datasets	Images	MSE	PSNR	UCIQE	UIQM
EUVP	Image 1	842.026	15.749	0.419	1.864
	Image 2	872.154	17.275	0.418	2.137
	Image 3	830.644	15.534	0.430	1.661
	Image 4	872.253	15.822	0.422	2.247
	Image 5	1022.762	17.987	0.445	2.156
	Image 6	922.121	18.654	0.556	3.654
	Image 7	913.356	18.123	0.456	2.355
	Image 8	1184.800	18.357	0.564	2.658
	Image 9	1045.131	18.456	0.598	3.325
	Image 10	1134.175	17.569	0.444	2.298
	Image Average	**963.942**	**17.353**	**0.475**	**2.436**

Table 5.5. Evaluation Metrics of our proposed model on UIEB dataset using MSE, PSNR, UCIQE and UIQM

Datasets	Images	MSE	PSNR	UCIQE	UIQM
UIEB	Image 1	606.608	16.095	0.465	1.887
	Image 2	662.074	17.776	0.459	2.107
	Image 3	767.527	16.592	0.401	1.888
	Image 4	727.181	17.663	0.410	1.904
	Image 5	798.359	18.862	0.625	2.632
	Image 6	780.157	18.426	0.588	2.231
	Image 7	759.153	19.842	0.564	3.214
	Image 8	684.953	19.874	0.489	3.278
	Image 9	763.759	18.896	0.525	3.865
	Image 10	763.486	19.632	0.608	2.536
	Image Average	**731.326**	**18.366**	**0.513**	**2.554**

Table 5.6. Evaluation Metrics of our proposed model on LSUI dataset using MSE, PSNR, UCIQE and UIQM

Datasets	Images	MSE	PSNR	UCIQE	UIQM
LSUI	Image 1	1043.574	15.366	0.441	1.827
	Image 2	1020.682	15.576	0.405	2.333
	Image 3	1252.697	15.006	0.467	1.921
	Image 4	955.570	16.066	0.477	2.259
	Image 5	1163.800	16.933	0.307	2.787
	Image 6	1255.143	17.116	0.369	2.636
	Image 7	908.869	15.056	0.309	2.462
	Image 8	1006.861	15.025	0.476	2.095
	Image 9	1241.307	16.407	0.471	3.168
	Image 10	915.795	15.664	0.404	3.221
	Image Average	**1093.794**	**15.878**	**0.415**	**2.420**

Table 5.7. Evaluation Metrics of our proposed model on UFO-120 dataset using MSE, PSNR, UCIQE and UIQM

Datasets	Images	MSE	PSNR	UCIQE	UIQM
UFO-120	Image 1	820.711	16.779	0.414	1.613
	Image 2	818.224	16.771	0.496	1.737
	Image 3	816.678	15.337	0.500	2.449
	Image 4	847.085	15.109	0.427	2.058
	Image 5	1060.826	17.567	0.472	2.905
	Image 6	976.274	17.779	0.487	2.202
	Image 7	1113.448	16.119	0.452	3.934
	Image 8	1150.686	18.752	0.420	3.876
	Image 9	1169.523	15.155	0.467	3.182
	Image 10	1128.895	15.343	0.428	2.584
	Image Average	**991.216**	**16.584**	**0.454**	**2.623**

Table 5.8. Evaluation Metrics of our proposed model on RUIE dataset using MSE, PSNR, UCIQE and UIQM

Datasets	Images	MSE	PSNR	UCIQE	UIQM
RUIE	Image 1	706.448	15.604	0.446	1.755
	Image 2	663.923	17.641	0.410	2.306
	Image 3	697.657	16.949	0.500	2.194
	Image 4	705.228	15.570	0.414	2.064
	Image 5	979.839	17.907	0.423	3.228
	Image 6	864.686	18.933	0.579	2.655
	Image 7	997.312	16.036	0.503	3.550
	Image 8	833.470	17.422	0.493	3.846
	Image 9	914.562	17.945	0.502	3.725
	Image 10	818.213	17.041	0.586	2.180
	Image Average	**818.134**	**17.105**	**0.486**	**2.750**

Table 5.9. Evaluation Metrics of our proposed model on Underwater MOT dataset using MSE, PSNR, UCIQE and UIQM

Datasets	Images	MSE	PSNR	UCIQE	UIQM
Underwater MOT	Image 1	1099.793	15.898	0.490	1.987
	Image 2	1253.287	15.166	0.464	1.601
	Image 3	1033.680	17.286	0.405	1.543
	Image 4	1129.493	17.313	0.415	2.484
	Image 5	1287.365	17.687	0.352	1.957
	Image 6	1343.265	15.572	0.342	1.938
	Image 7	1338.458	15.521	0.380	1.929
	Image 8	1254.369	17.355	0.435	2.018
	Image 9	1303.245	18.895	0.375	2.058
	Image 10	1281.365	17.529	0.323	1.837
	Image Average	**1232.432**	**16.822**	**0.398**	**1.935**

Table 5.10. Evaluation Metrics of our proposed model on DUO dataset using MSE, PSNR, UCIQE and UIQM

Datasets	Images	MSE	PSNR	UCIQE	UIQM
DUO	Image 1	1045.142	16.548	0.401	3.287
	Image 2	1037.716	16.674	0.441	2.129
	Image 3	960.472	15.987	0.353	2.019
	Image 4	1013.565	16.542	0.441	3.187
	Image 5	924.647	17.341	0.493	2.070
	Image 6	1074.894	16.993	0.437	3.182
	Image 7	813.642	17.086	0.412	2.183
	Image 8	1069.631	16.224	0.338	2.087
	Image 9	969.763	15.074	0.493	2.999
	Image 10	1047.834	16.461	0.431	2.529
	Image Average	**995.731**	**16.493**	**0.424**	**2.567**

Based on the mean square error (MSE) evaluation parameter, the top two results have been seen in the UIEB dataset, i.e., 731.326, and the RUIE dataset, i.e., 818.134, whereas the bottom two results have been seen in the LSUI dataset, i.e., 1093.794, and the Underwater MOT dataset, i.e., 1232.432.

With the PSNR evaluation parameter, the top two results have been seen in the UIEB dataset, i.e., 18.366, and the EUVP dataset, i.e., 17.353, whereas the bottom two results have been seen in the LSUI dataset, i.e., 15.878, and the DUO dataset, i.e., 16.493.

With the UCIQE evaluation parameter, the top two results have been seen in the UIEB dataset, i.e., 0.513, and the RUIE dataset, i.e., 0.486, whereas the bottom two results have been seen in the LSUI dataset, i.e., 0.415, and the Underwater MOT dataset, i.e., 0.398.

With the UIQM evaluation parameter, the top two results have been seen in the RUIE dataset, i.e., 2.750, and the UFO-120 dataset, i.e., 2.632, whereas the bottom two results have been seen in the LSUI dataset, i.e., 2.420, and the Underwater MOT dataset, i.e., 1.935.

The values that we are taking for all four evaluation parameters when considering the above- or below-average datasets are the combined average values with an efficiency greater than 85%. Whereas the overall average values that we are getting in all our datasets are above 75%. All values of each evaluation parameter and efficiency in terms of % have been evaluated with the help of tables 5.2–5.10.

We can consider the RUIE, EUVP, UFO-120, and U45 datasets as above average, while the LSUI, Underwater MOT, and DUO datasets as below

average. But the overall results of our proposed method on every dataset are far better compared to other methods.

To sum up, the research suggests that our approach is better than commonly used underwater image enhancement methods for producing high-quality underwater images.

5.2 Result analysis of DeepSeaNet Model

The quantitative findings are given in Tables 5.11 to 5.14. Table 5.11 represents the quantitative comparison of the EUVP dataset. Table 5.11 demonstrates how the suggested model outperformed the current research on nearly all image quality criteria. Whereas the proposed approach improved PSNR and SSIM by 5.3% and 2.4%, respectively. A significant increase of 0.05 and 11 was seen in the UIQM and NIQE evaluation parameters of Deep SESR [79]. In the perspective of underwater image enhancement, the suggested model has likewise obtained dominance on 8 out of 10 image quality measures.

In Figure 5.18, it has been observed that the methods UGAN, UGAN-P, and Funie-GAN are underperforming in comparison to other methods in the EUVP dataset. The results obtained in Deep SESR and DeepSeaNet are more enhanced and have higher accuracy in comparison to all methods. Our method, DeepSeaNet, is providing the best results in MSE, PSNR, SSIM, NIQE and UISM.

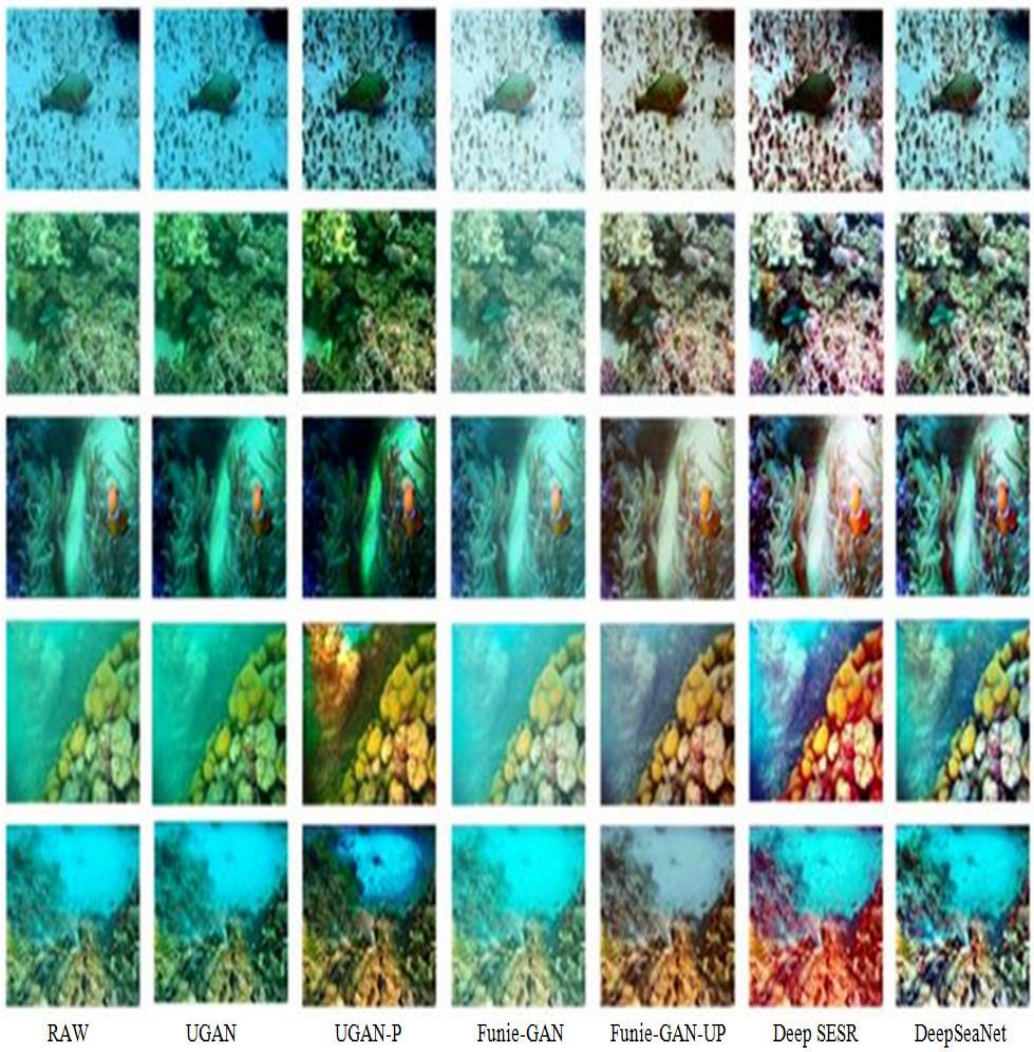

Figure 5.18. Qualitative representation of DeepSeaNet model for underwater image enhancement on EUVP dataset.

Table 5.11. Quantitative evaluation of DeepSeaNet model for underwater image enhancement on EUVP dataset. Ten parameters have been used to evaluate the result. Results are shown in two consecutive tables for EUVP dataset. The top two outcomes are represented in bold.

Methods	SSIM	MSE	PSNR	PCQI	VIF
UGAN	0.81	0.36	26.55	0.701	**0.402**
UGAN-P	0.81	0.36	26.54	**0.703**	0.401
Funie-GAN	0.79	0.39	26.22	**0.706**	0.384
Funie-GAN-UP	0.78	0.61	25.22	0.702	0.394
Deep SESR	**0.81**	**0.34**	**27.08**	0.679	0.384
DeepSeaNet	**0.83**	**0.29**	**28.62**	0.694	**0.438**

Methods	NIQE	UISM	UIQM	UIConM	UCIQE
UGAN	**49.91**	6.84	2.89	0.78	0.581
UGAN-P	50.17	6.83	2.93	0.78	0.559
Funie-GAN	50.51	6.91	2.97	**0.84**	**0.595**
Funie-GAN-UP	52.87	6.86	2.93	**0.79**	0.588
Deep SESR	55.68	**7.06**	**3.09**	0.78	0.572
DeepSeaNet	**44.89**	**7.06**	**3.04**	0.77	**0.591**

Table 5.11 has been further analyzed with the help of graphs for each evaluation parameter, as given in Figures 5.19.–5.26.

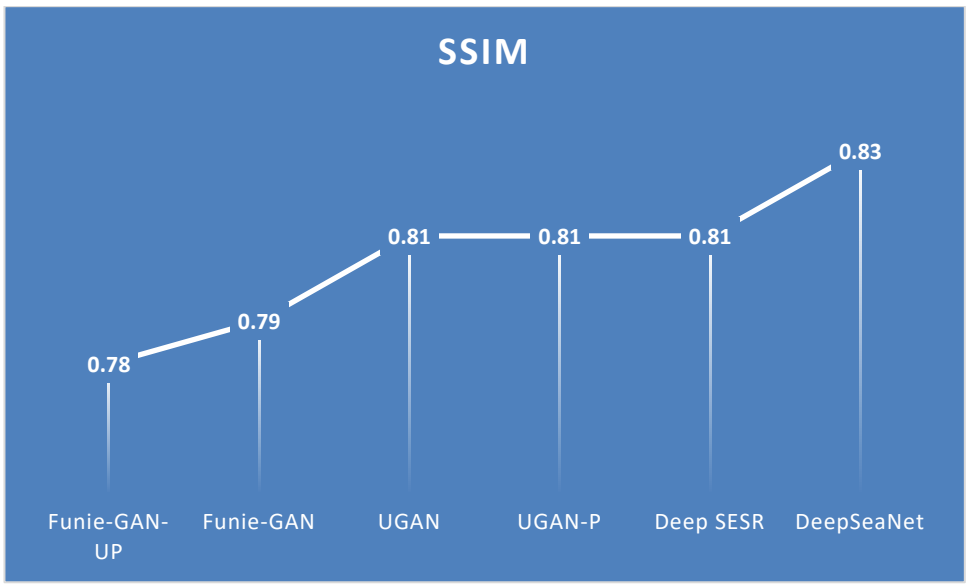

Figure 5.19. Analysis of the SSIM evaluation parameter present in Table 5.11

By analyzing Figure 5.19, we can easily understand that the FUNIE-GAN-UP method is performing the lowest with a SSIM value of 0.78 and the DeepSeaNet method is performing the best with a SSIM value of 0.83 among the methods that have been compared in Table 5.11.

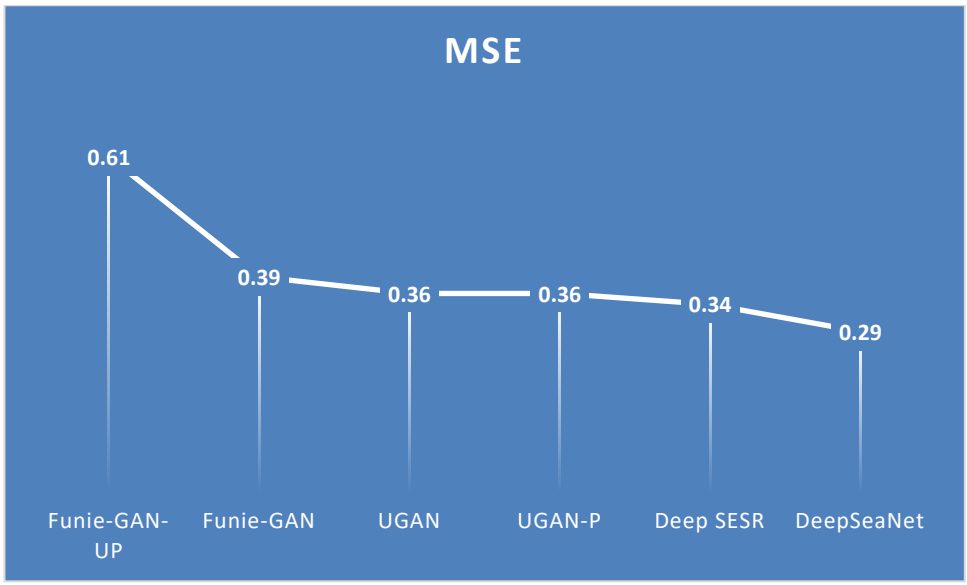

Figure 5.20. Analysis of the MSE evaluation parameter present in Table 5.11

By analyzing Figure 5.20, we can easily understand that the FUNIE-GAN-UP method is performing the lowest with a MSE value of 0.61 and the DeepSeaNet method is performing the best with a MSE value of 0.29 among the methods that have been compared in Table 5.11.

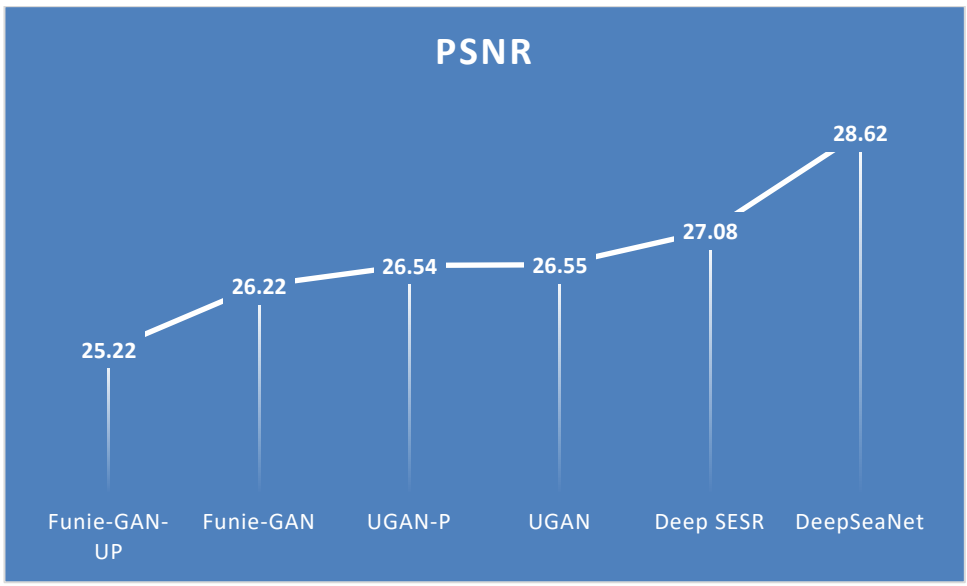

Figure 5.21. Analysis of the PSNR evaluation parameter present in Table 5.11

By analyzing Figure 5.21, we can easily understand that the FUNIE-GAN-UP method is performing the lowest with a PSNR value of 25.22 and the DeepSeaNet method is performing the best with a PSNR value of 28.62 among the methods that have been compared in Table 5.11.

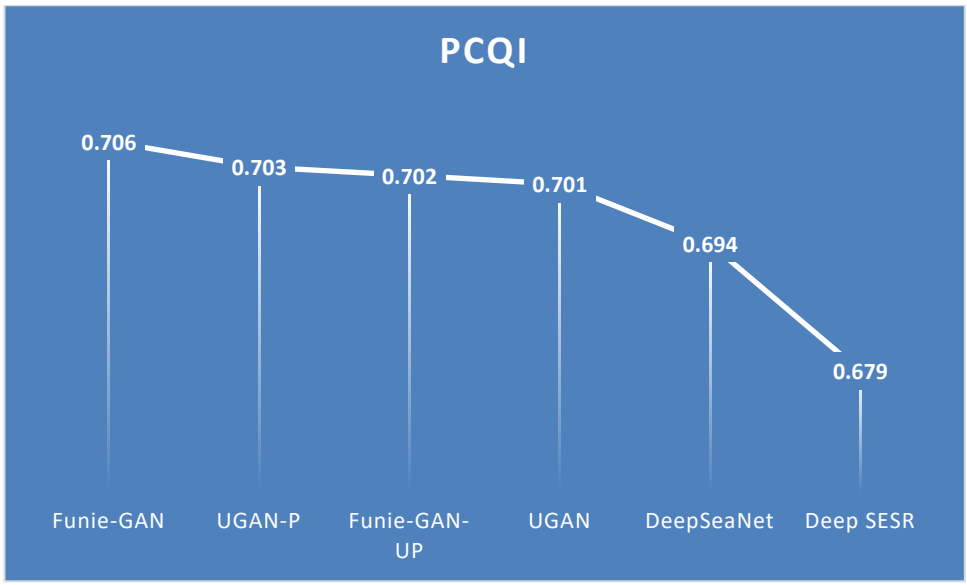

Figure 5.22. Analysis of the PCQI evaluation parameter present in Table 5.11

By analyzing Figure 5.22, we can easily understand that the FUNIE-GAN method is performing the lowest with a PCQI value of 0.706 and the DeepSeaNet method is performing the best with a PCQI value of 0.679 among the methods that have been compared in Table 5.11.

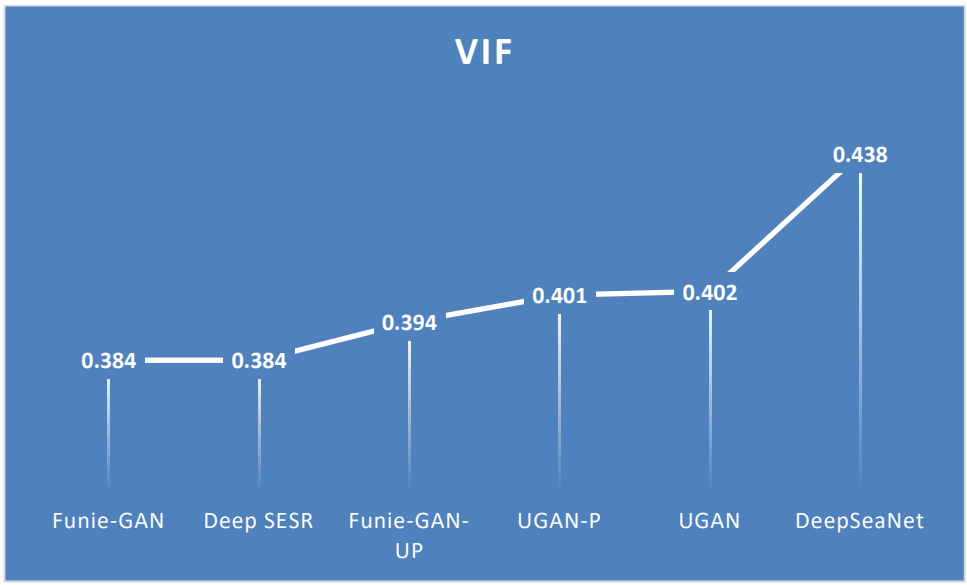

Figure 5.23. Analysis of the VIF evaluation parameter present in Table 5.11

By analyzing Figure 5.23, we can easily understand that the FUNIE-GAN method is performing the lowest with a VIF value of 0.384 and the DeepSeaNet method is performing the best with a PCQI value of 0.438 among the methods that have been compared in Table 5.11.

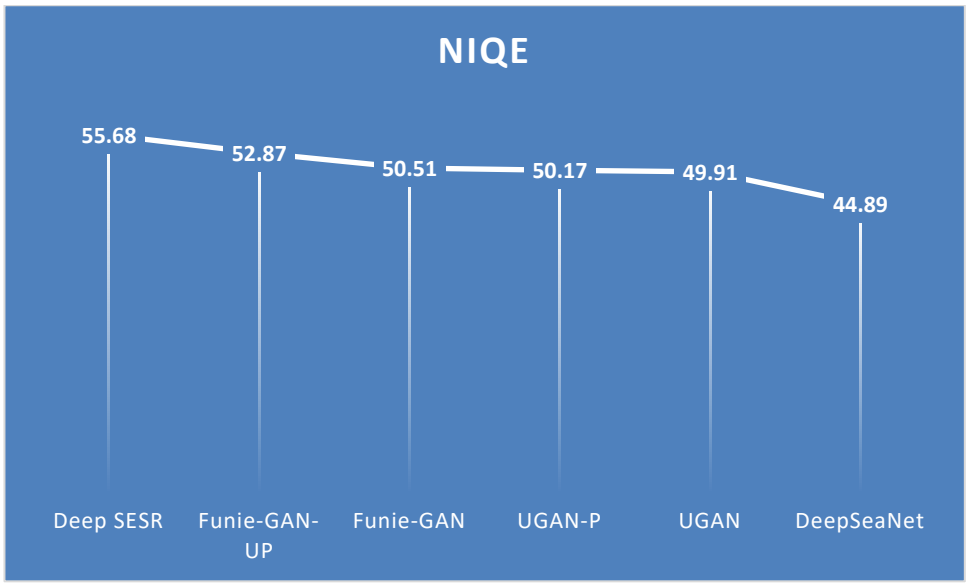

Figure 5.24. Analysis of the NIQE evaluation parameter present in Table 5.11

By analyzing Figure 5.24, we can easily understand that the DEEP SESR method is performing the lowest with a NIQE value of 55.68 and the DeepSeaNet method is performing the best with a NIQE value of 44.89 among the methods that have been compared in Table 5.11.

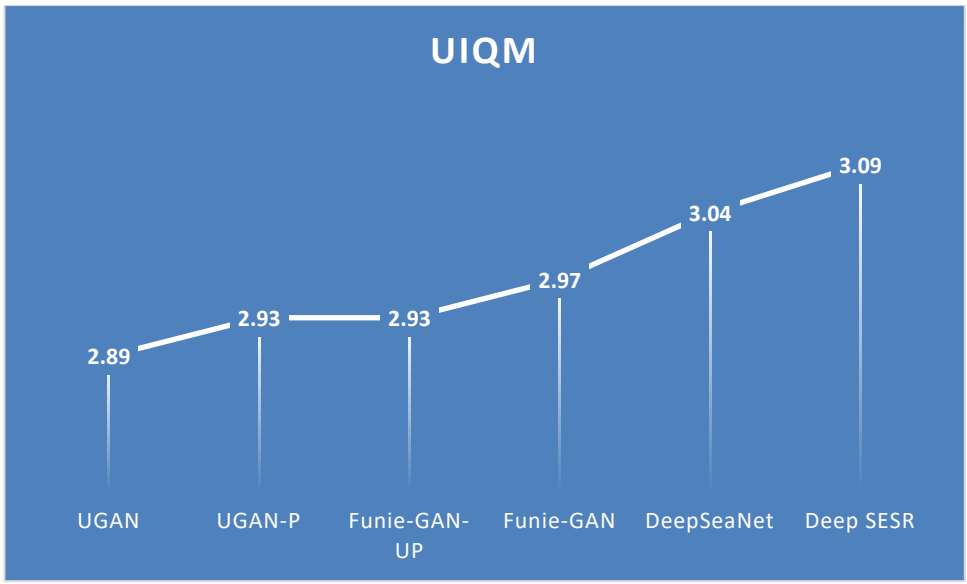

Figure 5.25. Analysis of the UIQM evaluation parameter present in Table 5.11

By analyzing Figure 5.25, we can easily understand that the UGAN method is performing the lowest with a UIQM value of 2.89 and the Deep SESR method is performing the best with a UIQM value of 3.09 among the methods that have been compared in Table 5.11. Our method, DeepSeaNet, shows the second highest efficiency with a UIQM value of 3.04.

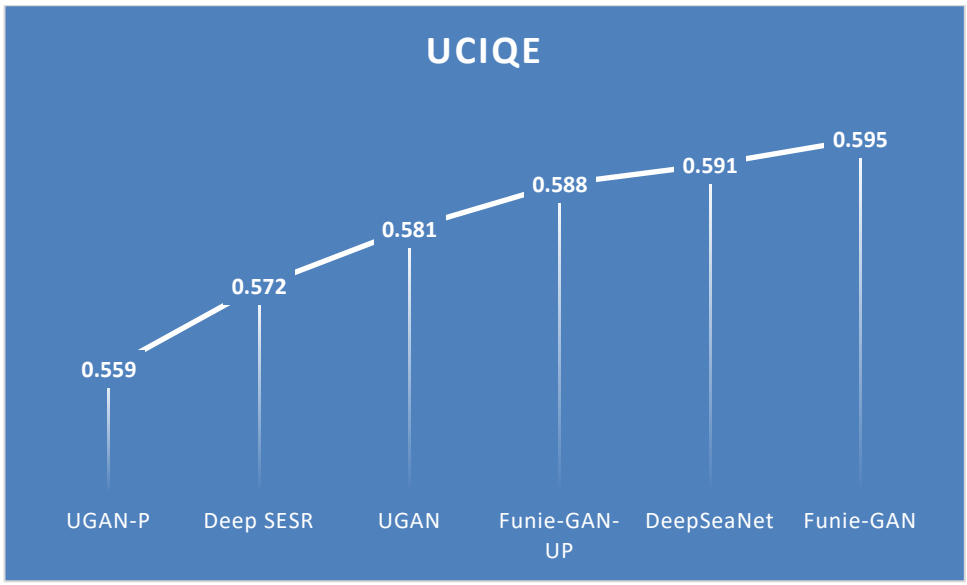

Figure 5.26. Analysis of the UCIQE evaluation parameter present in Table 5.11

By analyzing Figure 5.26, we can easily understand that the UGAN-P method is performing the lowest with a UCIQE value of 0.559 and the Funie-GAN method is performing the best with a UCIQE value of 0.595 among the methods that have been compared in Table 5.11. Our method, DeepSeaNet, shows the second highest efficiency with a UCIQE value of 0.591.

Table 5.12 shows the quantitative evaluation of the DeepSeaNet model for image enhancement on the UIEB dataset.

It shows that the suggested approach greatly performed on the current best-published studies on the UIEB dataset in every aspect. A significant increase of 0.18, 0.44, 0.02, 0.89, and 0.98 was seen in MSE, PSNR, SSIM, UIQM, and NIQE, respectively, in comparison to the best previously proposed methods.

In Figure 5.27, we also show a visual assessment of the designed model compared to existing approaches.

It shows that the previous approaches, Haze Lines [108] and Retinex [60], suffer from color oversaturation and undersaturation in improved images. Whereas Fusion-based [6] and GDCP [107] approaches fail to improve damaged images, the suggested DeepSeaNet model produces the most visually appealing enhanced underwater images.

After these quantitative and qualitative analyses, Table 5.12 has been further analyzed with the help of graphs for each evaluation parameter, as given in Figures 5.28–5.32.

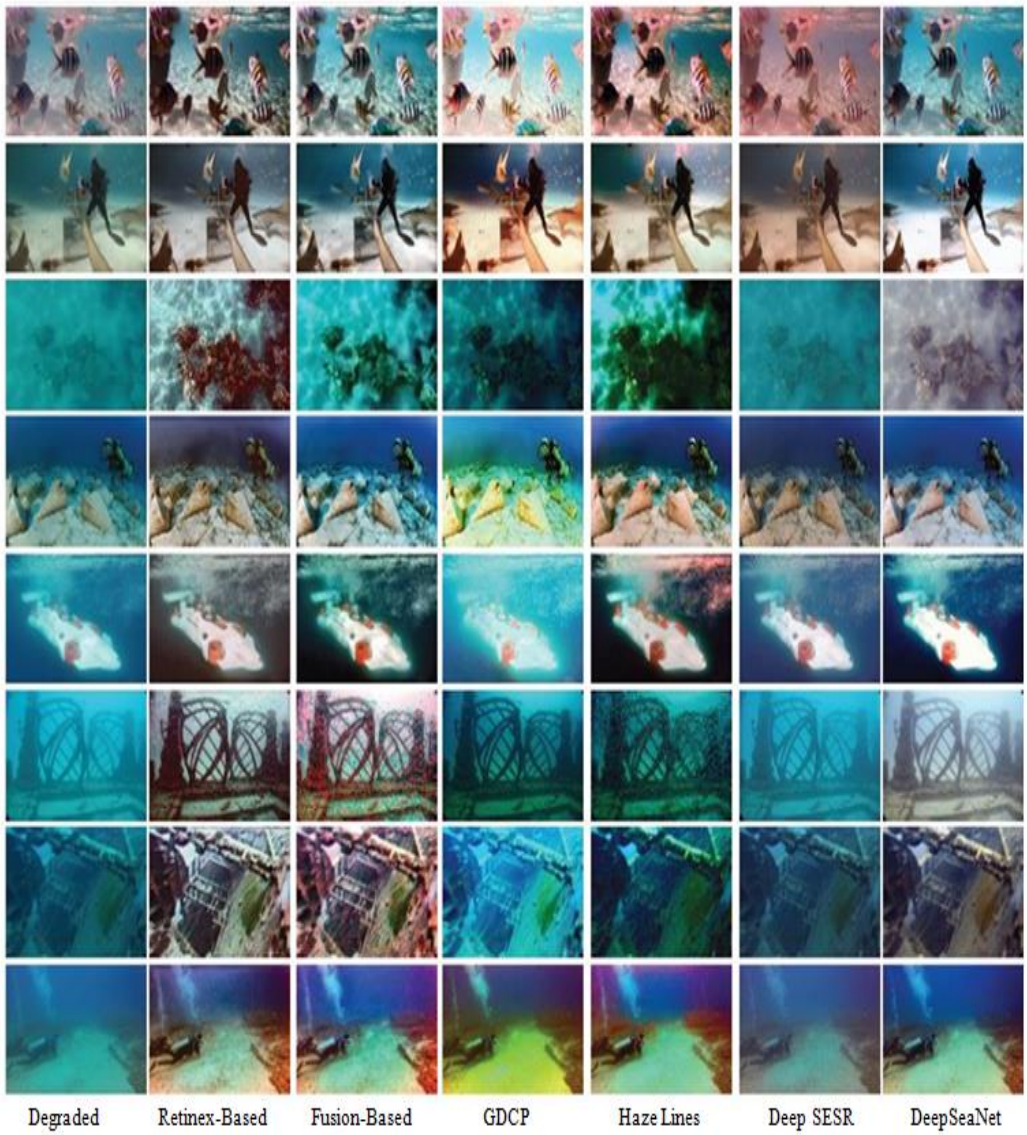

Figure 5.27. Qualitative representation of DeepSeaNet model for underwater image enhancement on UIEB dataset.

Table 5.12. Quantitative evaluation of DeepSeaNet model for underwater image enhancement on UIEB dataset. The top two outcomes are represented in bold.

Methods	MSE	PSNR	SSIM	UIQM	NIQE
Fusion-Based	0.91	**21.23**	0.78	1.22	**4.96**
Histogram Prior	1.71	15.85	0.53	**1.25**	5.29
Retinex-Based	1.34	17.66	0.61	1.15	5.66
GDCP	3.33	13.86	0.55	1.11	5.88
Blurriness-Based	1.91	15.31	0.61	1.16	6.11
Water Cycle GAN	1.72	15.75	0.52	0.91	7.67
Dense GAN	1.21	17.28	0.44	1.11	5.71
Water Net	**0.79**	19.11	**0.79**	0.97	6.04
Haze lines	2.44	15.17	0.57	1.09	5.95
Deep SESR	1.75	16.65	0.57	1.11	5.91
DeepSeaNet	**0.61**	**21.57**	**0.81**	**2.14**	**3.98**

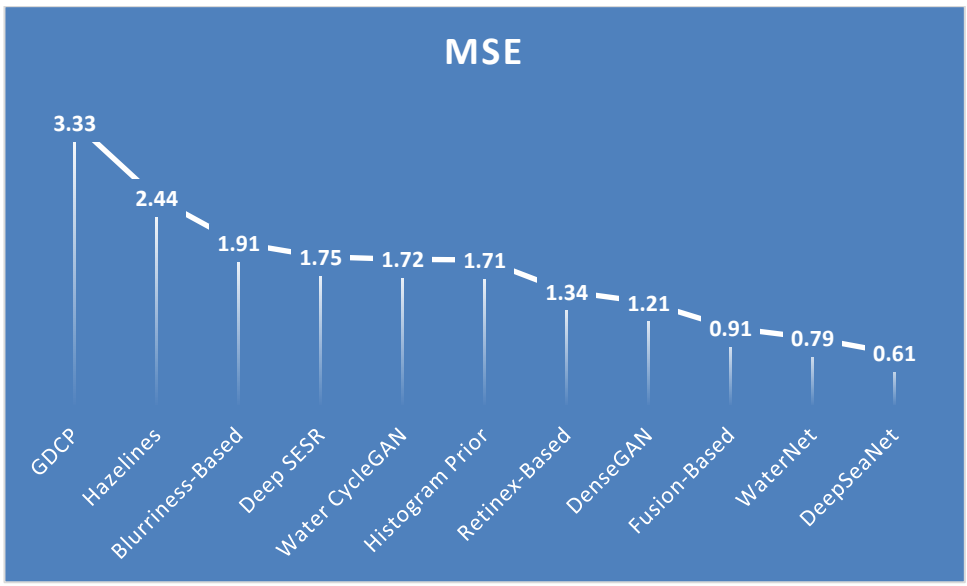

Figure 5.28. Analysis of the MSE evaluation parameter present in Table 5.12

By analyzing Figure 5.28, we can easily understand that the GDCP method is performing the lowest with a MSE value of 3.33 and the DeepSeaNet method is performing the best with a MSE value of 0.61 among the methods that have been compared in Table 5.12.

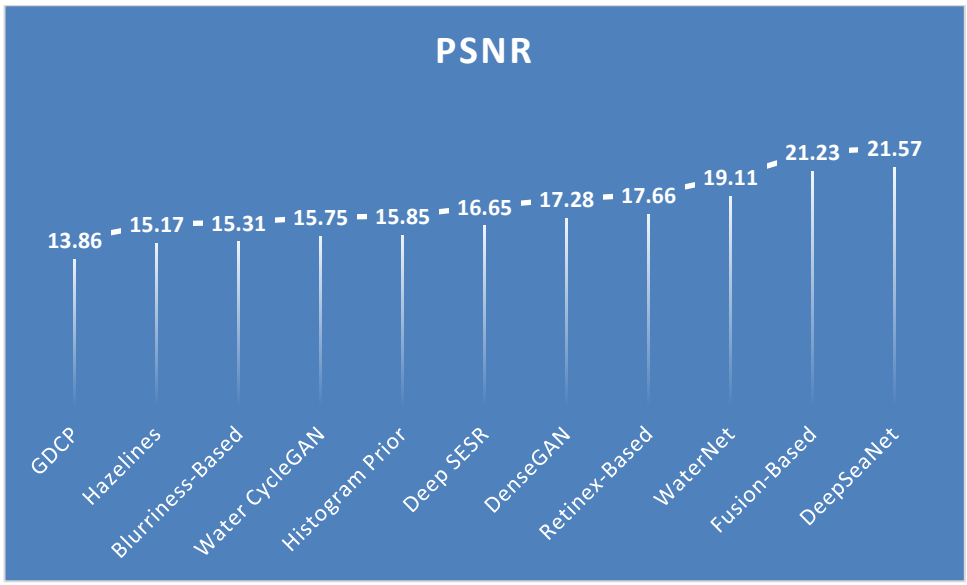

Figure 5.29. Analysis of the PSNR evaluation parameter present in Table 5.12

By analyzing Figure 5.29, we can easily understand that the GDCP method is performing the lowest with a PSNR value of 13.86 and the DeepSeaNet method is performing the best with a PSNR value of 21.57 among the methods that have been compared in Table 5.12.

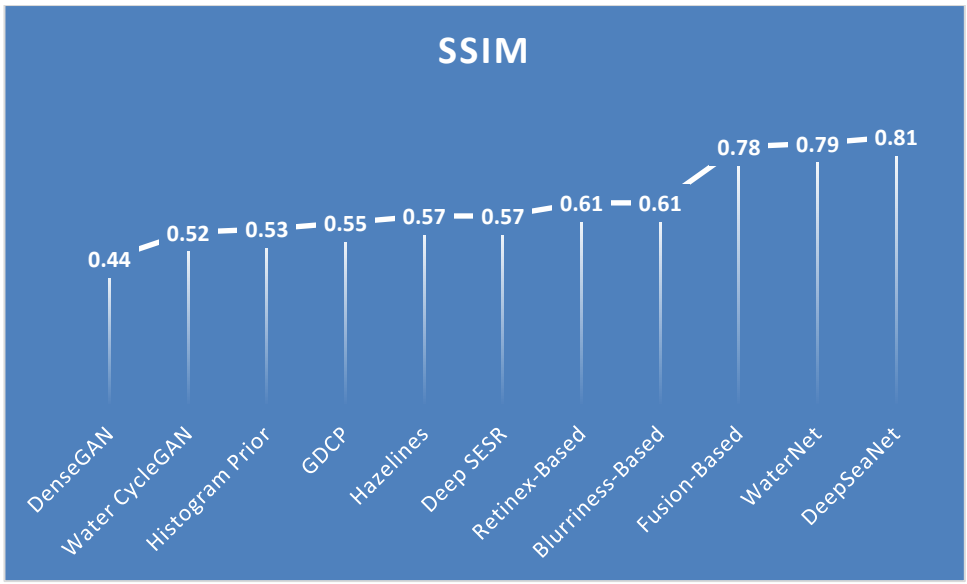

Figure 5.30. Analysis of the SSIM evaluation parameter present in Table 5.12

By analyzing Figure 5.30, we can easily understand that the DenseGAN method is performing the lowest with a SSIM value of 0.44 and the DeepSeaNet method is performing the best with a SSIM value of 0.81 among the methods that have been compared in Table 5.12.

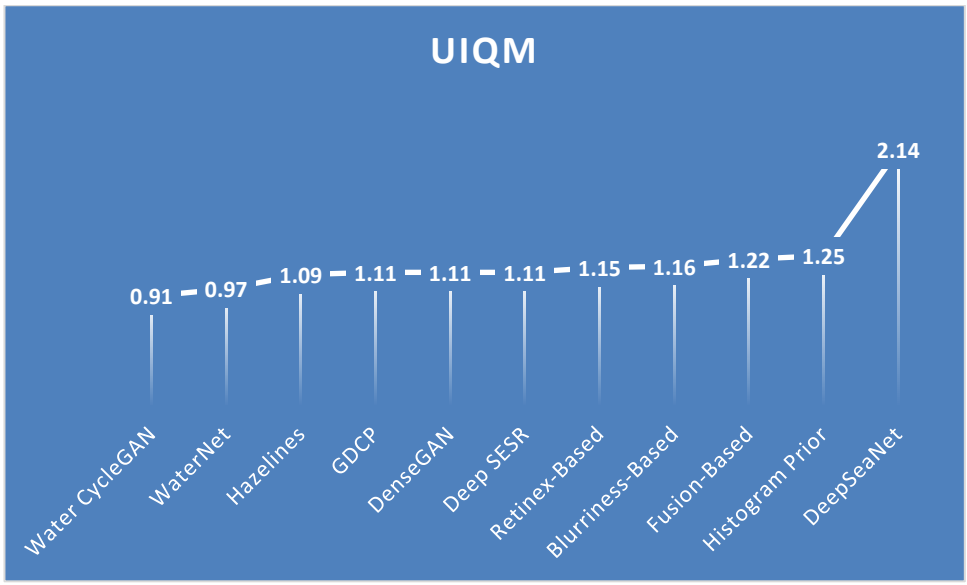

Figure 5.31. Analysis of the UIQM evaluation parameter present in Table 5.12

By analyzing Figure 5.31, we can easily understand that the Water CycleGAN method is performing the lowest with a UIQM value of 0.91 and the DeepSeaNet method is performing the best with a UIQM value of 2.14 among the methods that have been compared in Table 5.12.

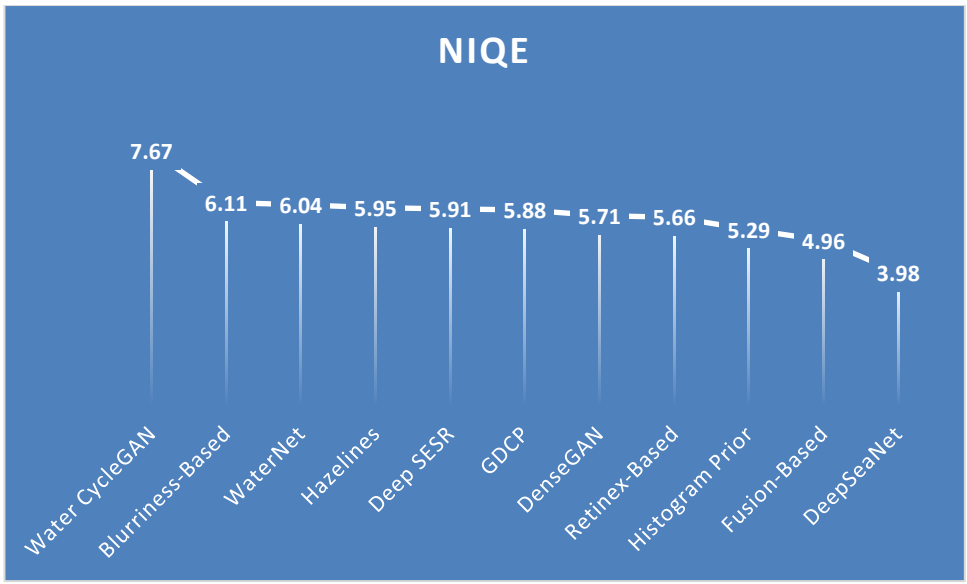

Figure 5.32. Analysis of the NIQE evaluation parameter present in Table 5.12

By analyzing Figure 5.32, we can easily understand that the Water CycleGAN method is performing the lowest with a NIQE value of 7.67 and the DeepSeaNet method is performing the best with a UIQM value of 3.98 among the methods that have been compared in Table 5.12.

A quantitative evaluation of the DeepSeaNet model for underwater image enhancement on the Challenge set of the UIEB dataset has also been shown. The improved results achieved by applying the suggested work keep the blue characteristic of the water stronger than current efforts like U-color [92].

Table 5.13 displays the quantitative evaluation of the DeepSeaNet model for underwater image enhancement on the Challenge set of the UIEB dataset. The suggested DeepSeaNet model outperforms the previous best published research through a considerable improvement in SSIM, NIQE, and UIQM.

Table 5.13 has been further analyzed with the help of graphs for each evaluation parameter, as given in Figures 5.33.–5.37.

Table 5.13. Quantitative evaluation of DeepSeaNet model for underwater image enhancement on UIEB dataset Challenge set. The top two outcomes are represented in bold.

Methods	MSE	PSNR	SSIM	UIQM	NIQE
Fusion-Based	0.88	15.68	0.65	1.45	5.88
Histogram Prior	1.32	13.55	0.46	**1.49**	5.55
Retinex-Based	1.15	15.36	0.58	1.25	5.89
GDCP	3.21	11.32	0.56	1.14	5.68
Blurriness-Based	1.52	14.56	0.52	1.36	6.35
Water Cycle GAN	1.38	**17.86**	0.45	1.03	6.65
Dense GAN	0.98	15.36	0.32	1.33	5.26
Water Net	**0.88**	16.35	**0.68**	1.09	6.34
Haze lines	2.11	14.65	0.46	1.23	5.75
Deep SESR	0.93	15.36	0.71	1.35	**4.97**
DeepSeaNet	**0.79**	**19.35**	**0.75**	**1.95**	**4.68**

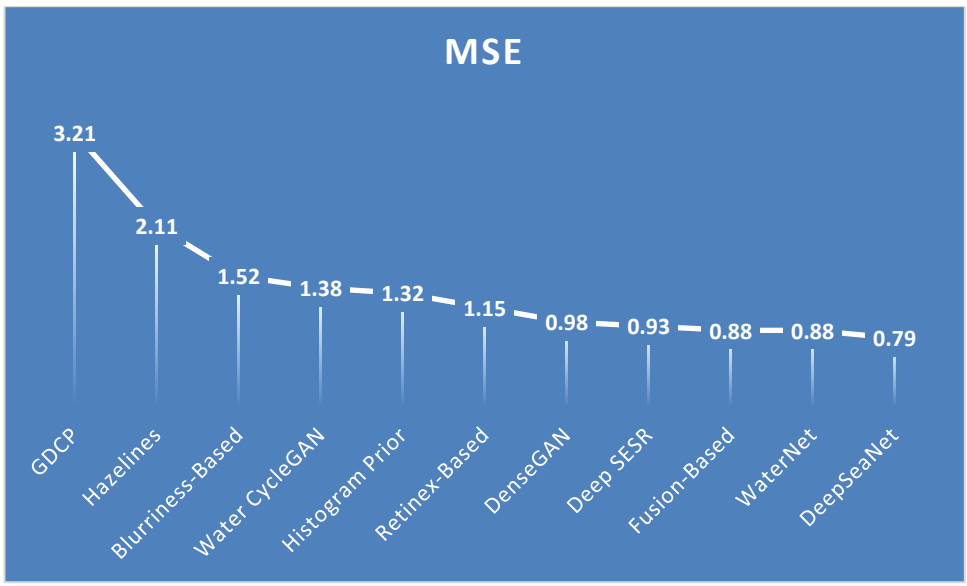

Figure 5.33. Analysis of the MSE evaluation parameter present in Table 5.13

By analyzing Figure 5.33, we can easily understand that the GDCP method is performing the lowest with a MSE value of 3.21 and the DeepSeaNet method is performing the best with a MSE value of 0.79 among the methods that have been compared in Table 5.13.

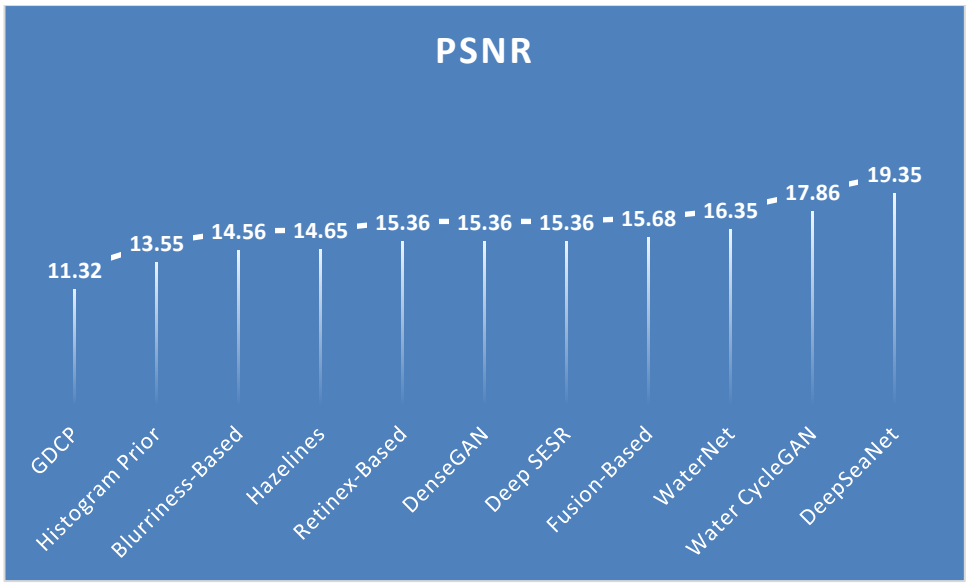

Figure 5.34. Analysis of the PSNR evaluation parameter present in Table 5.13

By analyzing Figure 5.34, we can easily understand that the GDCP method is performing the lowest with a PSNR value of 11.32 and the DeepSeaNet method is performing the best with a PSNR value of 19.35 among the methods that have been compared in Table 5.13.

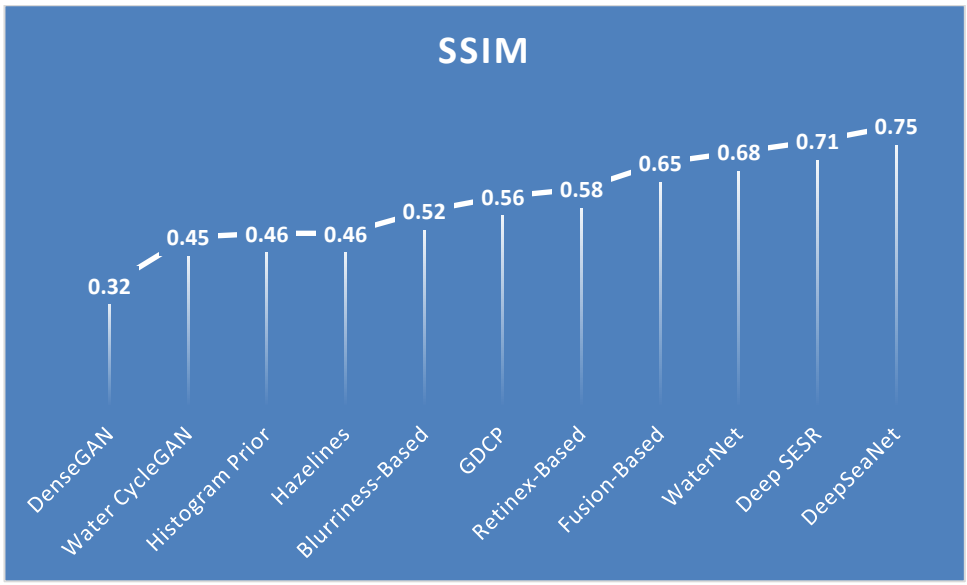

Figure 5.35. Analysis of the SSIM evaluation parameter present in Table 5.13

By analyzing Figure 5.35, we can easily understand that the DenseGAN method is performing the lowest with a SSIM value of 0.32 and the DeepSeaNet method is performing the best with a PSNR value of 0.75 among the methods that have been compared in Table 5.13.

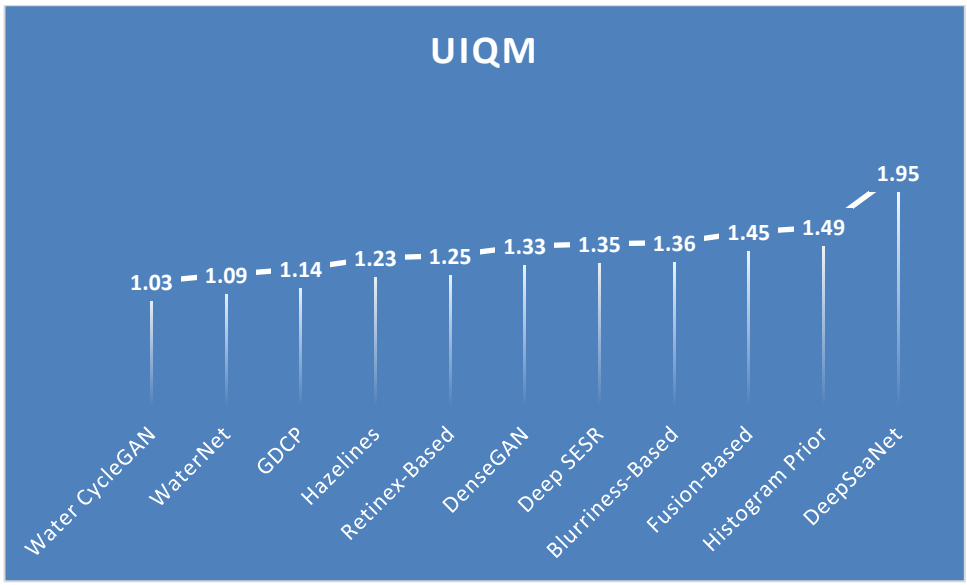

Figure 5.36. Analysis of the UIQM evaluation parameter present in Table 5.13

By analyzing Figure 5.36, we can easily understand that the Water CycleGAN method is performing the lowest with a UIQM value of 1.03 and the DeepSeaNet method is performing the best with a UIQM value of 1.95 among the methods that have been compared in Table 5.13.

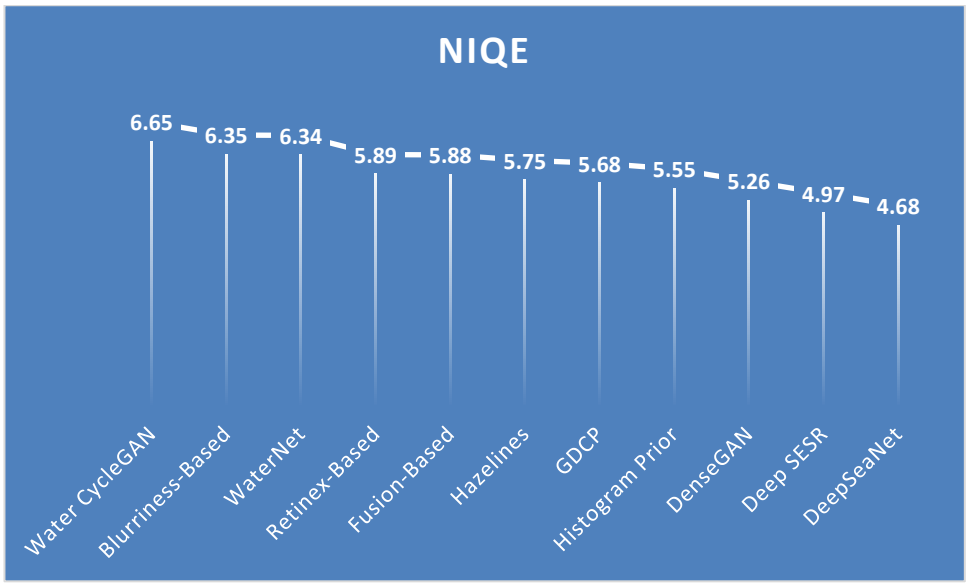

Figure 5.37. Analysis of the NIQE evaluation parameter present in Table 5.13

By analyzing Figure 5.37, we can easily understand that the Water CycleGAN method is performing the lowest with a NIQE value of 6.65 and the DeepSeaNet method is performing the best with a NIQE value of 4.68 among the methods that have been compared in Table 5.13.

Table 5.14 represents the quantitative evaluation of the DeepSeaNet algorithm for underwater image enhancement on the UFO-120 dataset. It illustrates how the proposed wavelength-specific multiple contextual deep convolutional

neural networks outperformed on an untrained dataset for the underwater image improvement task. Despite a minor loss in PSNR, there was a large efficiency improvement in MSE, SSIM, and NIQE. Our suggested approach beat the Deep SESR [79] by 3.04% in UIQM. Figure 5.38 represents the qualitative comparison between the various enhanced methods on the UFO-120 dataset. Our method, DeepSeaNet, provides the most enhanced resultant images in the UFO-120 dataset.

Table 5.14 has been further analyzed with the help of graphs for each evaluation parameter, as given in Figures 5.39.–5.43.

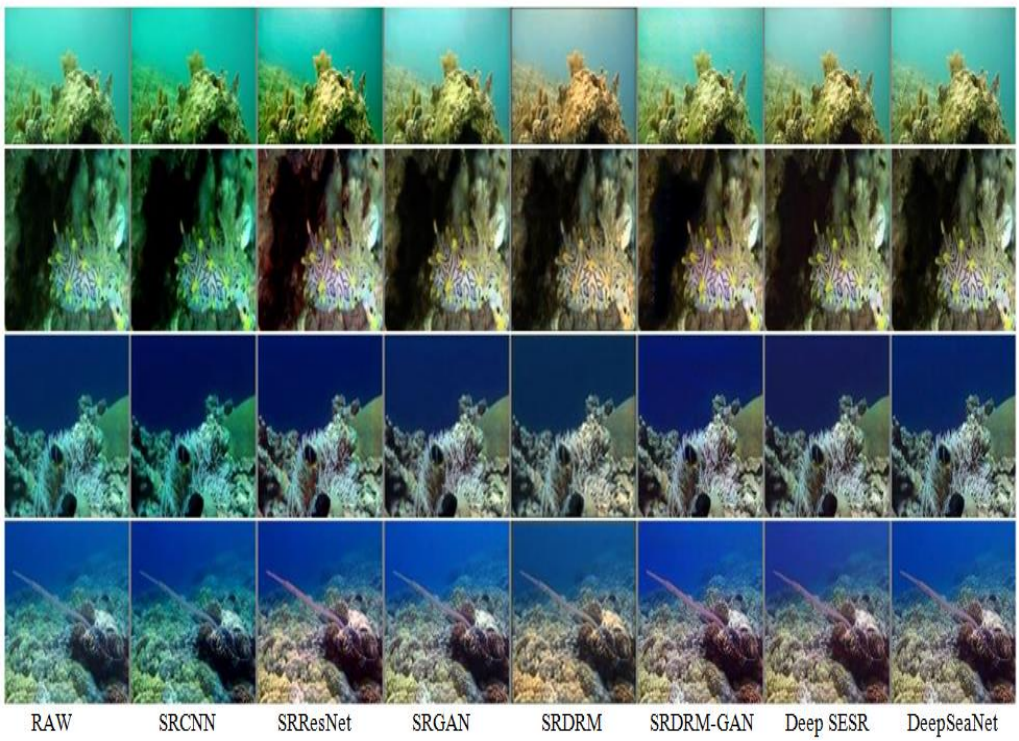

Figure 5.38. Qualitative representation of DeepSeaNet model for underwater image enhancement on UFO-120 dataset.

Table 5.14. Quantitative evaluation of DeepSeaNet model for underwater image enhancement on UFO-120 dataset. The top two results are shown in bold.

Methods	MSE	PSNR	SSIM	UIQM	NIQE
SRCNN	**0.82**	22.22	0.56	2.24	**5.52**
SRResNet	1.22	23.85	0.56	2.18	8.35
SRGAN	0.95	23.87	0.58	2.39	6.53
SRDRM	1.46	22.65	0.67	2.33	7.54
SRDRM-GAN	0.88	24.45	**0.68**	2.33	8.65
Deep SESR	0.96	**26.86**	0.66	**2.87**	7.36
DeepSeaNet	**0.75**	**25.23**	**0.74**	**2.96**	**4.66**

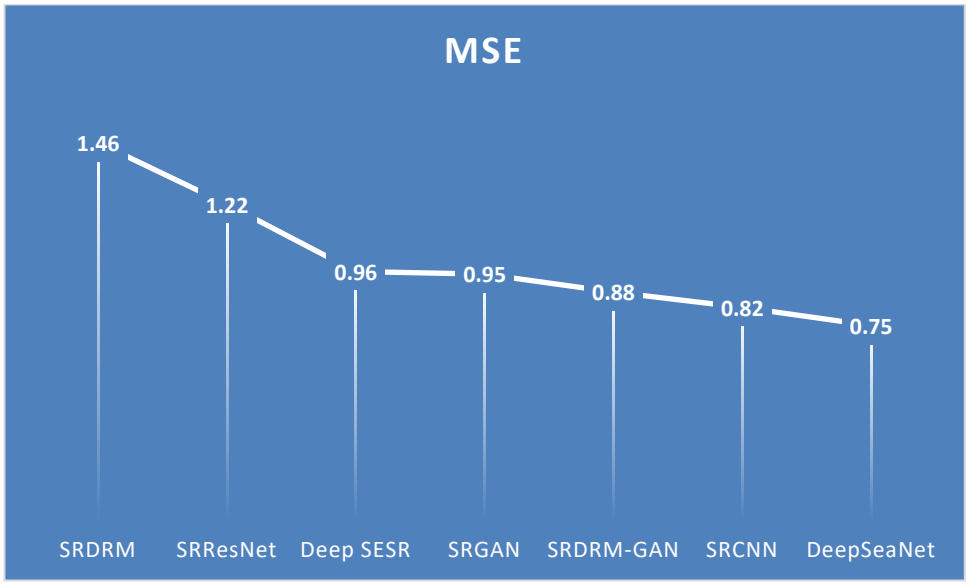

Figure 5.39. Analysis of the MSE evaluation parameter present in Table 5.14

By analyzing Figure 5.39, we can easily understand that the SRDRM method is performing the lowest with a MSE value of 1.46 and the DeepSeaNet method is performing the best with a NIQE value of 0.75 among the methods that have been compared in Table 5.14.

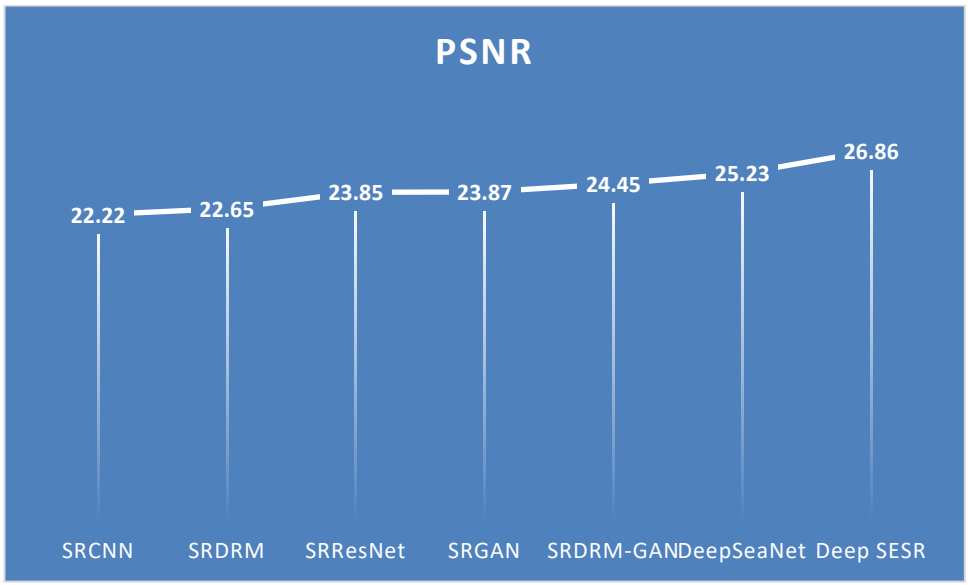

Figure 5.40. Analysis of the PSNR evaluation parameter present in Table 5.14

By analyzing Figure 5.40, we can easily understand that the SRCNN method is performing the lowest with a PSNR value of 22.22 and the Deep SESR method is performing the best with a PSNR value of 26.86 among the methods that have been compared in Table 5.14. Our method, DeepSeaNet, shows the second highest efficiency with a PSNR value of 25.23.

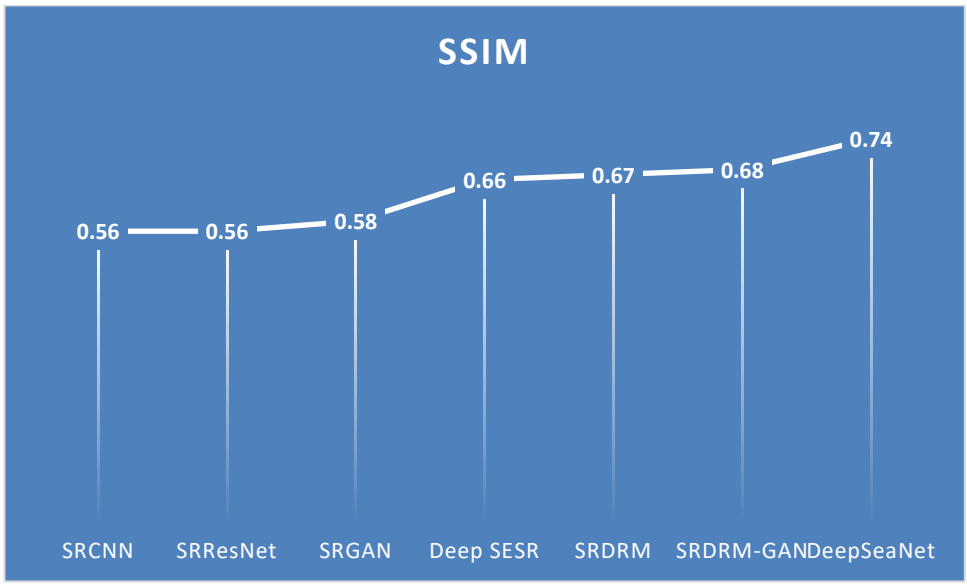

Figure 5.41. Analysis of the SSIM evaluation parameter present in Table 5.14

By analyzing Figure 5.41, we can easily understand that the SRCNN method is performing the lowest with a SSIM value of 0.56 and the DeepSeaNet method is performing the best with a SSIM value of 0.74 among the methods that have been compared in Table 5.14.

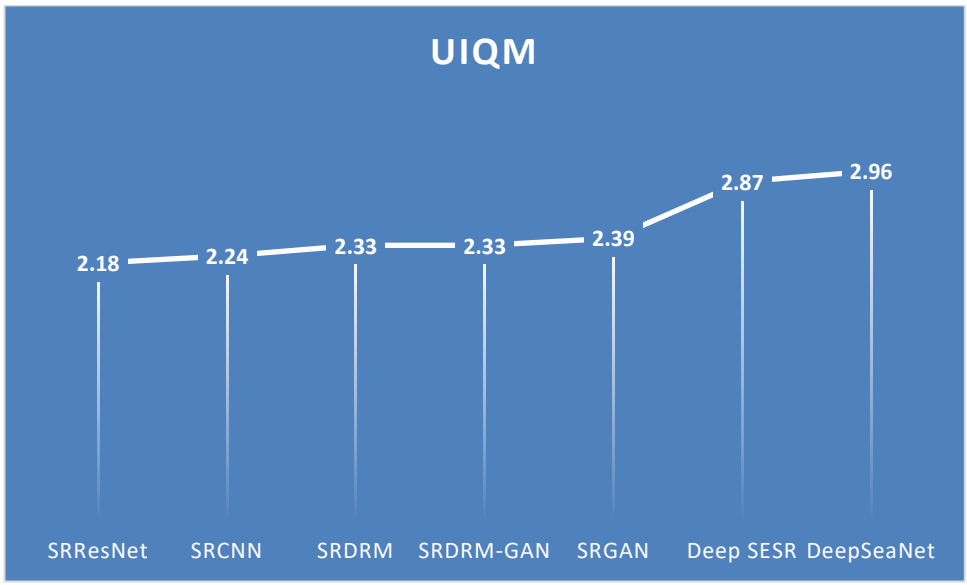

Figure 5.42. Analysis of the UIQM evaluation parameter present in Table 5.14

By analyzing Figure 5.42, we can easily understand that the SRResNet method is performing the lowest with a UIQM value of 2.18 and the DeepSeaNet method is performing the best with a UIQM value of 2.96 among the methods that have been compared in Table 5.14.

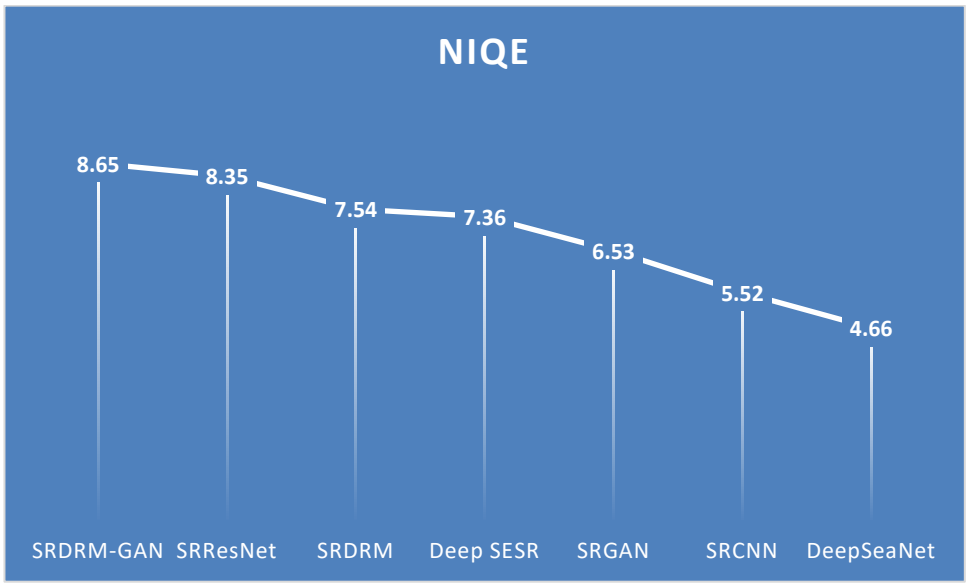

Figure 5.43. Analysis of the NIQE evaluation parameter present in Table 5.14

By analyzing Figure 5.43, we can easily understand that the SRResNet method is performing the lowest with a NIQE value of 8.65 and the DeepSeaNet method is performing the best with a NIQE value of 4.66 among the methods that have been compared in Table 5.14.

5.3 Conclusion

We performed a comparison and analysis of various methods with our CUS model and DeepSeaNet model of underwater image enhancement for enhancing underwater and deep-sea images and increasing their overall quality in this detailed discussion. In the CUS model, color expansion, bilateral filtering, and contrast improvement have been employed to deal with the challenges of underwater circumstances. A contrast correction as well as a color correction approach are used in a fusion-based approach one after another to enhance the contrast, color, and other features of underwater images and to remove different noise particles.

In the DeepSeaNet model, a four-stage architecture is designed where, in the first three stages, a degraded image is converted into a global color correction residual. This is further passed to the fourth stage, where the final enhanced deep-sea underwater image has been generated by applying deconvolutional operations. We also used CBAM in our DeepSeaNet model to increase the efficiency of the convolutional and deconvolutional operations.

We evaluated our both models with the help of qualitative and quantitative analysis. We use tables, images, and graphs to show and compare our results with various pre-existing models. Our collaborative efforts are proposed to provide enhanced underwater image quality while addressing the unique problems connected with this area.

CHAPTER 6

CONCLUSION AND FUTURE WORK

In this final chapter we summarize our thesis work, it provides the deep detailed discoveries and their contributions. The proposed model explained their overall contribution, showing their superiority in underwater image enhancement. We also included various possibilities for future research and their development.

The main summary of the thesis is summarized in the conclusion, which provides a discrete summary of the models, their explanation with result. This complete research has been focused on the major findings and the perception learned from the development and the use of the designed models.

In last the chapter discussed the major contribution of the proposed model in underwater image enhancement. It contains the development of the model, their approach, and their possible uses. The chapter also highlights the future work that will make the significance new thought in the research evident.

This research work proposes underwater image enhancement models with the help of enhancement techniques as well as enhancement using deep learning techniques to enhance the quality of underwater images. The first proposed underwater image enhancement framework implements a CUS model with the help of image enhancement techniques. The implemented algorithm utilizes contrast improvement using histogram stretching and color correction using CIELAB color space to increase the quality of images. The second proposed underwater image enhancement framework implements a DeepSeaNet model with the help of image enhancement techniques using deep learning techniques to enhance the quality of underwater images. The implemented algorithm utilizes color improvement using CBAM to improve the quality of images. The efficiency of the suggested models was compared to the most recent methods, generating significant improvements for many metrics like MSE, PSNR, UIQM, UCIQE, and UICM for all techniques that were studied. The quantitative and qualitative results, as well as the comparative analysis, indicate the efficiency and effectiveness of the suggested models.

6.1 Summary of the Thesis

This section discusses the thesis to solve the limitations as well as the difficulties addressed in underwater image methods using restoration and enhancement techniques.

Firstly, to address the improvement challenges of the underwater image enhancement model, this research work suggested novel CUS and DeepSeaNet models for the underwater image enhancement system to enhance the quality of underwater images.

Secondly, to provide robustness in the underwater image enhancement system, the proposed CUS architecture provides a promising solution using a single image-based system with independent datasets that provides equal weight to any dataset image and improves image quality.

Thirdly, to improve deep sea underwater image quality, the suggested model deploys CBAM-based algorithms to provide efficiency, achieve improvement, and enhance the quality of images, depending upon the wavelength criteria for each channel.

Lastly, we provide the result analysis and comparative analysis of our framework with various other techniques and have given significant results in terms of various evaluation criteria.

6.2 Contribution of the Research

This study discusses the technique used to handle the issues of underwater image enhancement systems. We have suggested the CUS and DeepSeaNet frameworks for the improvement of the underwater image's quality.

6.2.1 CUS Model

In this research, we analyzed challenges with water images and videos and current underwater image improvement techniques and successfully suggested a novel image enhancement approach called CUS for a variety of underwater images. Various underwater image enhancement algorithms have been used to enhance the images, but they are mostly dataset specific. We worked not only on the color element but also on the contrast element. This fusion-based enhancement

approach is a single image-based system that not only improves the result over other standard methods but also works well on various datasets. That's why it is also dataset independent. This dataset-independent approach provides robustness to our model, which makes it superior in comparison to other methods. Our suggested model initially conducts contrast improvement using a basic histogram stretching with adaptive characteristics obtained in the RGB color space that considers both the raw image's histogram distribution parameter and the underwater propagation capabilities of distinct light channels. The CIE Lab color model is then used to perform adaptive stretching for color improvement. After that, our proposed technique is compared to other standard dehazing models, such as DCP, as well as other enhancement models like UCM and ICM. These enhancement models also use histogram stretching in HSI/HSV and R-G-B color spaces. Qualitative and quantitative findings show that our technique is more successful at increasing visibility, improving details, and reducing artifacts and noise from images. Other underwater image datasets can also benefit from the incorporation of histogram restructuring in RGB and CIE Lab color models. Hence, it shows that our system is highly robust in nature, which provides a fruitful output for different datasets.

6.2.2 DeepSeaNet Framework

In this research, we developed a unique deep learning-based algorithm for underwater images. We designed it by using the unique receptive field size of every image channel, which is determined by their wavelength. These multi-contextual features aids in understanding many global as well as local characteristics based on each channel of every images. Further, these characteristics are again modified with the help of convolutional block attention module, which significantly increased the suggested approach performance. Our suggested model is structurally adaptable to allow increased underwater image

spatial resolution. We demonstrated the superiority of the designed method above existing best-published research across many standard datasets.

6.3 Future Work

Even though our method outperforms the competition, it has following aspects that should be considered in future research:

1) On one side, our method may have over-enhanced regions for underwater images taken in artificial light in the DeepSeaNet framework. We can do this by applying some dehazing approach before passing the dataset into the neural network. On the other hand, the process of choosing the CIE lab color space may increase the algorithm's complexity in the CUS framework. We can reduce the complexity of CUS framework by processing the image directly using the RGB color space with some advance techniques.

2) Developing underwater image enhancement systems that are more robust and computationally efficient. The proposed image enhancement approach should be capable of adapting to various underwater environments and developing an effective enhancement approach for various types of underwater image applications. We may conclude from this research that only a few of the techniques can increase the quality of underwater images.

3) Creating a own underwater image dataset, and then test the algorithms whether it will perform well or not.

4) Providing a relationship between low-level image processing and high-level classification and detection Existing underwater image enhancement approaches concentrate on increasing image intuitive effects while ignoring whether the improved images may improve the precision of high-level characteristic analysis like object classification and recognition.

5) Designing an efficient underwater image quality evaluation measure. Although few image quality evaluation measures have been published, only a few are applicable to underwater images. Here, the commonly used UIQM and UCIQE, which are motivated by human vision structure properties to evaluate underwater color images, failed to give a valid evaluation of the quality of the underwater image. Their assessment prefers overly enhanced colored images, which contradicts subjective preferences for naturalness. Future work must be given to the sensible combination of both objective and subjective evaluation, as well as the continuous improvement of non-reference evaluation models.

List of Publications

Research Papers Details in International Journals:

- N. Singh and A. Bhat, "A systematic review of the methodologies for the processing and enhancement of the underwater images", *Multimedia Tools and Applications*, vol. 82, pp. 38371-38396, 2023. DOI: 10.1007/s11042-023-15156-9. (SCIE, IF: 3.6)

- N. Singh and A. Bhat, "A Robust Model for Improving the Quality of Underwater Images using Enhancement Techniques", *Multimedia Tools and Applications*, vol. 83, pp. 2267-2288, 2023. DOI: 10.1007/s11042-023-15617-1. (SCIE, IF: 3.6)

- N. Singh and A. Bhat, "Deep Sea Underwater Image Enhancement using Convolutional Module", *Expert System* (2023). (Accepted) (SCIE, IF: 3.3)

- N. Singh and A. Bhat, "Underwater Image Enhancement using Contrast Correction", *New Generation Computing* (2024) (Under Review) (SCIE, IF: 2.6)

Research Papers Published in International Conferences:

- N. Singh and A. Bhat, "A Detailed Understanding of Underwater Image Enhancement using Deep Learning", *International Conference on Information Systems and Computer Networks (ISCON)*, pp. 1-6, 2021. DOI: 10.1109/ISCON52037.2021.9702312.

- N. Singh and A. Bhat, “Underwater Image Enhancement using Convolutional Block Attention Module”, *International Conference on Information Systems and Computer Networks (ISCON)*, pp. 1-5, 2023. DOI: 10.1109/ISCON57294.2023.10111974.

- N. Singh and A. Bhat, “Comparative Result Analysis of Underwater Image Enhancement methods”, *International Conference on Computing, Communication and Networking Technologies (ICCCNT)*, pp. 1-5, 2023. DOI: 10.1109/ICCCNT56998.2023.10307108.

References

[1] G. Buchsbaum, “A spatial processor model for object colour perception”, *Journal of the Franklin Institute*, vol. 310, no. 1, pp. 1–26, 1980.

[2] R. Hummel, “Image enhancement by histogram transformation”, *Computer Graphics and Image Processing*, vol. 6, no. 2, pp. 184–195, 1977.

[3] Y. C. Liu, W. H. Chan and Y. Q. Chen, “Automatic white balance for digital still camera”, *IEEE Transactions on Consumer Electronics*, vol. 41, no. 3, pp. 460–466, 2004.

[4] S. M. Pizer, R. E. Johnston, J. P. Ericksen, B. C. Yankaskas and K. E. Muller, “Contrast-limited adaptive histogram equalization: speed and effectiveness”, *Visualization in Biomedical Computing*, vol. 337, no. 2, 1990.

[5] D. H. Foster, “Color constancy”, *Vision Research*, vol. 51, no. 7, pp. 674–700, 2011.

[6] C. Ancuti, C. O. Ancuti, T. Haber and P. Bekaert, “Enhancing underwater images and videos by fusion”, *IEEE Conference on Computer Vision and Pattern Recognition*, pp. 81-88, 2012.

[7] D. J. Jobson, Z. Rahman, and G. A. Woodell, “A multiscale retinex for bridging the gap between color images and the human observation of scenes”, *IEEE Transactions on Image Processing*, vol. 6, no. 7, pp. 965–976, 2002.

[8] K. Iqbal, M. O. Odetayo, A. E. James, R. A. Salam, and A. Z. Talib, “Enhancing the low-quality images using unsupervised colour correction method”, *IEEE International Conference on Systems Man and Cybernetics*, pp. 1703-1709, 2010.

[9] M. S. Hitam, E. A. Awalludin, N. J. H. W. Y. Wan, and Z. Bachok, "Mixture contrast limited adaptive histogram equalization for underwater image enhancement", *International Conference on Computer Applications Technology*, pp. 1-5, 2013.

[10] A. S. A. Ghani and N. A. M. Isa, "Underwater image quality enhancement through integrated color model with Rayleigh distribution", *Applied Soft Computing*, vol. 27, pp. 219–230, 2015.

[11] J. S. Jaffe, "Computer modeling and the design of optimal underwater imaging systems", *IEEE Journal of Oceanic Engineering*, vol. 15, no. 2, pp. 101–111, 1990.

[12] K. He, J. Sun, and X. Tang, "Single image haze removal using dark channel prior", *Computer Vision and Pattern Recognition*, vol. 33, no. 12, pp. 2341-2353, 2009.

[13] J. Y. Chiang and Y. Chen, "Underwater image enhancement by wavelength compensation and dehazing", *IEEE Transactions on Image Processing*, vol. 21, no. 4, pp. 1756–1769, 2012.

[14] P. D. Jr, E. D. Nascimento, F. Moraes, and S. Botelho, "Transmission estimation in underwater single images", *IEEE International Conference on Computer Vision Workshops*, pp. 825–830, 2013.

[15] A. Galdran, D. Pardo, A. Picon, and A. Alvarez-Gila, "Automatic red channel underwater image restoration", *Journal of Visual Communication and Image Representation*, vol. 26, pp. 132–145, 2015.

[16] N. Carlevaris-Bianco, A. Mohan, and R. M. Eustice, "Initial results in underwater single image dehazing", *Oceans Engineering*, pp. 1-8, 2010.

[17] N. Wang, H. Zheng and B. Zheng, “Underwater image restoration via maximum attenuation identification”, *IEEE Access*, vol. 5, no. 99, pp. 18941-18952, 2017.

[18] Y. T. Peng and P. C. Cosman, “Underwater image restoration based on image blurriness and light absorption”, *IEEE Transactions on Image Processing*, vol. 26, no. 4, pp. 1579–1594, 2017.

[19] Y. Wang, H. Liu, and L. P. Chau, “Single underwater image restoration using adaptive attenuation-curve prior”, *IEEE Transactions on Circuits and Systems*, vol. PP, no. 99, pp. 1–11, 2017.

[20] Y. Li, S. Takahashi and S. Serikawa, “Cognitive Ocean of things: a comprehensive review and future trends”, *Wireless Networks,* pp. 1-10, 2019.

[21] T. Uemura, H. Lu and H. Kim, “Marine organisms tracking and recognizing using Dehazing and Deep Learning”, *International Conference on Robotic Sensor Networks*, pp. 53-58, 2020.

[22] F. Almabouada, M. A. Abreu, J. M. P. Coelho and K. E. Aiadi, “Experimental and simulation assessments of underwater light propagation”, *Frontiers of Optoelectronics*, vol. 12, no. 4, pp. 405-412, 2019.

[23] R. E. Hufnagel and N. R. Stanley, “Modulation transfer function associated with image transmission through turbulent media”, *Journal of the Optical Society of America,* vol. 54, no. 1, pp. 52-60, 1964.

[24] M. Yang and C. Gong C, “Underwater image restoration by turbulence model based on image gradient distribution”, *International Conference on Uncertainty Reasoning and Knowledge Engineering*, pp. 296-299, 2012.

[25] B. L. McGlamery, “A computer model for underwater camera systems”, *International Society for Optics and Photonics,* vol. 208, pp, 221-231,1980.

[26] S. Honjo, K. W. Doherty and Y. C. Agrawal, “Direct optical assessment of large amorphous aggregates (marine snow) in the deep ocean”, *Oceanographic Research Papers,* vol. 31, no. 1, pp. 67-76, 1984.

[27] E. Trucco and A. T. Olmos-Antillon, “Self-tuning underwater image restoration”, *IEEE Journal of Oceanic Engineering,* vol. 31, no. 2, pp. 511-519, 2006.

[28] W. Hou, D. J. Gray and A. D. Weidemann, “Automated underwater image restoration and retrieval of related optical properties”, *IEEE International Geoscience and Remote Sensing Symposium,* pp. 1889-1892, 2007.

[29] W. Hou, A. D. Weidemann and D. J. Gray, “Imagery derived modulation transfer function and its applications for underwater imaging”, *International Society for Optics and Photonics,* vol. 6696, pp. 707-714, 2007.

[30] W. Hou, D. J. Gray and A. D. Weidemann, “Comparison and validation of point spread models for imaging in natural waters”, *Optics Express,* vol. 16, no. 13, pp. 9958-9965, 2008.

[31] V. A. D. Grosso, “Modulation transfer function of water”, *Oceans 75 Conference,* pp. 331-347, 1975.

[32] V. A. D. Grosso, “Optical transfer function measurements in the Sargasso Sea”, *International Society for Optics and Photonics,* pp. 74-101, 1978.

[33] K. J. Voss and A. L. Chapin, “Measurement of the point spread function in the ocean”, *Applied optics,* vol. 29, no. 25, pp. 3638-3642, 1990.

[34] J. Y. Chiang, Y. C. Chen, and Y. F. Chen, "Underwater image enhancement: using wavelength compensation and image dehazing (WCID)", *In International Conference on Advanced Concepts for Intelligent Vision Systems,* pp. 372-383, 2011.

[35] T. Li, S. Rong, W. Zhao, L. Chen, Y. Liu, H. Zhou and B. He, "Underwater image enhancement using adaptive color restoration and dehazing", *Optics Express*, vol. 30, no. 4, pp. 6216-6235, 2022.

[36] Y. T. Peng, X. Zhao and P. C. Cosman, "Single underwater image enhancement using depth estimation based on blurriness", *Proceeding IEEE International Conference on Image Processing*, pp. 4952-4956, 2015.

[37] Y. T. Peng and P. C. Cosman, "Single image restoration using scene ambient light differential", *Proceeding IEEE International Conference on Image Processing (ICIP 2016)*, pp. 1953-1957, 2016.

[38] X. Ding, Y. Wang and J. Zhang, "Underwater image dehaze using scene depth estimation with adaptive color correction", *Proceeding of IEEE Oceans,* pp. 1-5, 2017.

[39] Y. Cho, Y. S. Shin and A. Kim, "Online depth estimation and application to underwater image dehazing", *Oceans 2016 MTS/IEEE Monterey*, pp. 1-7, 2016.

[40] C. O. Ancuti, C. Ancuti, C. De, "Locally adaptive color correction for underwater image dehazing and matching", *Proceeding on IEEE Computer Vision and Pattern Recognition,* pp. 1-9, 2017.

[41] Y. Wang, H. Liu and H. P. Chau, “Single underwater image restoration using attenuation-curve prior”, *IEEE International Symposium on Circuits and Systems (ISCAS 2017),* pp. 1-4, 2017.

[42] S. Emberton, L. Chittka and A. Cavallaro, “Underwater image and video dehazing with pure haze region segmentation”, *Computer Vision and Image Understanding,* vol. 168, pp. 145-156, 2018.

[43] C. Ancuti, C. O. Ancuti and C. De, “Multi-scale underwater descattering”, *International Conference on Pattern Recognition (ICPR 2016),* pp. 4202-4207, 2016.

[44] C. Li, J. Guo and S. Chen, “Underwater image restoration based on minimum information loss principle and optical properties of underwater imaging”, *Proceeding IEEE International Conference on Image Processing, (ICIP 2016),* pp. 1993-1997, 2016.

[45] C. Li, J. Guo and C. Guo, “A hybrid method for underwater image correction”, *Pattern Recognition Letters,* vol. 94, pp. 62-67, 2017.

[46] S. Emberton, L. Chittka and A. Cavallaro, “Hierarchical rank-based veiling light estimation for underwater dehazing”, *Proceedings of the British Machine Vision Conference,* pp. 1-12, 2015.

[47] K. Wang, E. Dunn and J. Tighe, “Combining scene priors and haze removal for single image depth estimation”, *IEEE Winter Conference on Applications of Computer Vision,* pp. 800-807, 2014.

[48] K. R. Rai, P. Gour and B. Singh, “Underwater image segmentation using CLAHE enhancement and thresholding”, *International Journal of Emerging Technology and Advanced Engineering,* vol. 2, no. 1, pp. 118-123, 2012.

[49] S. Vasamsetti, N. Mittal and B. C. Neelapu, “Wavelet based perspective on variational enhancement technique for underwater imagery”, *Ocean Engineering,* vol. 141, pp. 88-100, 2017.

[50] H. W. Han, X. H. Zhang and W. L. Ge, “A mixed noise reduction algorithm for underwater laser images based on soft-morphological filter”, *Acta Photonica Sinica,* vol. 40, no. 1, pp. 136-141, 2011.

[51] A. Arnold-Bos, J. P. Malkasse and G. Kervern, “A preprocessing framework for automatic underwater images denoising”, *European Conference on Propagation and Systems,* pp. 15-18, 2005.

[52] S. Bazeille, I. Quidu and L. Jaulin and J. P. Malkasse, “Automatic underwater image pre-processing”, *Proceeding Caracterisation Du Milieu Marin (CMM06),* pp. 16-19, 2006.

[53] D. X. Jia and Y. R. Ge, “Underwater image de-noising algorithm based on non-sub sampled contour let transform and total variation”, *International Conference on Computer Science and Information Processing (CSIP 2012),* pp. 76-80, 2012.

[54] M. Chambah, D. Semani and A. Renouf A, “Underwater color constancy: Enhancement of automatic live fish recognition”, *Color Imaging IX: Processing, Hardcopy, and Applications,* pp. 157-168, 2003.

[55] Z. Fu, X. Fu, Y. Huang, and X. Ding, “Twice mixing: a rank learning-based quality assessment approach for underwater image enhancement”, *Signal Processing: Image Communication,* vol. 102, pp.116622, 2022.

[56] G. Hou, Z. Pan, B. Huang, G. Wang and X. Luan, “Hue preserving-based approach for underwater colour image enhancement”, *IET Image Processing*, vol. 12, no. 2, pp.292-298, 2018.

[57] L. A. Torres-Méndez and G. Dudek, “Color correction of underwater images for aquatic robot inspection”, *Proceeding of International Workshop Energy Minimization Methods Computer Vision and Pattern Recognition*, pp. 60-73, 2005.

[58] K. Iqbal, R. A. Salam and A. Osman, “Underwater image enhancement using an integrated color model”, *International Journal of Computer Science*, vol. 34, no. 2, pp. 1-6, 2007.

[59] F. Petit, A. S. Capelle-Laize and P. Carre, “Underwater image enhancement by attenuation inversion with quaternions”, *IEEE International Conference on Acoustics, Speech and Signal Processing, (ICASSP 2009)*, pp. 1177-1180, 2009.

[60] X. Fu, P. Zhuang and Y. Huang, “A retinex-based enhancing approach for single underwater image”, *IEEE International Conference on Image Processing (ICIP 2014)*, pp. 4572-4576, 2014.

[61] C. O. Ancuti, C, Ancuti, C. D. Vleeschouwer and P. Bekaert, “Color balance and fusion for underwater image enhancement”, *IEEE Transaction on Image Processing*, vol. 27, no. 1, pp. 379-393, 2018.

[62] M. Bryson, M. Johnson-Roberson, O. Pizarro and S. B. Williams, “True color correction of autonomous underwater vehicle imagery”, *Journal of Field Robotics*, vol. 33, no. 6, pp. 853-874, 2016.

[63] J. Perez, A. C. Attanasio, N. Nechyporenko and P. J. Sanz, "A deep learning approach for underwater image enhancement", *International Conference on the Interplay Between Natural and Artificial Computation,* pp. 183-192, 2017.

[64] J. Li, K. A. Skinner, R. M. Eustice and M. Johnson-Roberson, "Water-GAN: Unsupervised generative network to enable real-time color correction of monocular underwater images", *IEEE Robotics and Automation letters,* vol. 3, no. 1, pp. 387-394, 2017.

[65] A. Creswell, T. White, V. Dumoulin, K. Arulkumaran, B. Sengupta and A. A. Bharath, "Generative adversarial networks: An overview", *IEEE signal processing magazine,* vol. 35, no. 1, pp. 53-65, 2018.

[66] J. Y. Zhu, T. Park, P. Isola and A. A. Efros, "Unpaired image-to-image translation using cycle-consistent adversarial networks", *Proceeding IEEE International Conference on Computer Vision (ICCV 2017)*, pp. 2223-2232, 2017.

[67] C. Li, J. Guo and C. Guo, "Emerging from water: Underwater image color correction based on weakly supervised color transfer", *IEEE Signal Processing Letters,* vol. 25, no. 3, pp.323-327, 2018.

[68] M. J. Islam, Y. Xia and J. Sattar, "Fast underwater image enhancement for improved visual perception", *IEEE Robotics and Automation Letters*, vol. 5, no. 2, pp. 3227-3234, 2020.

[69] R. Han, G. Yang, Y. Zhibin, L. Peng and Z. Haiyong, "Underwater Image Enhancement Based on a Spiral Generative Adversarial Framework", *IEEE Access*, vol. 8, pp. 218838-218852, 2020.

[70] L. Shen, Y. Zhao, Q. Peng, J. C. W. Chan and S. G. Kong, “An iterative image dehazing method with polarization”, *IEEE Transactions on Multimedia*, vol. 21, no. 5, pp. 1093-1107, 2018

[71] W. E. K. Middleton, “Vision through the atmosphere”, *In geophysik ii/geophysics ii Springer, Berlin, Heidelberg*, pp. 254-287, 1957.

[72] B. H. Chen, Y. S. Tseng and J. L. Yin, “Gaussian-adaptive bilateral filter”, *IEEE Signal Processing Letters*, vol. 27, pp. 1670-1674, 2020.

[73] K. Iqbal, M. Odetayo, A. James, R. A. Salam, and A. Z. H, Talib, “Enhancing the low-quality images using Unsupervised Color Improvement Method”, *IEEE International Conference on Systems, Man and Cybernetics*, pp. 1703–1709, 2010.

[74] A. S. A . Ghani and N. A. M. Isa, “Underwater image quality enhancement through Rayleigh-stretching and averaging image planes”, *International Journal of Naval Architecture and Ocean Engineering*, vol. 6, no. 4, pp. 840-866, 2014.

[75] A. Bhat, A. Tyagi, A. Verdhan and V. Verma, “Fast Under Water Image Enhancement for Real Time Applications”, *International Conference for Convergence in Technology (I2CT)*, pp. 1-8, 2021.

[76] H. G. Daway and E. G. Daway, “Underwater image enhancement using colour restoration based on YCbCr colour model”, In *IOP Conference Series: Materials Science and Engineering*, vol. 571, no. 1, pp. 012125, 2019.

[77] C. Li, C. Guo, W. Ren, R. Cong, J. Hou, S. Kwong and D. Tao, “An underwater image enhancement benchmark dataset and beyond”, *IEEE Transactions on Image Processing*, vol. 29, pp. 4376-4389, 2019.

[78] L. Peng, C. Zhu and L. Bian, “U-shape Transformer for Underwater Image Enhancement”, *arXiv preprint arXiv:2111.11843*, 2021.

[79] M. J. Islam, P. Luo and J. Sattar, “Simultaneous enhancement and super-resolution of underwater imagery for improved visual perception”, *arXiv preprint arXiv:2002.01155*, 2020.

[80] R. Liu, X. Fan, M. Zhu, M. Hou and Z. Luo, “Real-world underwater enhancement: Challenges, benchmarks, and solutions under natural light”, *IEEE Transactions on Circuits and Systems for Video Technology*, vol. *30, no.* 12, pp. 4861-4875, 2020.

[81] C. Liu, H. Li, S. Wang, M. Zhu, D. Wang, X. Fan and Z. Wang, “A dataset and benchmark of underwater object detection for robot picking”, *IEEE International Conference on Multimedia & Expo Workshops (ICMEW)*, pp. 1-6, 2021.

[82] H. Wen, Y. Tian, T. Huang and W. Gao, “Single underwater image enhancement with a new optical model”, *IEEE International Symposium on Circuits and Systems (ISCAS)*, pp. 753-756, 2013.

[83] A. B. Tamou, A. Benzinou, K. Nasreddine and L. Ballihi, “Underwater live fish recognition by deep learning”, *International Conference on Image and Signal Processing*, Springer, Cham, pp. 275-283, 2018.

[84] G. Ulutas and B. Ustubioglu, “Underwater image enhancement using contrast limited adaptive histogram equalization and layered difference representation”, *Multimedia Tools and Applications*, vol. 80, no. 10, pp. 15067-15091, 2021.

[85] M. Narwaria, R. Mantiuk, M. P. Da Silva and P. Le Callet, “HDR-VDP-2.2: a calibrated method for objective quality prediction of high-dynamic range and standard images”, *Journal of Electronic Imaging,* vol. 24, no. 1, pp. 010501-010501, 2015.

[86] M. Yang and A. Sowmya, “An underwater color image quality evaluation metric”, *IEEE Transactions on Image Processing,* vol. 24, no. 12, pp. 6062-6071, 2015.

[87] C. Li, J. Quo, Y. Pang, S. Chen and J. Wang, “Single underwater image restoration by blue-green channels dehazing and red channel correction”, *IEEE International Conference on Acoustics, Speech and Signal Processing (ICASSP),* pp. 1731–1735, 2013.

[88] C. Fabbri, Md. J. Islam and J. Sattar, “Enhancing Underwater Imagery Using Generative Adversarial Networks”, *IEEE International Conference on Robotics and Automation (ICRA),* pp. 7159-7165, 2018.

[89] Y. Guo, H. Li and P. Zhuang, “Underwater Image Enhancement Using a Multiscale Dense Generative Adversarial Network”, *IEEE Journal of Oceanic Engineering,* vol. 45, no. 3, pp. 862–870, 2020.

[90] M. J. Islam, S. S. Enan, P. Luo and J. Sattar, “Underwater Image Super-Resolution using Deep Residual Multipliers”, *IEEE International Conference on Robotics and Automation (ICRA,)* pp. 900-906, 2020.

[91] N. Divakar and R. V. Babu, “Image Denoising via CNNs: An Adversarial Approach”, *Proceedings of the IEEE Conference on Computer Vision and Pattern Recognition (CVPR),* pp. 80-87, 2017.

[92] C. Li, S. Anwar, J. Hou, R. Cong, C. Guo and W. Ren, “Underwater Image Enhancement via Medium Transmission-Guided Multi-Color Space Embedding”, *IEEE Transactions on Image Processing*, vol. 30, pp. 4985-5000, 2021.

[93] Q. Yu, J. Zhang, H. Zhang, Y. Wang, Z. Lin, N. Xu, Y. Bai and A. Yuille, “Mask Guided Matting via Progressive Refinement Network”, *Proceedings of the IEEE/CVF Conference on Computer Vision and Pattern Recognition (CVPR)*, pp. 1154–1163, 2021.

[94] Y. Zhang, Y. Tian, Y. Kong, B. Zhong and Y. Fu, “Residual Dense Network for Image Super-Resolution”, *Proceedings of the IEEE Conference on Computer Vision and Pattern Recognition (CVPR)*, pp. 2472-2481, 2018.

[95] S. Woo, J. Park, J. Y. Lee and I. S. Kweon, “CBAM: Convolutional Block Attention Module”, *Proceedings of the European Conference on Computer Vision (ECCV)*, pp. 3-19, 2018.

[96] J. Johnson, A. Alahi and L. Fei-Fei, “Perceptual losses for real-time style transfer and super-resolution”, *European Conference on Computer Vision*, pp. 694-711, 2016.

[97] P. Sharma, I. Bisht and A. Sur, “Wavelength-based attributed deep neural network for underwater image restoration”, *ACM Transactions on Multimedia Computing, Communications and Applications*, vol. 19, no. 1, pp. 1-23, 2023.

[98] N. Singh, S. R. Dubey, P. Dixit and J. P. Gupta, “Semantic Image Retrieval Using Multiple Features”, *International Conference on Technical and Managerial Innovation in Computing and Communications in Industry and Academia*, pp. 277-284, 2012.

[99] G. Pchai, Z. Wang, G. Guo, Y. Chen, Y. Jin, W. Wang and X. Zhao, "Recurrent attention dense network for single image de-raining", *IEEE Access,* vol. 8, pp. 111278-111288, 2020.

[100] K. Simonyan and A. Zisserman, "Very Deep Convolutional Networks for Large-Scale Image Recognition", *arXiv preprint arXiv:1409.1556,* 2014.

[101] J. Deng, W. Dong, R. Socher, L.-J. Li, K. Li and L. Fei-Fei, "ImageNet: A large-scale hierarchical image database", *IEEE Conference on Computer Vision and Pattern Recognition*, pp. 248–255, 2009.

[102] Y. Wang, J. Zhang, Y. Cao and Z. Wang, "A deep CNN method for underwater image enhancement", *IEEE International Conference on Image Processing (ICIP*), pp. 1382–1386, 2017.

[103] Z. Wang, A. C. Bovik, H. R. Sheikh and E. P. Simoncelli, "Image Quality Assessment: From Error Visibility to Structural Similarity", *IEEE Transaction on Image Processing,* vol. 13, no. 4, pp. 600-612, 2004.

[104] A. Paszke, S. Gross, F. Massa, A. Lerer, J. Bradbury, G. Chanan, T. Killeen, Z. Lin, N. Gimelshein, L. Antiga, A. Desmaison, A. Kopf, E. Yang, Z. DeVito, M. Raison, A. Tejani, S. Chilamkurthy, B. Steiner, L. Fang, J. Bai and S. Chintala, "PyTorch: An Imperative Style, High-Performance Deep Learning Library", *Advances in Neural Information Processing Systems,* vol. 32, pp. 8024–8035, 2019.

[105] P. Diederik, J. Kingma and A. Ba, "A Method for Stochastic Optimization", *International Conference on Learning Representations (ICLR),* vol. 5, 2015.

[106] C. Li, J. Guo, R. Cong, Y. Pang and B. Wang, "Underwater Image Enhancement by Dehazing with Minimum Information Loss and Histogram

Distribution Prior", *IEEE Transactions on Image Processing,* vol. 25, no. 12, pp. 5664–5677, 2016.

[107] Y.-T. Peng, K. Cao and P. C. Cosman, "Generalization of the Dark Channel Prior for Single Image Restoration", *IEEE Transactions on Image Processing*, vol. 27, no. 6, pp. 2856–2868, 2018.

[108] D. Berman, D. Levy, S. Avidan and T. Treibitz, "Underwater Single Image Color Restoration Using Haze-Lines and a New Quantitative Dataset", *IEEE Transactions on Pattern Analysis and Machine Intelligence,* vol. 43, no. 8, pp. 2822-2837, 2020.

[109] H. Lu, Y. Li, S. Nakashima, H. Kim and S. Serikawa, "Underwater image super-resolution by descattering and fusion", *IEEE Access,* vol. 5, pp. 670-679, 2017.

[110] S. Wang, K. Ma, H. Yeganeh and Z. Wang, W. Lin, "A Patch-Structure Representation Method for Quality Assessment of Contrast Changed Images", *IEEE Signal Processing Letters*, vol. 22, no. 12, pp. 2387-2390, 2015.

[111] A. Mittal, R. Soundararajan and A. C. Bovik, "Making a "Completely Blind" Image Quality Analyzer", *IEEE Signal Processing Letters*, vol. 20, no. 3, pp. 209-212, 2013.

[112] K. Panetta, C. Gao and S. Agaian, "Human-Visual-System-Inspired Underwater Image Quality Measures", *IEEE Journal of Oceanic Engineering*, vol. 41, no. 3, pp. 541-551, 2016.

[113] A. S. A. Ghani, R.S.N.A.R. Aris, and M. L. M. Zain, "Unsupervised contrast correction for underwater image quality enhancement through

integrated-intensity stretched-Rayleigh histograms", *Journal of Telecommunication, Electronic and Computer Engineering (JTEC),* vol. 8, no. 3, pp. 1-7, 2016.

[114] A. S. A. Ghani and N. A. M. Isa, "Enhancement of low-quality underwater image through integrated global and local contrast correction", *Applied Soft Computing*, vol. 37, pp. 332-344, 2015.

[115] C. Dong, C. C. Loy, K. He and X. Tang, "Image Super-Resolution Using Deep Convolutional Networks", *IEEE Transactions on Pattern Analysis and Machine Intelligence*, vol. 38, no. 2, pp. 295–307, 2016.

[116] C. Ledig, L. Theis, F. Huszar, J. Caballero, A. Cunningham, A. Acosta, A. Aitken, A. Tejani, J. Totz, Z. Wang and W. Shi, "Photo-Realistic Single Image Super-Resolution Using a Generative Adversarial Network", *Proceedings of the IEEE Conference on Computer Vision and Pattern Recognition (CVPR)*, pp. 4681-4690, 2017.

Curriculum Vitae

Nishant Singh

Registration Number: 2K20/PHDCO/02

Department of Computer Science and Engineering

Delhi Technological University, Delhi-110042

Email: singhnishant88@gmail.com

Google Scholar:

https://scholar.google.com/citations?user=PkIvs-QAAAAJ&hl=en

Mr. Nishant Singh is currently pursuing a Ph.D. in the Department of Computer Science and Engineering from Delhi Technological University, Delhi. His Research interests include Image Processing, Neural Networks, Machine Learning, Computer Vision, and Deep Learning. He has eleven years of total experience including academic and research experience.

He is currently working as an Assistant Professor in the Department of Computer Engineering and Application, Institute of Engineering and Technology (IET) at GLA University, Mathura, Uttar Pradesh, India. Previously, he had worked as an Assistant Professor in the Department of Computer Science and Engineering at Poornima Institute of Engineering and Technology (PIET), Jaipur, Rajasthan, India. Before that, he had worked as an Assistant Professor in the Department of Computer Science and Engineering at Shree Digamber Institute of Technology (SDIT), Dausa, Rajasthan, India.